**University of Alberta**

# Sedimentology, Ichnology, Stratigraphy and Depositional History of the Contact Between the Triassic Doig and Montney Formations in West-Central Alberta, Canada – Presence of an Unconformity Bound Sand Wedge

by

Jonathan T. LaMothe

©

A thesis submitted to the Faculty of Graduate Studies and Research
in partial fulfillment of the requirements for the degree of

Master of Science

Department of Earth and Atmospheric Sciences

Edmonton, Alberta
Spring 2008

Library and Archives Canada

Published Heritage Branch

395 Wellington Street
Ottawa ON K1A 0N4
Canada

Bibliothèque et Archives Canada

Direction du Patrimoine de l'édition

395, rue Wellington
Ottawa ON K1A 0N4
Canada

*Your file Votre référence*
*ISBN: 978-0-494-45839-6*
*Our file Notre référence*
*ISBN: 978-0-494-45839-6*

NOTICE:
The author has granted a non-exclusive license allowing Library and Archives Canada to reproduce, publish, archive, preserve, conserve, communicate to the public by telecommunication or on the Internet, loan, distribute and sell theses worldwide, for commercial or non-commercial purposes, in microform, paper, electronic and/or any other formats.

The author retains copyright ownership and moral rights in this thesis. Neither the thesis nor substantial extracts from it may be printed or otherwise reproduced without the author's permission.

AVIS:
L'auteur a accordé une licence non exclusive permettant à la Bibliothèque et Archives Canada de reproduire, publier, archiver, sauvegarder, conserver, transmettre au public par télécommunication ou par l'Internet, prêter, distribuer et vendre des thèses partout dans le monde, à des fins commerciales ou autres, sur support microforme, papier, électronique et/ou autres formats.

L'auteur conserve la propriété du droit d'auteur et des droits moraux qui protège cette thèse. Ni la thèse ni des extraits substantiels de celle-ci ne doivent être imprimés ou autrement reproduits sans son autorisation.

---

In compliance with the Canadian Privacy Act some supporting forms may have been removed from this thesis.

While these forms may be included in the document page count, their removal does not represent any loss of content from the thesis.

Conformément à la loi canadienne sur la protection de la vie privée, quelques formulaires secondaires ont été enlevés de cette thèse.

Bien que ces formulaires aient inclus dans la pagination, il n'y aura aucun contenu manquant.

Canada

**Abstract**

In west-central Alberta during the Early (Spathian) Triassic the Moig Siltstone, Moig Sandstone and Lower Doig Formation were deposited. Analysis of core, well logs, cross-sections and maps suggests that these units were emplaced in an overall transgressive system with occasional stillstand deposition. The Moig Siltstone and Moig Sandstone form two unconformity bound sand wedges. Mapping and cross-sections suggests that high energy flooding surfaces influenced morphology of the units. Theses three units studied were also affected by the underlying Paleozoic faults.

From core analysis three facies associations (SO, B, and SS) were developed based on fifteen facies (F1-F11). The three associations relate to sheltered shelf deposits (FA SS), storm dominated upper offshore to transition zone deposits (FA SO), and low energy transition zone to proximal lower shoreface deposits (FA B). Ichnology was crucial in delineating the Moig Sandstone (FA B) since all sedimentary structures had been biogenically altered.

**Acknowledgements**

First and foremost, I would like to address the acknowledgements of my two supervisors Dr. George Pemberton and Dr. Murray Gingras. Their wealth of knowledge, enthusiasm and endless stories have kept me driven over the past two years.

Thanks to my committee members Dr. Caldwell and Dr. Heming. Your suggestions are very much appreciated.

I would also like to thank Lynn Dafoe. Lynn, thank you for your countless suggestions and edits they are greatly appreciated. I look forward to our continued friendship.

I would like to thank all the other IRG lab rats; (as Sue liked to call us) Tyler Hawk, Sarah Gunn, Kevin Balshaw, Trevor Hoffman, Curtis Lettley, Marilyn Zorn, Ryan Lemiski and Zaki. You all made my time here fun and definitely interesting.

Support and guidance of this thesis was generously given from Talisman Energy and Dan Edwards of Krishelle Enterprises. Talisman provided financial and technical support (Thanks for the Surfer help Matt!) while Dan Edwards (a guru of Triassic rocks) provided great insight.

Teddi is also thanked for her friendship and guidance during my early days of thesis writing.

My family played a huge roll in encouraging me to continue my education. Without their drive I don't now where I would be today. Thanks mom, dad, Jer and Mel.

Last and not least I would like to thank my wife Kathryn who had to put up with my constant ramblings and twice a week drive from Edmonton to Calgary. I know this was difficult for you so thanks.

**Table of Contents**


CHAPTER ONE: INTRODUCTION AND OVERVIEW ..... 1
1.1 INTRODUCTION ..... 1
1.2 STUDY AREA ..... 3
1.3 PREVIOUS WORK ..... 3
1.4 REGIONAL STRATIGRAPHY ..... 11
1.5 THE DOIG FORMATION AND ITS VARYING INTERPRETATIONS ..... 17
1.6 TECTONIC HISTORY ..... 19
1.7 PALEOGEOGRAPHY AND PALEOCLIMATE ..... 24
1.8 SEDIMENT PROVENANCE ..... 27
1.9 SOURCE ROCKS ..... 29
1.10 METHODS AND OBJECTIVES ..... 37

CHAPTER TWO: FACIES, FACIES ASSOCIATIONS, DISCRPTIONS AND INTERPRETATIONS ..... 38
2.1 INTRODUCTION ..... 38
2.2 FACIES DESCRIPTION AND INTERPRETATION ..... 38
2.2.1 Facies F1: Heavily bioturbated silty sand ..... 41
2.2.2 Facies F2: Dark grey massive sandy silt ..... 44
2.2.3 Facies F3: Rhythmic to wavy laminated sandy silt ..... 47
2.2.4 Facies F4: Deformed sandy silt ..... 50
2.2.5 Facies f5: Transgressive surfaces of erosion ..... 54
2.2.5.1 Facies F5a: Transgressive surface of erosion ..... 54
2.2.5.2 Facies F5b: Transgressive surface of erosion ..... 55
2.2.5.3 Facies F5c: Transgressive surface of erosion ..... 62
2.2.5.4 Facies F5d: Transgressive surface of erosion ..... 62
2.2.6 Facies F6: Heavily bioturbated mottled sandstone ..... 65
2.2.7 Facies F7a: Heavily bioturbated archetypal Cruziana suite ..... 70
2.2.8 Facies F7b: Heavily bioturbated proximal Cruziana suite: ..... 73
2.2.9 Facies F8: Organic rich black shale ..... 77
2.2.10 Facies F9: Muddy siltstone ..... 82
2.2.11 Facies F10: Muddy silt with deformed lenticular sands ..... 83
2.2.12 Facies F11: Silty sand with flame structures ..... 86
2.3 FACIES ASSOCIATIONS ..... 90
2.3.1 Facies Association SO (Moig Siltstone) ..... 90
2.3.2 Facies Association B (Moig Sandstone) ..... 90
2.3.3 Facies Association SS (Lower Doig) ..... 91

CHAPTER THREE: STRATIGRAPHY, DEPOSITIONAL ENVIRONMENTS, AND DISTROBUTION OF THE MOIG AND DOIG UNITS ..... 93
3.1 INTRODUCTION ..... 93
3.2 MAPS ..... 93
3.3 STRATIGRAPHIC EVOLUTION ..... 106
3.4 CROSS-SECTIONS ..... 110

3.5 DEPOSITIONAL MODEL....119
3.5.1 Depositional model 1 Moig Siltstone....119
3.5.2 Depositional model 2 Moig Sandstone....122
3.5.3 Depositional model 3 Lower Doig Formation....124
3.6 FUTURE WORK....125

CHAPTER FOUR: CONCLUSION....127

REFERENCES....128

APPENDIX A: CORE LOGS....143

## List of Tables

Table 2.1 Facies and Facies Associations ..... 8

**List of Figures**

Figure 1. Table of formations found within the Triassic of the Western Canadian Sedimentary Basin. From Bird et al. (1994). ..... 2

Figure 2. Stratigraphic Chart ..... 4

Figure 3. Diagram representing the study area. ..... 5

Figure 4. Study area showing wells. ..... 6

Figure 5. Schematic cross-section representing the 8 parasequences. ..... 9

Figure 6. Diagrammatic cross-sections representing three dominant cycles. ..... 12

Figure 7. Schematic cross-section representing Triassic stratigraphy. ..... 13

Figure 8. Outcrop and subsurface stratigraphy from the Triassic. ..... 15

Figure 9. Study area in relation to Peace River Embayment. ..... 20

Figure 10. Paleogeography of early Triassic time.. ..... 21

Figure 11. Distribution of Triassic rocks in the Western Canadian Sedimentary Basin.. . 22

Figure 12. Five stage, diagrammatic summary of the Peace River Arch ..... 23

Figure 13. Global view of Supercontinent Pangea. ..... 26

Figure 14. This map indicates palaeocurrents in the Triassic. ..... 28

Figure 15. Sand map, of porous Montney sandstone in Sturgeon Lake. ..... 30

Figure 16. Gamma ray log showing upper and lower Phosphate Zone sediments. ..... 31

Figure 17. Hydrogen Index versus Oxygen Index from the Doig Phosphate Zone ..... 32

Figure 18. Map showing the study area in relation to Tmax thermal maturity. ..... 34

Figure 19. Early Triassic Paleogeography showing zones of upwelling. ..... 35

Figure 20. Modern analog of trade winds and coastal upwelling ..... 36

Figure 2.1. Facies F1 ..... 43

Figure 2.2. Facies F2 ..... 46

Figure 2.3. Facies F3 ..... 49

Figure 2.4. Facies F4 ..... 53

Figure 2.5a. Facies F5a ..... 57
Figure 2.5b. Facies F5b ..... 61
Figure 2.5c. Facies F5c ..... 64
Figure 2.5d. Facies F5d ..... 67
Figure 2.6. Facies F6 ..... 69
Figure 2.7a. Facies F7a ..... 72
Figure 2.7b. Facies F7b ..... 76
Figure 2.8. Facies F8 ..... 79
Figure 2.9. Facies F9 ..... 82
Figure 2.10. Facies F10 ..... 85
Figure 2.11. Facies F11 ..... 89
Figure 3.1. Gross thickness map of the Moig Siltstone ..... 94
Figure 3.2. Structure map of the Paleozoic Belloy Formation ..... 96
Figure 3.3. Gross thickness map of the Moig Siltstone ..... 97
Figure 3.4. Net sand isopach of the Moig Sandstone ..... 99
Figure 3.5. Paleozoic faults overlain on the net sand isopach of the Moig Sandstone ..... 100
Figure 3.6. Gross thickness map of the Lower Doig Formation ..... 103
Figure 3.7. Gross thickness map of the Lower Doig Formation ..... 104
Figure 3.8. Stillstand Deposits ..... 108
Figure 3.9. Base map illustrating cross-section placement and fault location ..... 114
Figure 3.10. Well-log cross-section S1-S1'. ..... 115
Figure 3.11. Well-log cross-section S2-S2'. ..... 116
Figure 3.12. Well-log cross-section D1-D1'. ..... 117
Figure 3.13. Well-log cross-section D2-D2'. ..... 118
Figure 3.14. Depositional Model. ..... 120

# CHAPTER ONE

## 1.1 INTRODUCTION

This study describes the Triassic Doig Formation with special emphasis on the contact with the Montney Formation found within west-central Alberta and northeastern British Columbia. The complex nature of this contact reveals a number of unconformity bound wedges.

The Montney, Doig, Halfway, and Charlie Lake formations are Triassic sediments of the Peace River Arch area (Figure 1). Willis (1992) described the Upper-Middle Doig, Halfway, and Charlie Lake as part of the same time equivalent depositional system. Current papers disagree on the Halfway/Charlie Lake depositional timing; however, it is generally accepted that the Doig/Halfway formations are part of the same time equivalent system with the Halfway Formation representing nearshore deposits like barrier bars and the Doig Formation representing more basinal silts and muds. In a typical stratigraphic section the Doig Formation is a clastic unit found below the Halfway Formation. The division between the two has been a cause for many issues since the Halfway strata may prograde and cut into the underlying Doig sandstone (Young, 1997). Where this does not occur the division may be where intebedded sands and shales of the Doig pass suddenly into a sand rich Halfway Formation (Gibson and Edwards, 1990a).

The Lower Doig Formation is represented by a highly radioactive phosphatic shale up to 9 m thick, which downlaps west near the Toad/Grayling contact (Gibson and Edwards, 1990a). Studies by Riediger et al. (1990a,b) suggested that this Phosphate Zone may be a source rock for some of the Triassic hydrocarbons. Across the study area, the base of the Phosphate Zone is characterized by a thin sand, which is called the Gordondale sand by Davies (1997a) (Figure 2). More work needs to be performed on this

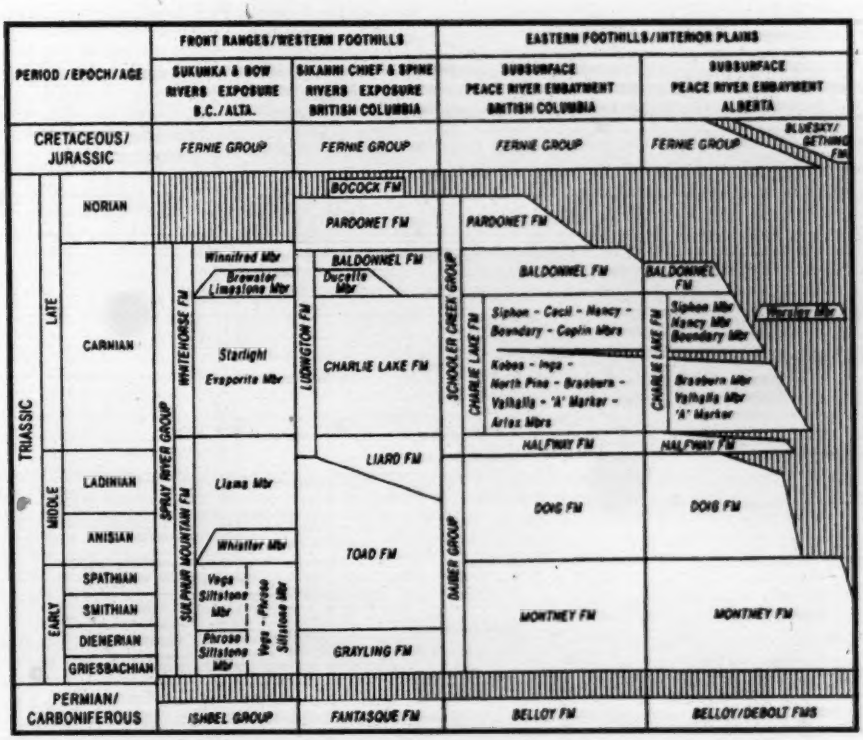


**Figure 1.** Table of formations found within the Triassic of the Western Canadian Sedimentary Basin. From Bird et al. (1994).

productive unit to get an idea of depositional style and stratigraphic setting.

## 1.2 STUDY AREA

The study area is contained within west central Alberta, close to British Columbia. The main Doig hydrocarbon pools in the study area are Pouce Coupe, Pouce Coupe South, Progress, and the Gordondale fields (Figure 3). These four pools are producing from thick Doig sands similar to Wembley and Sinclair fields; however, pools in the study area are smaller in geographical extent. Discovery dates were in the late 70's to early 80's and a hydrocarbon assessment by Bird et al. (1994) showed that porosity values of the fields are 8-11%. As of 1994 the greatest in place hydrocarbon volume belonged to Pouce Coupe South at 2,973 $10^6m^3$ and the least was found in Gordondale with an in place volume of 704 $10^6m^3$ (Bird et al., 1994).

Within the study area there are over 800 wells that penetrate the Doig Formation and approximately 200 of those wells have been cored (Figure 4). The typical cored section in the study area is approximately 30m in length and contains the Halfway and the Doig formations.

The Gordondale Sand is present and productive at the base of the Phosphate Zone in certain locations within the study area. There are 11 cores through this unit that can be utilized.

## 1.3 PREVIOUS WORK

Dawson (1881) first wrote about exposed Triassic rock present in the Pine River Valley. Subsequently McConnell (1891) recorded data on exposed Triassic rock in the Liard River Valley (Edwards et al., 1994). Then in 1917, McLearn worked on Triassic sediments found within northeastern British Columbia (Edwards et al., 1994). McLearn

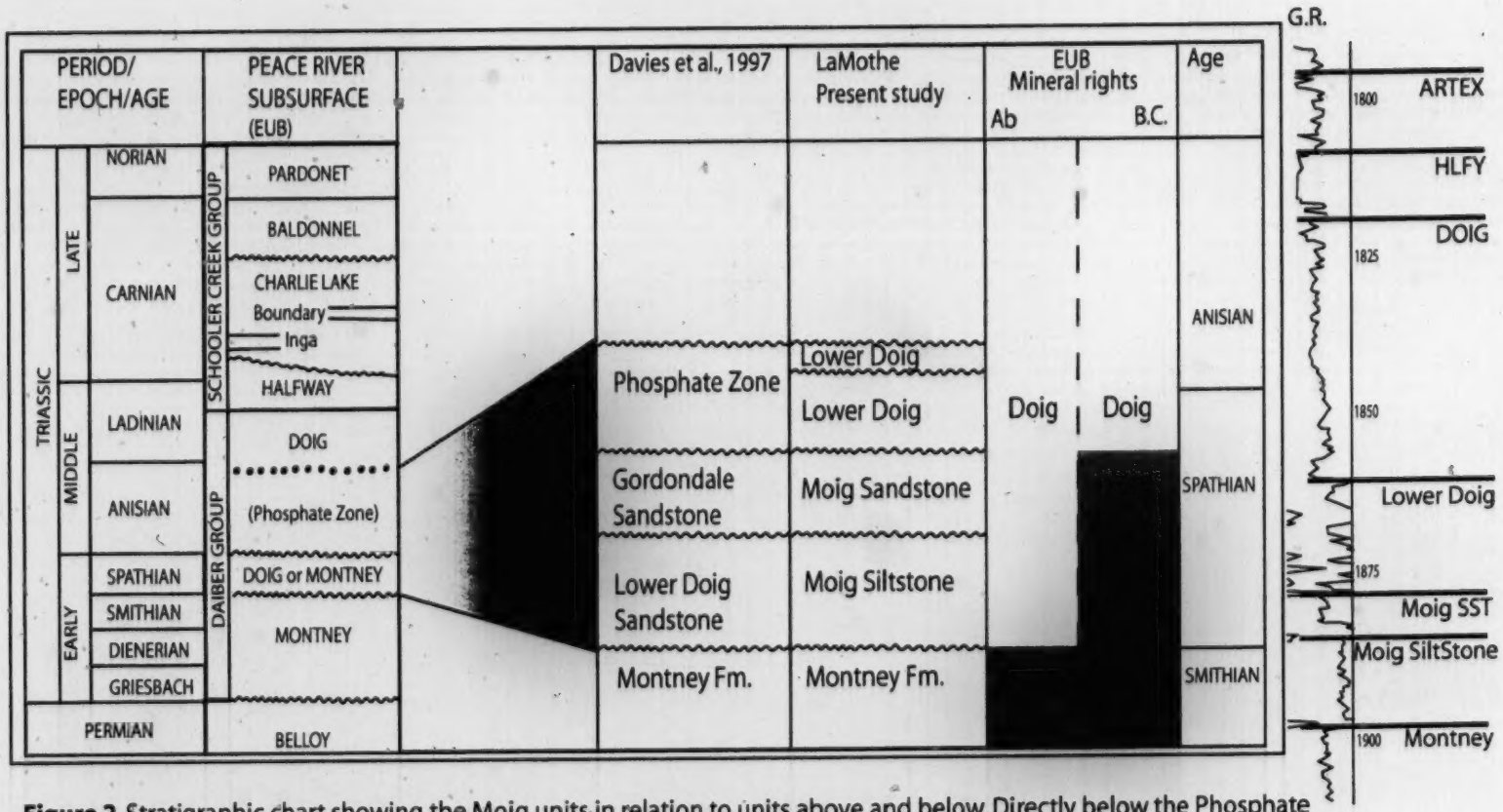


**Figure 2.** Stratigraphic chart showing the Moig units in relation to units above and below. Directly below the Phosphate Zone, is the Moig Sandstone as represented on the gamma ray log in well 11-10-78-10W6/2. This unit is bounded above and below by an unconformity surface. Modified after Gibson (1997) and Podruski et al., (1988)

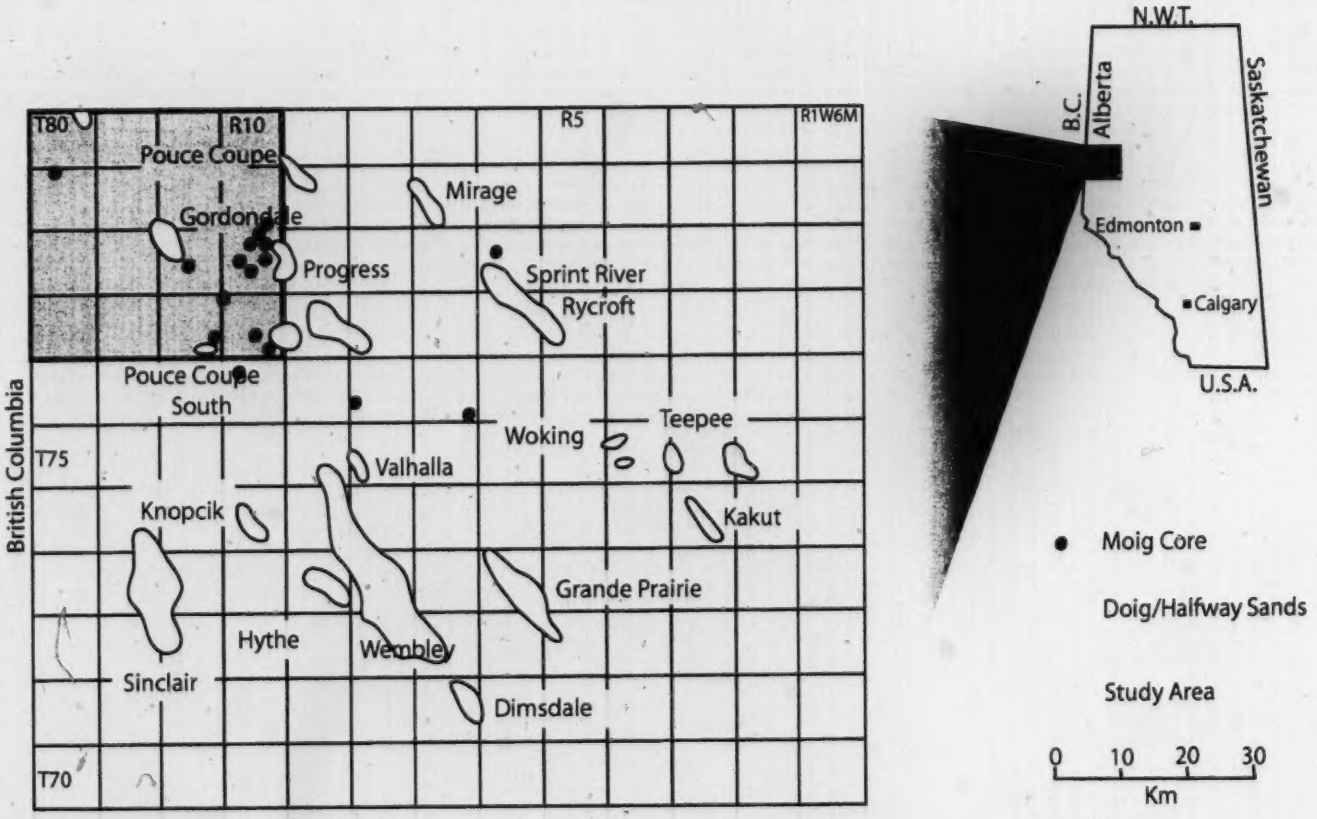


**Figure 3.** Diagram representing the study area with refrence to the Doig/Halfway pools. Modified after Wittenberg (1992).

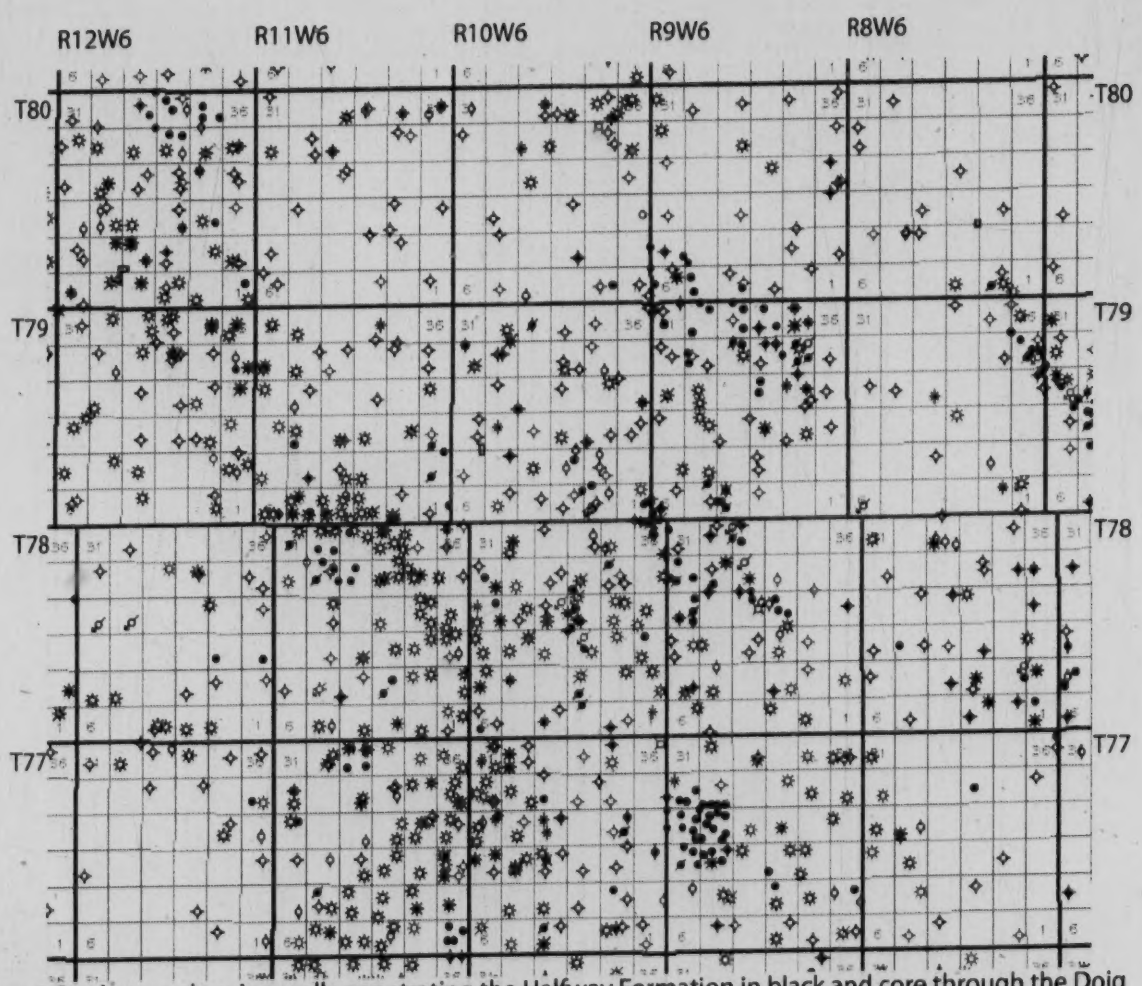


**Figure 4.** Study area showing wells penetrating the Halfway Formation in black and core through the Doig Formation in red.

and Kindle then modified and summarized this work in a Geological Survey of Canada report (McLearn and Kindle, 1950). Stelck (1941), Warren (1945), Pelletier (1960, 1961, 1963, 1964, 1965), Tozer (1961, 1962, 1963, 1965, 1967, 1982a,b, 1984), and Gibson (1970, 1971a,b, 1972, 1975) authored other works on Triassic outcrop strata postdating that of Mclearn and Kindle. Warren (1945), Tozer (1961, 1962, 1963, 1965, 1967, 1982a,b, 1984, 1994), Silberling and Tozer (1968), Orchard and Tozer (1997), Schaeffer and Mangus (1976), and Callaway and Brinkman (1989) prepared most of the research about Triassic biostratigraphy dating methods using ammonites, conodonts, and early Triassic fish.

After the realization of the importance of Triassic rocks and the discovery of hydrocarbons contained within them, many subsurface studies were performed, giving an overview of the Triassic section. Some of these early works were by Hunt and Ratcliffe (1959), Armitage (1962), and Barss et al. (1964). In 1964, Barss et al. published the first Atlas of the Western Canadian Sedimentary Basin. This fundamental work inspired updates and other overviews of the Triassic by Gibson (1968a,b, 1969, 1970, 1971a,b, 1972, 1975), Tozer (1965, 1967, 1982a,b, 1984, 1994), Cant (1984, 1986), Aukes and Web (1986), Campbell and Horne (1986), Prodruski et al. (1988), Brack et al. (1989), Gibson and Barclay (1989), Moslow and Davies (1992), Gibson and Edwards (1990a,b), Edwards et al. (1994), Bird et al. (1994), and Davies (1997a,b).

Armitage (1962) reviewed Triassic resources in northeastern British Columbia. In his report, Armitage relates outcrop data of the Toad – Grayling Formations to the subsurface. In this correlation, he renames the above so they apply to subsurface units called the Montney and the Doig formations found within the Diaber Group. Furthermore, Armitage (1962) named the Diaber Group for the units of sediments found from the base of the Paleozoic unconformity to the Schooler Creek Group. His subdivision was based on the well 06-26-87-21W6, which is the type section for subsurface Diaber strata. Armitage (1962) also recognized the Doig phosphate interval,

described by Creaney and Allan (1990) and Riediger et al. (1990) as a source rock for Triassic hydrocarbons.

Subsurface Doig Formation depositional models, predominantly of northeastern British Columbia strata, have been compiled by Evoy (1995, 1997), Evoy and Moslow (1995), and Harris and Bustin (2000). Most other works on western Alberta Doig strata have been authored by Campbell and Horne (1986), Cant (1986), Campbell and Hassler (1989), Campbell et al. (1989), Gibson and Edwards (1990a,b), Wittenberg and Moslow (1991), Wittenberg (1992, 1993), Evoy (1995, 1997), Evoy and Moslow (1995), Harris (2000), and Rahman and Henderson (2005). All the above authors and their depositional models are described later in this chapter.

Diagenesis and Doig mineralogy were studied by Wittenberg (1992), Harris and Bustin (2000), and Kirste et al. (1997). Wittenberg (1992) mapped out trends in dolomite, anhydrite, and quartz cement found in the PRA area, emphasizing the Wembley and Sinclair fields. Harris and Bustin (2000) showed that diagenetic events and cementation directly influence reservoir quality contained within the Doig. In addition to diagenetic trends, Kirste et al. (1997) described fluid flow, water chemistry, and gas chemistry of the Charlie Lake, Halfway, Doig, and Montney formations in Alberta and British Columbia.

Campbell and Hassler (1989) and Campbell et al. (1989) discussed the Halfway and Doig formations found within west-central Alberta. Their research recognizes two parasequences in the Halfway and six parasequences in the Doig, all of which present an upward coarsening style, as similarly described by Aukes and Webb (1986). In 1992, Wittenberg's studies of the Doig in west-central Alberta revealed the same parasequences found by Campbell and Hassler (1989) and Campbell et al. (1989) (Figure 5). Wittenberg (1992) further recognized that each progradational cycle is capped or bounded by a phosphatic shale, which he interprets as a condensed section associated with a transgressive event. By correlating each parasequence, Wittenberg deduced that the

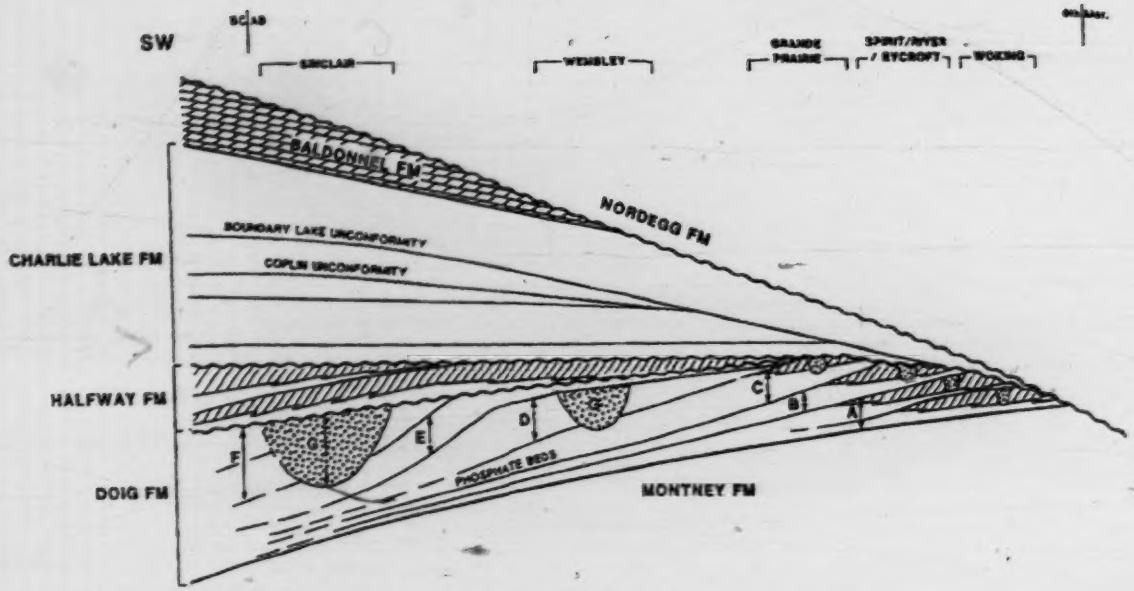


**Figure 5**. Schematic cross-section representing the 8 parasequences found within the Doig and the Halfway formations of west-central Alberta. From Campbell et al. (1989).

Halfway and Doig formations are part of the same time equivalent unit and depositional system, with the Halfway representing shoreline sands and the Doig representing shelf muds and shelf slump deposits. This correlation allows Wittenberg to disagree with the valley incision model of the Doig Formation developed by Campbell et al. (1989).

From an ichnological perspective, most work pertaining to the Liard Formation has focused on outcrop data along Williston Lake in northeastern British Columbia. This section of outcrop has been described in detail by Zonneveld (1999) in his PhD thesis. Further studies of Triassic trace fossil assemblages, brackish-water ichnofaunas, *Lingulid* derived traces, *Lingulid* trace distribution, and biostromes are outlined in Zonneveld et al. (2001), Buatois et al. (2004), Zonneveld and Pemberton (2003), Zonneveld, Beatty, and Pemberton (2005), and Zonneveld (2001) respectively. Large, robust *Cruziana* were also described by Zonneveld, Pemberton, Saunders, and Pickerill (2002) along Williston Lake with emphasis on applicability for biostratigraphy. Most other studies, in particular thesis projects by Wittenberg (1992), Evoy (1997), and Harris (2000) touched on trace fossils as described in core.

The Gordondale Sand, a thin sand found at the base of the Phosphate Zone, was first discussed briefly by Davies et al. (1997a). Their research describes this unit as an unconformity-bounded wedge composed of bioturbated locally productive shoreface sands of siliclastic sediments in and around the Gordondale Field. Davies et al. (1997a) recommend that more work must be completed to understand this unit's relationship with others above and below it. The next brief mention of the unit appears in sequence stratigraphic terms with no specific mention of the Gordondale Sand (Kendall, 1999). In Kendall's interpretation, the Uppermost Montney is contained in a 3rd order transgressive sequence of Spathian-Anisian age; furthermore, she suggests that the Upper Spathian-Doig contact displays considerable erosional truncation and that the Doig Phosphate Zone may represent a maximum flooding surface of the 3rd order sequence. The most recent information on this unit comes from a personal communication with Dan Edwards

(personal communication, 2005) in which he speculates that the Gordondale Sand is part of the Montney Formation and is bounded at the upper surface by the Doig Phosphate Zone and at the lower surface by an erosional phosphatic layer (Figure 2). For the purpose of this thesis the Gordondale sand named by Davies et al. (1997a) has been informally renamed to the Moig Sandstone to reduce confusion with published data on the Jurassic Gordondale Member also found in the area. The base of the Moig Sandstone contains the Upper Montney transgressive deposits briefly described by Kendall (1999). These Upper Montney deposits have been informally renamed to the Moig Siltstone since in Alberta mineral rights are designated to the Doig Formation. Mineral rights in Alberta designate the Moig units as Doig; however, they are most likely Montney deposits.

## 1.4 REGIONAL STRATIGRAPHY

Triassic strata of the PRA can be broken down into three major stages/cycles of transgression and regression based on third or forth order cycles contained within the Diaber and Schooler Creek groups (Gibson and Barclay, 1989; Podruski et al., 1988). These are the Montney Formation in cycle one, the Doig, Halfway, and Charlie Lake formations in cycle two, and the Baldonnel and Pardonet formations in cycle three (Figure 6). Depending on location, all formations found within the three cycles are eroded away by the pre-Jurrassic unconformity in the east (Figure 7). Within the three cycles there are varying amounts of transgressions and regressions on a local scale because of tectonic activity, sediment supply, underlying topography, eustatic sea level changes, and climate (Bird et al., 1994).

The Triassic Montney Formation in cycle one unconformably overlays Permian chert and sand of the Belloy Formation (Robbins, 1999). The Montney Formation is equivalent to the Vega-Phroso Member of Sukunka – Smokey River and Pine Pass as described in outcrop by Gibson (1971, 1972, 1975). Other equivalents of the Montney

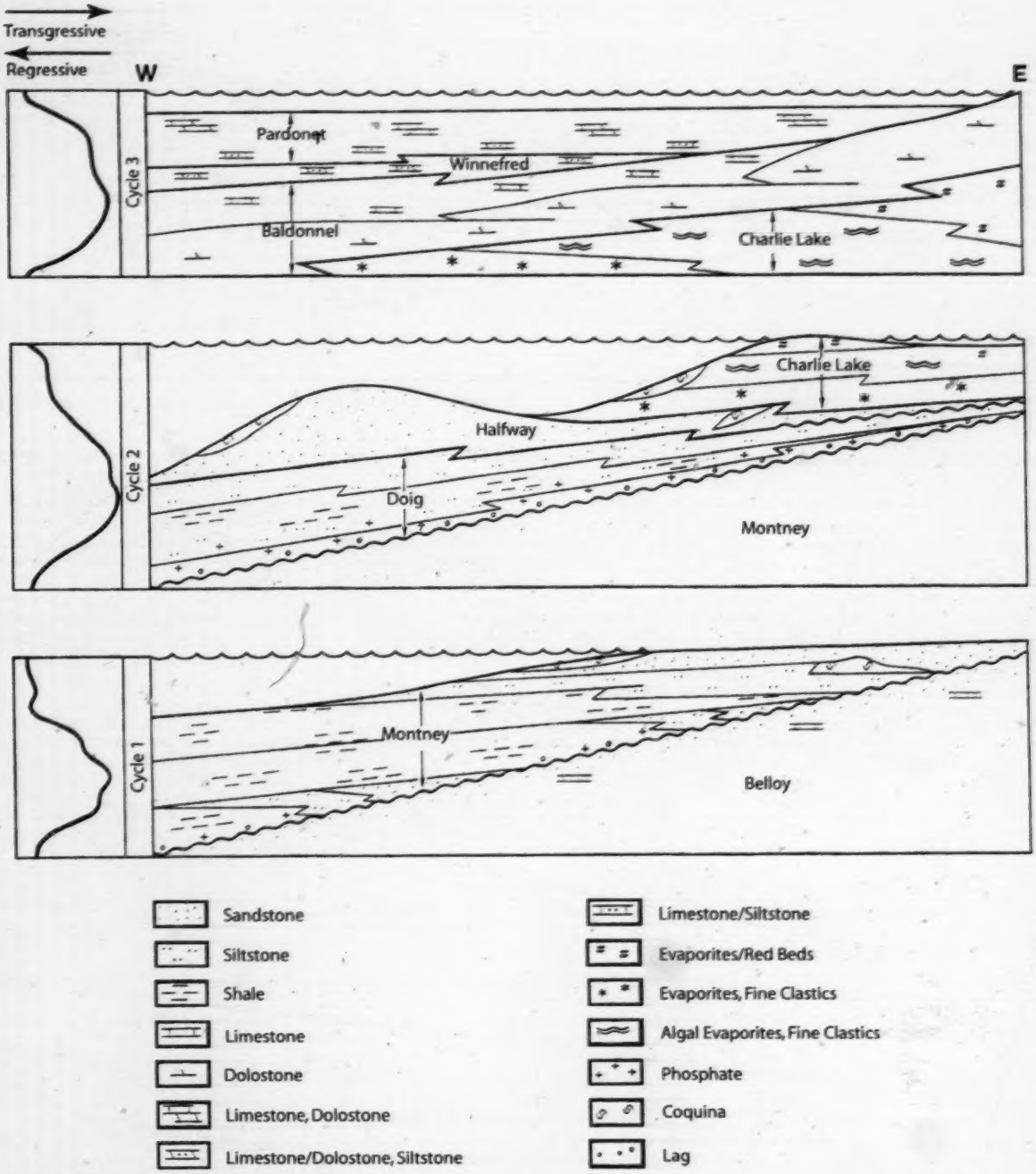


**Figure 6.** Diagrammatic cross-sections representing three dominant cycles found within the Triassic. The end of cycle one is represented by a regressive package and when combined with post-Triassic erosion the result may have been removal of the eastern edge of the cycle (Bird et al., 1994). Middle to beginning of cycle two has a major transgressive event responsible for the deposition of the Doig phosphates. Modified after Bird et al. (1994).

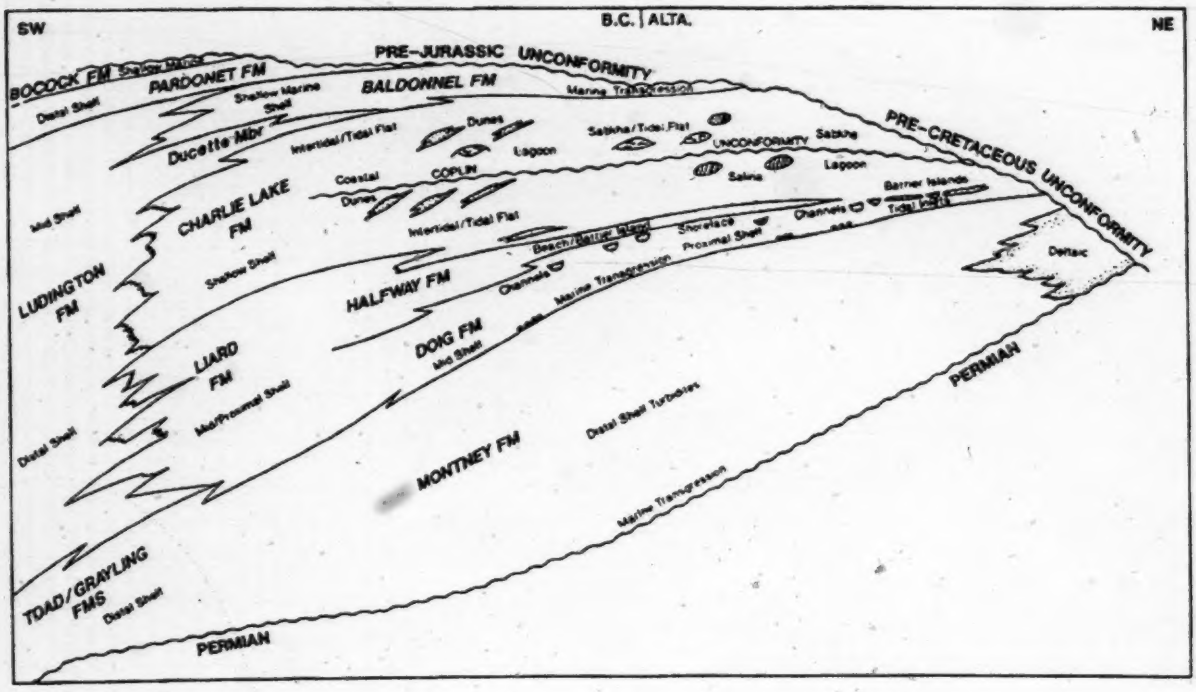


**Figure 7.** Schematic cross-section representing Triassic startigraphy in relation to the Pre-Jurassic Unconformity. Modified after Gibson and Edwards (1990).

Formation are the Grayling and lower part of the Toad formations in Sikanni – Pine Pass area (Gibson, 1971a, 1975; Figure 8). In the PRA subsurface, the Montney contains argillaceous siltstones and dark shale with the Upper Montney containing phosphates, which are easily confused with the Doig Phosphate Zone (Riediger et al., 1990a,b). Miall (1976) discovered that the Montney also contains dolomitized coquina beds associated with a shelf margin wedge. This lowest most cycle is interpreted as deltaic, emphasized by a tidally influenced coastline with distal shelf deposits offshore (Gibson and Barclay, 1989; Edwards et al., 1994). More recent studies interpret the Montney as a wave-dominated shoreline containing sands and coquina that gradationally move out into offshore siltstone and mud from turbidite deposition (Moslow and Davies, 1997; Davies, 1997a).

The Montney Formation of cycle one is conformably and unconformibly overlain by the Triassic Doig, Halfway, and Charlie Lake formations of cycle two. Particularly within the study area the Doig Phosphate Zone as recognized by Armitage (1962), is a major marine transgression that overlies the Montney and is composed of nodular phosphates, silt, shale, shells, and some bone fragments. It has been suggested by Edwards et al. (1994) that the abrupt nature of the contact with the lower cycle and the presence of phosphates indicates an interval of non-deposition or submarine erosion pretransgression and predeposition of cycle two. The equivalent units of the Doig Phosphates are the Whistler Member of Sukunka area and Middle Toad Formation of Sikanni Chief area (Edwards et al., 1994). Postdating this transgression is a regression depositing sands, silts, and bioclastics of the Upper Doig and Halfway formations equivalent to the Llama Member of Sukunka, and Upper Toad and Liard formations of Sikanni (Gibson, 1972, 1975; Figure 8). In most instances the Doig Formation represents an offshore environment grading up into barrier bars, tidal inlets, and shoreface environments of the Halfway Formation (Gibson and Edwards 1990b; Gibson, 1968a,b; Cant, 1986; Aukes and Webb 1986). Where there are anomalously

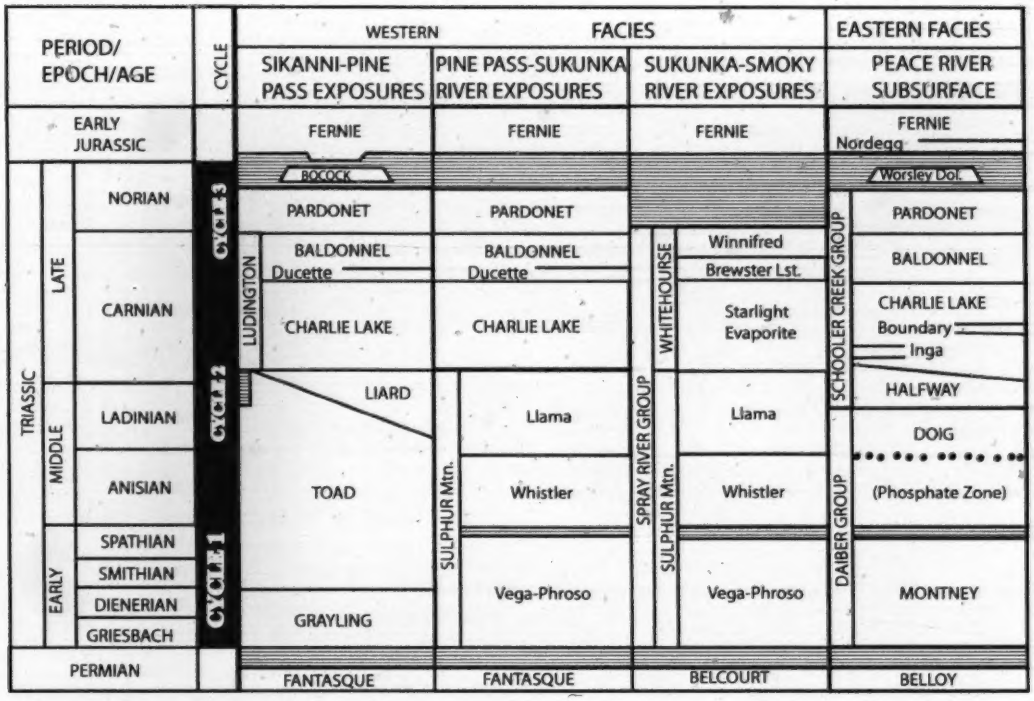


**Figure 8.** Outcrop and subsurface stratigraphy from the Triassic. From Gibson (1997) and Podruski et al. (1988).

thick Doig sands, interpretation of depositional style can be difficult and therefore many different interpretations have been placed on these thick sand bodies. Following sections in this chapter will discuss varying interpretations of the thick Doig sands. In a westerly direction, Halfway sands become increasingly continuous and thick due to stacking of shorface units. When in the extreme reaches of the west, the Doig and Halfway Formations grade into distal shelf and slope sands, silts, and shales present in the Ludington Formation (Edwards et al., 1994). The contact between the Doig and Halfway is in most cases conformable in the west except for instances where tidal inlet sands or pebbly lags of the Halfway have scoured into the underlying Doig Formation (Edwards et al., 1994). In the western foothills the erosional surface is absent therefore lending to the interpretation of a conformable Doig – Halfway unit.

The upper contact of cycle two involves the Halfway and Charlie Lake formations. The Charlie Lake Formation is equivelent to the Starlight Evaporite Member of the Sukunka area. It is typically composed of evapoitic dolomite muds, shale and siltstone redbeds, stromatolitic carbonates, dissolution breccias, dune sands, and salt of a supratidal or intratidal environment (Gibson, 1975; Aukes and Webb, 1986; Cant 1986; Higgs, 1990; Edwards et al, 1994). In the basin an unconformity separates the Charlie Lake and the Halfway formations, representing a period of subarial exposure and erosion (Dixon, 2005).

The Baldonnel and Pardonet formations of cycle three represent shallow to deep water shelf and shoreline carbonates such as limestone or dololstone with smaller amounts of siltstones and shales, intraformational breccia, supratidal algal laminations, and siltstone redbeds (Gibson and Barclay, 1989). The transgressive Baldonnel and Pardonet are equivalent to the Bocock Formation of Sikanni area and the Winnifred and Brewster limestone members of the Sukunka area (Gibson and Barclay, 1989; Figure 8). Transgression of the sea continued after cycle three giving way to deep-water siliclastics and carbonates of the Jurassic Fernie.

## 1.5 THE UPPER DOIG FORMATION AND ITS VARYING INTERPRETATIONS

As previously noted, the Triassic Doig Formation is equivalent to the outcrop units of the Liard from Sikanni – Pine Pass and the Llama/Whistler from Sukunka – Pine Pass; as well as the Middle to Upper Toad from Sikanni and Sukunka – Smoky River Sikanni (Gibson, 1972, 1975; Figure 15). The Doig is predominantly dark grey siltstone and shale with isolated linear fine-grained sands up to 55 m in thickness (Dixon, 2002a). The lowest portion of the Doig Formation, as represented on the gamma ray logs, contains a highly radioactive bed corresponding to the Phosphate Zone, which directly overlays the Montney Formation. Above the Doig Formation rests the Halfway Formation, which typically contains silicalastic sediments and in some situations thick coquina beds. The contact between the Halfway and the Doig can be problematic in the study area since progradation of the Halfway sands/coquinas can cut directly into the top of the thick Doig sands (Edwards et al., 1994; Young, 1997). Where this does not occur, the transition of lower shoreface sediments into basinal shales and then into thick Doig sand represents the division between the two formations. On the gamma ray log, this represents a shale break between the two formations (Edwards et al., 1994). Young (1997) discusses in detail many of the varying interpretations of the Doig - Halfway contact. Within the study area contact interpretations are transgressive and unconformable (Hunt and Ratcliffe, 1959), regressive normal and abrupt (Barss et al., 1964; Wittenberg, 1993; Willis and Moslow, 1994), regressive (Aukes and Web, 1986; Podruski et al., 1987), regressive and unconformable (Campbell et al., 1989), regressive gradational (Gibson and Barclay, 1989; Embry and Gibson, 1995; Dixon, 2005), and regressive gradational or erosionaly unconformable (Gibson and Edwards, 1990; Edwards et al., 1994).

Mineralogy of the thick Doig sands reveals predominantly well sorted sublithic to quartz arenites and bioclastic packstones to grainstones (Harris and Bustin, 2000).

Detailed studies by Harris and Bustin (2000) show that diagenetic events and cementation directly influence reservoir quality. Typical cementation or diagenetic minerals found in the Doig are calcite, dolomite, anhydrite, and to a lesser extent apatite, pyrite and feldspar. Across the study area the predominant diagenetic mineral is dolomite, which can be seen in core analysis sheets. This trend in dolomite can be traced from other Doig fields in the south, such as Sinclair, where dolomite cement prevails (Wittenberg, 1992).

Isolated thick sands or "anomalously thick sandstone bodies" (ATSB) as described by many previous authors contain the most productive unit within the Doig. These ATSB's have a south-southeast trend and a westerly dip into the PRA, likely caused by intermittent reactivation events found in the DCGC and loading of sediments (Harris and Bustin, 2000; Wittenberg, 1992). The thick isolated linear Doig sands are far from understood because thickened sands do not correlate on a regional extent nor do they parallel the paleoshoreline. Progress Field in the study area exemplifies this pattern, with sands of the Doig ranging from 2 – 55 m. Thinner linear sands of a regressive shoreface cycle nature typically occur in northeastern British Columbia (Evoy, 1995; Evoy and Moslow, 1995; Evoy, 1997; Harris and Bustin, 2000). Once outside of British Columbia and into Alberta, these thin linear sands become thicker and more complex. There are currently five interpretations for the thick Doig sands:

1) incised valley fill (Campbell and Horne, 1986; Campbell and Hassler, 1989; Campbell et al., 1989; Cant, 1986),

2) small shelf slump features filled with shoreface sands (Munroe, 1991; Harris, 2000; Wittenberg and Moslow, 1991; Wittenberg, 1992, 1993),

3) lowstand shorefaces scoured into and filled upon transgression (Evoy, 1995; Evoy and Moslow, 1995; Evoy, 1997),

4) channels representing abandoned submarine canyons, which infill with clastic material from the prograding Halfway Formation (Gibson and Edwards, 1990),

5) faults paralleling the shore line that fill with shoreface/barrier bar sands upon

transgression (Rahman and Henderson, 2005).

## 1.6 TECTONIC HISTORY

Triassic strata of the Peace River Arch (PRA) area were deposited into the Peace River Embayment (Figure 9), which developed due to block faulting and tectonic subsidence along the ENE-WSW arc axis during Early Carboniferous and Permian times (Henderson, 1989; Richards, 1989). During this time sediments were deposited on the northwest portion of the Pangaea Supercontinent (Davies, 1997a,b) (Fig 10). In the west, amongst stable continental shelves and shorelines, Triassic thicknesses can be up to 1200 m. This contrasts with eastern sediments that thin and come to an end at the eroded zero edge (Figure 11) (Edwards et al., 1994).

Across the study area, the PRA formed in five stages of development as described by Cant (1988). From oldest to youngest the five stages are Early Paleozoic uplift phase, Mid to Late Devonian faulting and onlap, Mississippian block subsidence, Pennsylvanian faulting phase, and Mesozoic downwarp phase (Figure 12). O'Connell et al. (1990) further breaks this down into three structural phases of development in the Arch.

The first phase, Precambrian to Early Carboniferous, contains uplift, onlap, and burial. Uplift possibly occurred in the late Proterozic and was followed by onlap in the Mid to Late Devonian (O'Connell et al., 1990). As ages of the Arch approach the Mid Cambrian, the PRA was almost completely buried (O'Connell et al., 1990).

The second phase is composed of Early Carboniferous to Jurassic extension, uplift, and subsidence. This phase formed the Peace River Embayment (PRE). Richards (1989) and Henderson (1989) described the PRE as forming in the Early Carboniferous and Permian times apparently in response to block faulting and subsidence. In the study area, the PRE encompasses the Stoddart Group, Belloy Formation, and Triassic sediments (Barclay et al., 1990). Uplift occurred in the Early Carboniferous and signified a change

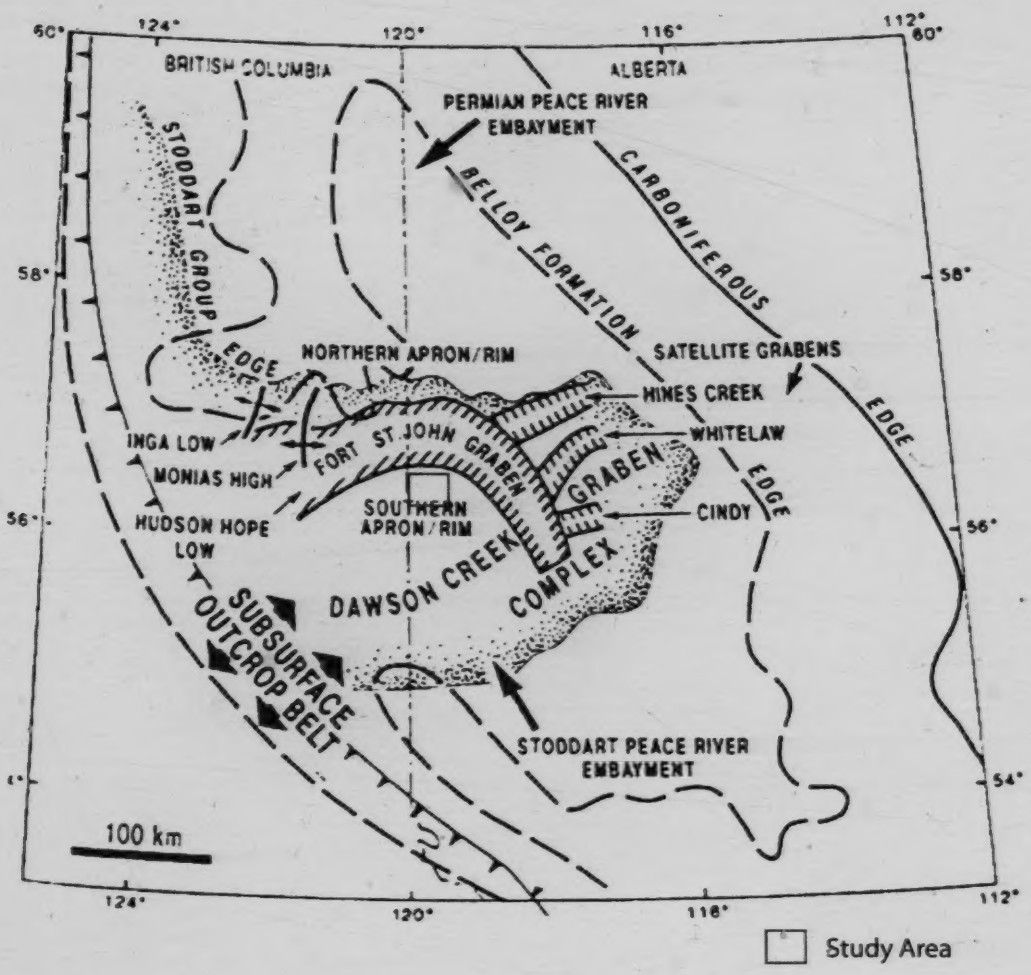


**Figure 9.** Study area in relation to Peace River Embayment and its structural elements. Modified from Macauley et al. (1964); Richards (1989); Henderson (1989); and Barclay et al. (1990).

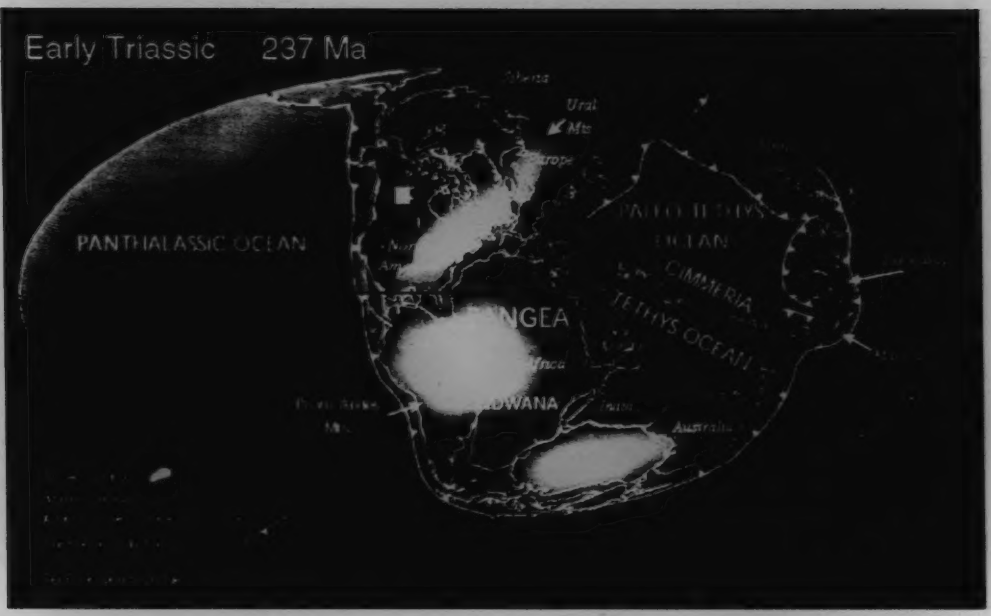


□ Triassic of WCSB

**Figure 10**. Paleogeography of early Triassic time. Modified after www.scotese.com/newpage8.htm (2006).

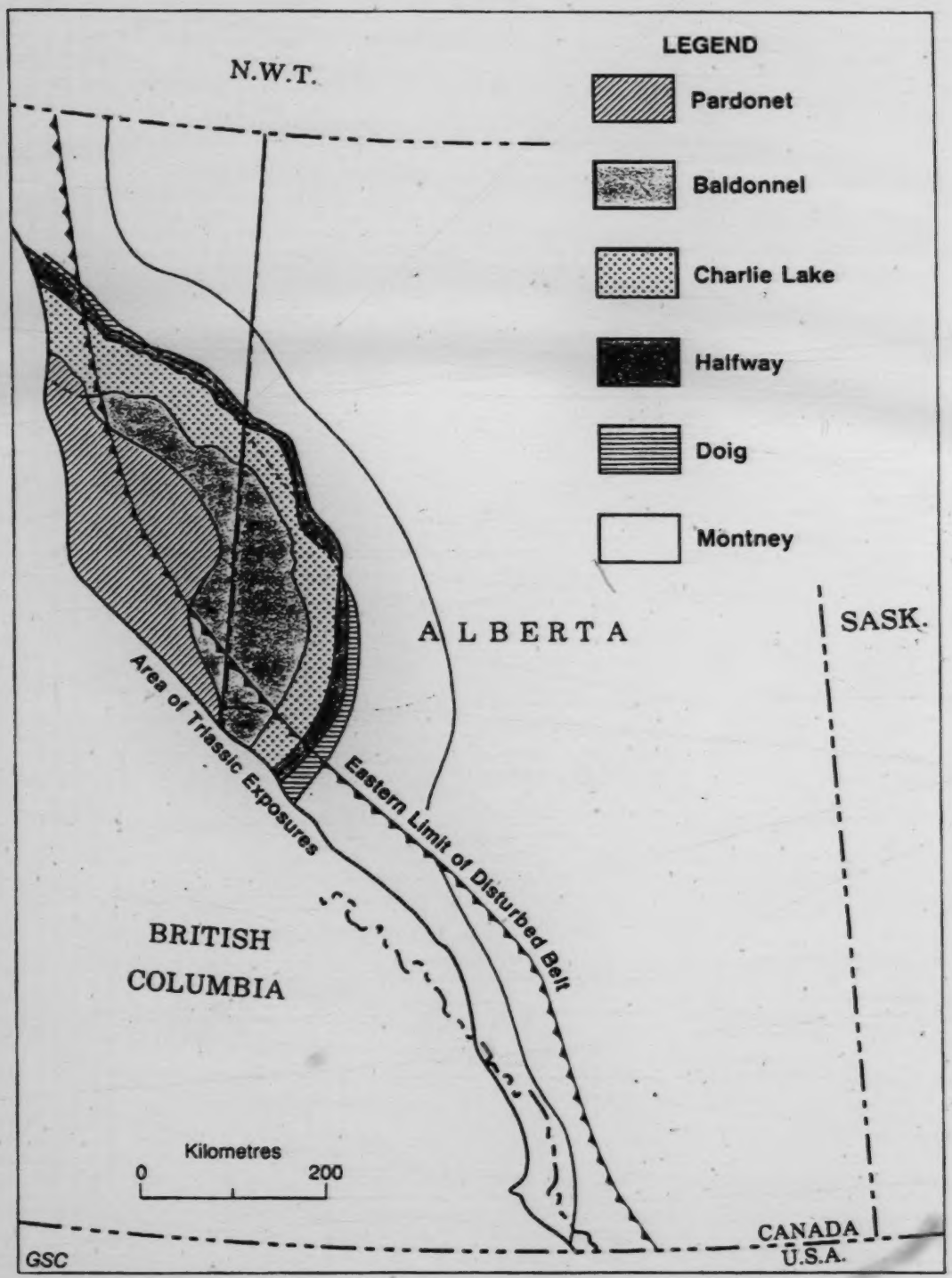


**Figure 11.** Distribution of Triassic rocks in the Western Canadian Sedimentary Basin. Zero eroded edge is represented by eastern limit of sediment. Taken from Podruski et al. (1988).

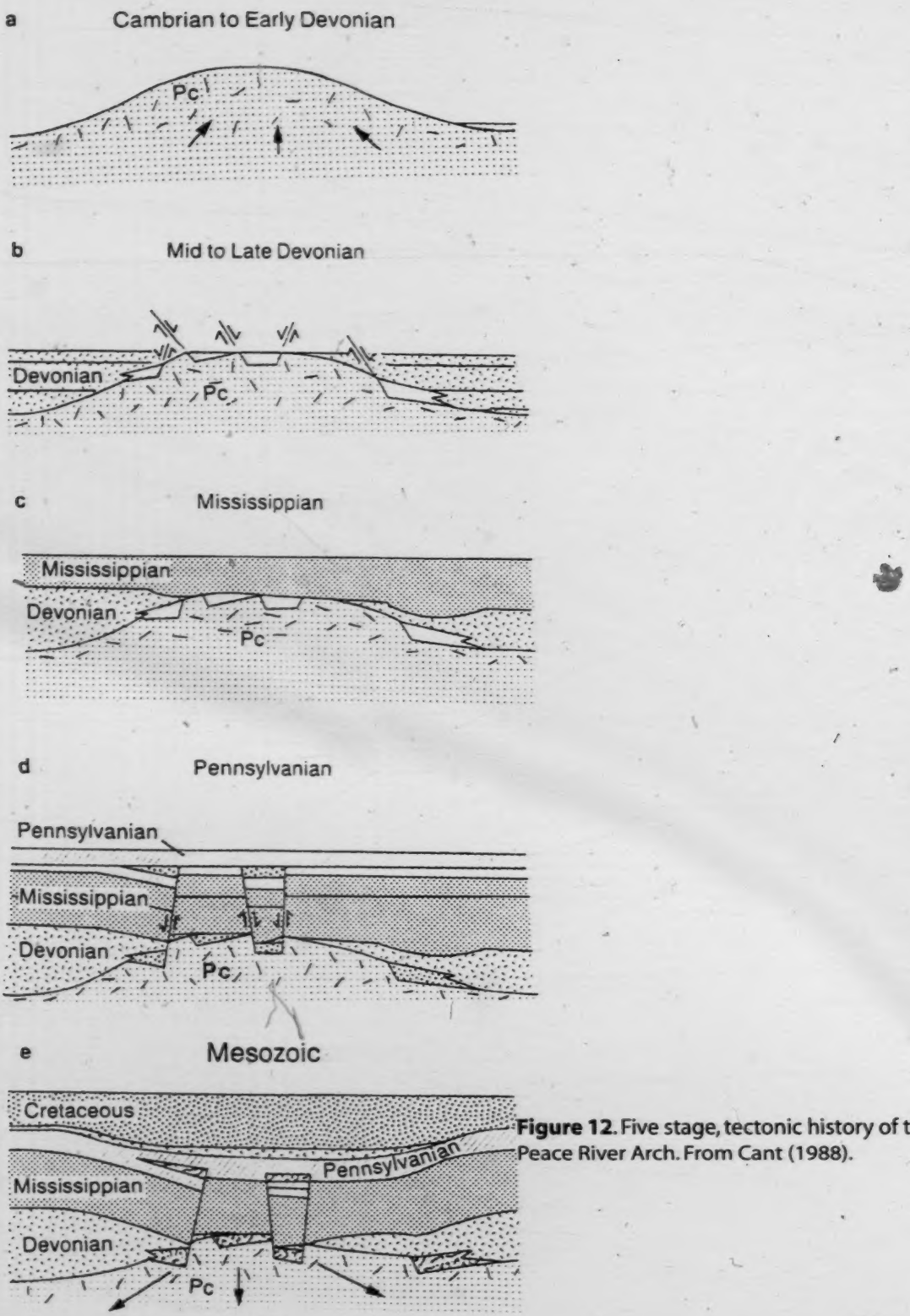


**Figure 12.** Five stage, tectonic history of the Peace River Arch. From Cant (1988).

in deposition from the cratonic platform to deposition into the Embayment, which is found only in west-central Alberta (O'Connell et al., 1990). Following deposition into the PRE, local subsidence occurred during Permian, Triassic, and Jurassic times (O'Connell et al., 1990).

The third phase, as described by O'Connell et al. (1990), contains regional loading in the Jurassic and Cretaceous periods. During this last phase, loading due to deposition of sediments caused reactivation of underlying structures, thus creating subsidence of the Dawson Creek Graben Complex (DCGC) for a second time.

Cant (1986) believes that during Doig deposition a series of minor structures were readjusting below the Triassic sediments. He further suggested that the Wembley Field contains synsedimentary deposition features. These deposition features drape over an underlying horst on the basement structure, which may be the cause of micro faults or gravity faults in Wembley Field (Cant, 1988). These small-scale gravity faults will therefore not be evident on isopach or structure maps of a regional scale (Edwards et al., 1994). Reactivation of these underlying horst structures may be the cause for depositional patterns found within the Doig Formation. Furthermore, these horst structures may have resulted from development of the North American Plate subduction and formation of a magmatic arc resulting in rifting found in the Ouachita region. This rifting opened the modern Atlantic Ocean, which lay to the south of the Western Canadian Sedimentary Basin (WCSB). This intense tectonic activity may have had some significance in reactivating underlying structures such as the DCGC during the relatively quiet tectonic Triassic time (Davies, 1997a).

## 1.7 PALEOGEOGRAPHY AND PALEOCLIMATE

Paleogeography of the Triassic is crucial to understand the depositional setting of the Doig Formation. During the Anisian and Ladinian stages, approximately 241 – 228

ma, the Doig Formation was deposited on the west facing shoreline of the Panthalassa Ocean (Edwards et al., 1994). This clastic deposition occurred at approximately 26 °-34°N paleolatitude on the Supercontinent Pangea as described by Davies (1997a) (Figure 13). At this time, the PRA lay in a slightly skewed location as compared to the present day position. Studies by Golonka et al. (1994), illustrate a roughly 30° clockwise rotation placing the Doig Formation at a lower to middle paleolatitude.

At this location and time, researchers' interpretations of the paleoclimate differ: from temperate (Gibson and Barclay, 1989; Gibson and Edwards, 1990a,b) and arid to semiarid (Habicht, 1979; Dickens, 1993). Davies (1997) describes the Triassic as a period that incorporated some of the most extreme paleoclimate conditions, as represented in evaporite formations, redbeds, and aeolian deposits. This seasonally arid environment experienced prevailing northeast trade winds, which at various times may have been deflected by "megamonsoonal" weather, south and east of the WCSB (Davies 1997a). Furthermore, a west flowing jet-stream may have influenced the climate found in the study area (Davies, 1997a). Davies (1997a) supports his argument for a seasonally arid Triassic climate in the PRA by stating that the extremely arid Triassic period should have been evident in reduced-flooding environments, hypersaline environments in a restricted shallow internal shelf or embayment, and reduction of fluvial discharge. These environments would be ideal for formation of early diagenetic dolomite in pore fluid, seen in the Montney, Doig, and other Triassic formations in the PRA (Davies, 1997a). From a fluvial perspective, determining significant flooding events creates considerable difficulty, since most of the fluvial systems would have been eroded by the pre-Jurassic unconformity, with the exception of deltaic systems found in the Toad – Grayling Formation in the Sturgeon Lake South and Kaybob fields east of Grande Prairie.

The Doig Formation, sandwiched between the Lower and Upper Triassic strata in the PRA, was likely deposited in an arid to semiarid environment. The Upper Triassic, composed of the Charlie Lake Formation containing redbeds, evaporates, and dune

**Figure 13.** Global view of Supercontinent Pangea during late Triassic time. Triassic strata of the PRA is shown in yellow along the western margin, mid-latitudinal location with subduction zones in the offshore. Modified after Dilek (1994) and Davies (1997a).

deposits in the Artex Member, represents a typically arid environment as described by numerous individuals (Barclay and Leckie, 1986; Aukes and Webb, 1986; Gibson and Barclay, 1989; Gibson and Edwards, 1990a,b, Edwards et al., 1994; Davies, 1997a). The Upper Triassic Charlie Lake, Baldonnel, and Pardonet formations in addition to the Lower Triassic Montney Formation of the PRA also contain desert loess deposits, which implies a coastal arid to semiarid environment (Davies, 1997b). A comparison of modern day analogs links this environment to the offshore Saharan, Atacama, and Namib deserts (Davies, 1997b; Wittenberg, 1992).

## 1.8 SEDIMENT PROVENANCE

Studies by Pelletier (1963, 1964, 1965) and Gibson (1968, 1975) illustrated a paleocurrent direction proceeding from the east or northeast as seen in outcrop and core (Figure 14). This indicates sedimentary erosion and deposition from Permian and Upper Mississippian clastic sediments in the east (Gibson, 1975; Gibson and Barclay, 1989). At this time, source from the west was highly unlikely since accretion of western North America had not yet occurred. Moreover, the lack of clastic detritus from the volcanic island arc system, which implies a distance far too great for a significant sediment supply, presents another dispute against a western sediment source (Willis, 1992).

Found within the study area, fine grained Doig sediments with high quartz content and moderate lithics and feldspar, suggest a texturally and mineralogically mature sediment that originated from the east (Gibson and Barclay, 1989). As discussed earlier in this chapter, due to the pre-Jurassic unconformity no fluvial systems have been discovered or preserved in the Doig. Miall (1976) mapped out a delta found in the Sturgeon Lake South and Kaybob fields in the Toad – Grayling Formation, revealing a trend in depositional styles to the southwest; therefore, sediments would have originated from the northeast (Figure 15). Depositional trends may have been skewed or weakened

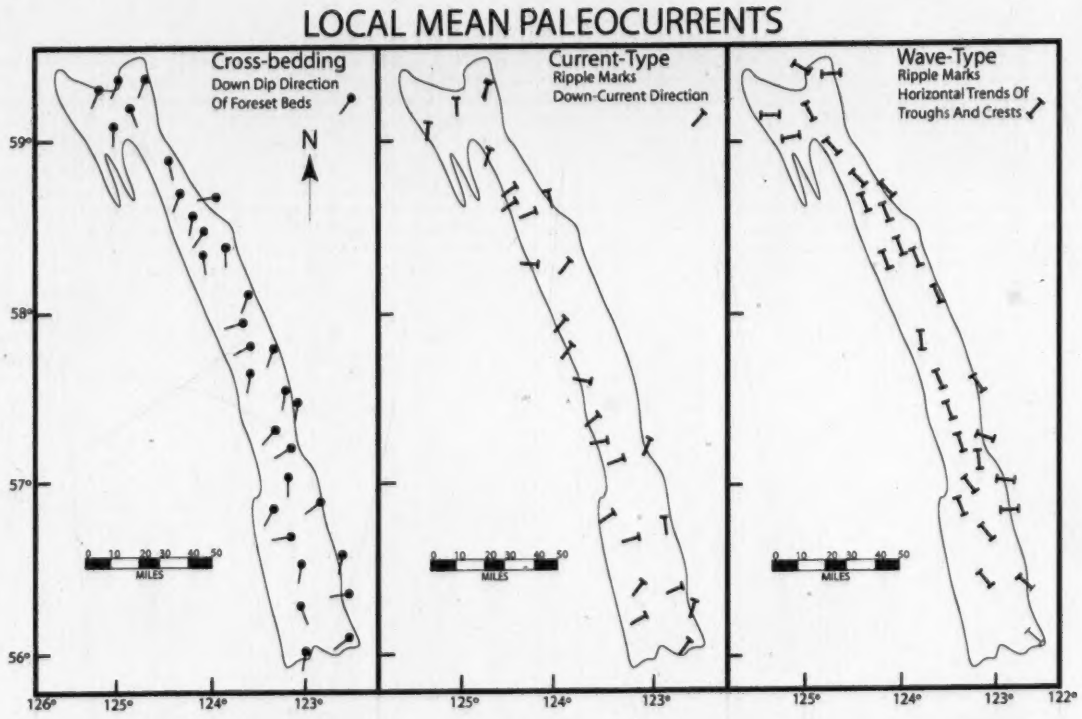


**Figure 14.** This map indicates palaeocurrents in the Triassic Toad – Grayling, Liard, and Halfway formations of northeastern British Columbia described in outcrop by Pelletier (1965). Sediment transport is in a southwesterly direction as indicated by cross-bedding and current ripples. Wave ripples indicate a palaeoshoreline perpendicular to the trend. From Pelletier (1965).

due to longshore drift or currents paralleling the eastern portions of the basin (Gibson, 1975).

## 1.9 SOURCE ROCKS

The Lower Doig Formation harbors a highly radioactive, organic rich Phosphate Zone. Across the study area, this zone has a thickness of approximately 20 m, with the lower 5 m composed of thin beds of siltstone and shale housing shelly/boney fragments, phosphate, and phosphate nodules (Figure 16). Using biomarker signatures, Creaney and Allan (1990) first identified this zone as a source rock for Triasssic oil and gas in the PRA. Since its first definite identification as a source rock for Triassic reserves, several different studies place the Phosphate Zone's total organic carbon (TOC) at 1.12-11 % and its Kerogen levels at type II (Riedeger et al., 1990a; 1990b; Creaney and Allan, 1990; Faraj, 2003). Hydrogen and oxygen index levels (Figure 17) illustrate the presence of Kerogen type II. Slightly above the lowest 5 m of the Phosphate Zone, an area with moderate phosphate composition leads to a TOC of 2 – 7 %. TOC values of less than 2 % in the Upper Doig indicate that this area is probably not a significant source for hydrocarbons (Riediger et al., 1990a).

Across the PRA, thermal maturity increases toward the deformed belt (Tmax >460°C) in the southwest and decreases toward the pre-Jurassic unconformity (Tmax ~440°C) in the northeast (Riediger et al., 1990a). A more imature sample provides greater oil generation; consequently, the southwest produces more oil, when confined to the oil window. In the study area, the Tmax values of approximately 445°C - 450°C place this zone in the oil window; however, most of the production in the area stems from gas (Figure 18). The TOC percentage and Kerogen type make this zone an excellent source rock and allow a viable gas/oil shale target above and within this zone.

Upwelling of ocean currents formed phosphates, which in turn became source

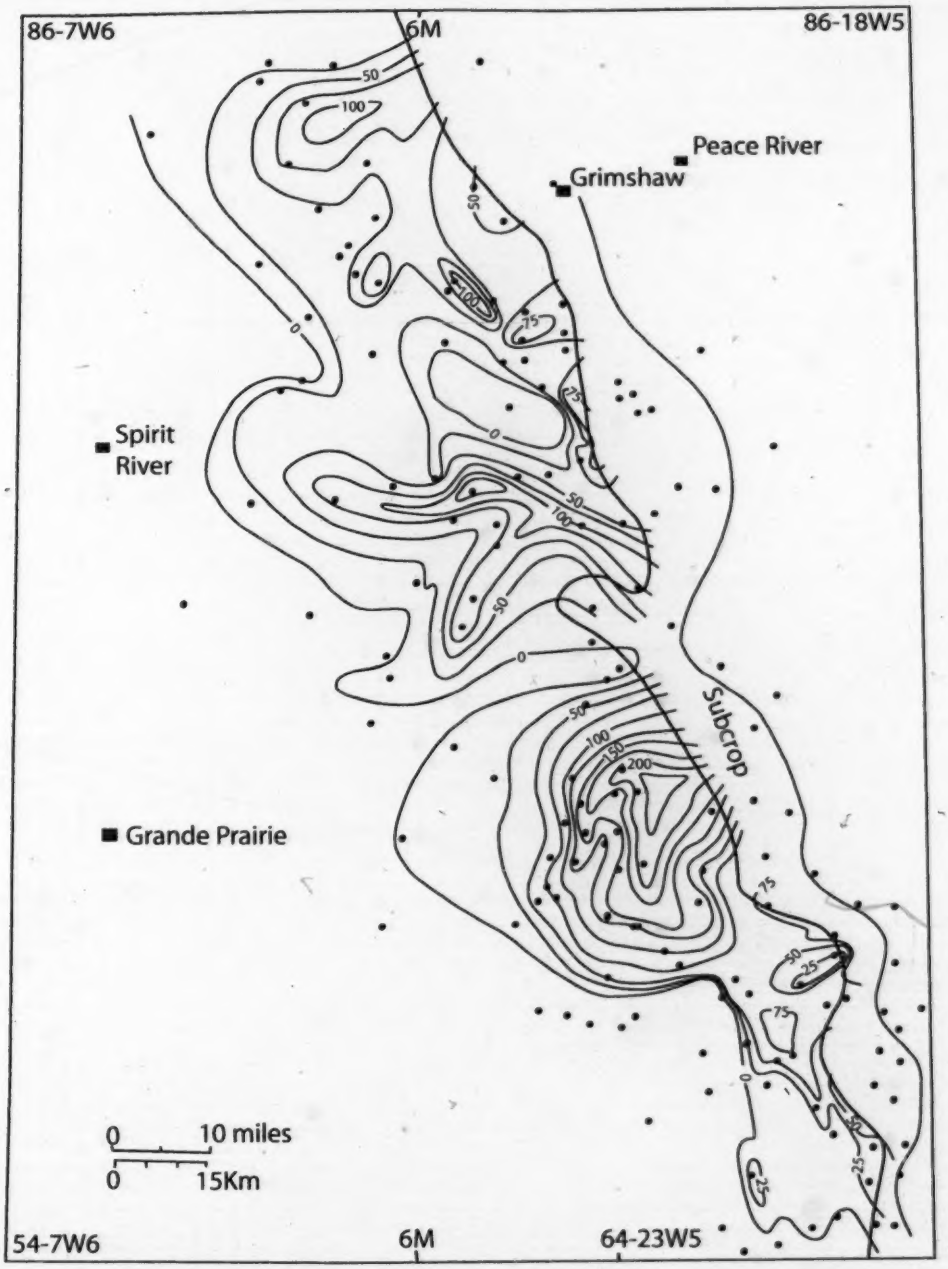


**Figure 15.** Sand map, of the porous Montney sandstones in Sturgeon Lake - South area (Miall, 1976). Thick northeast - southwest trends represent distributary channels. Modifed from Miall (1976)

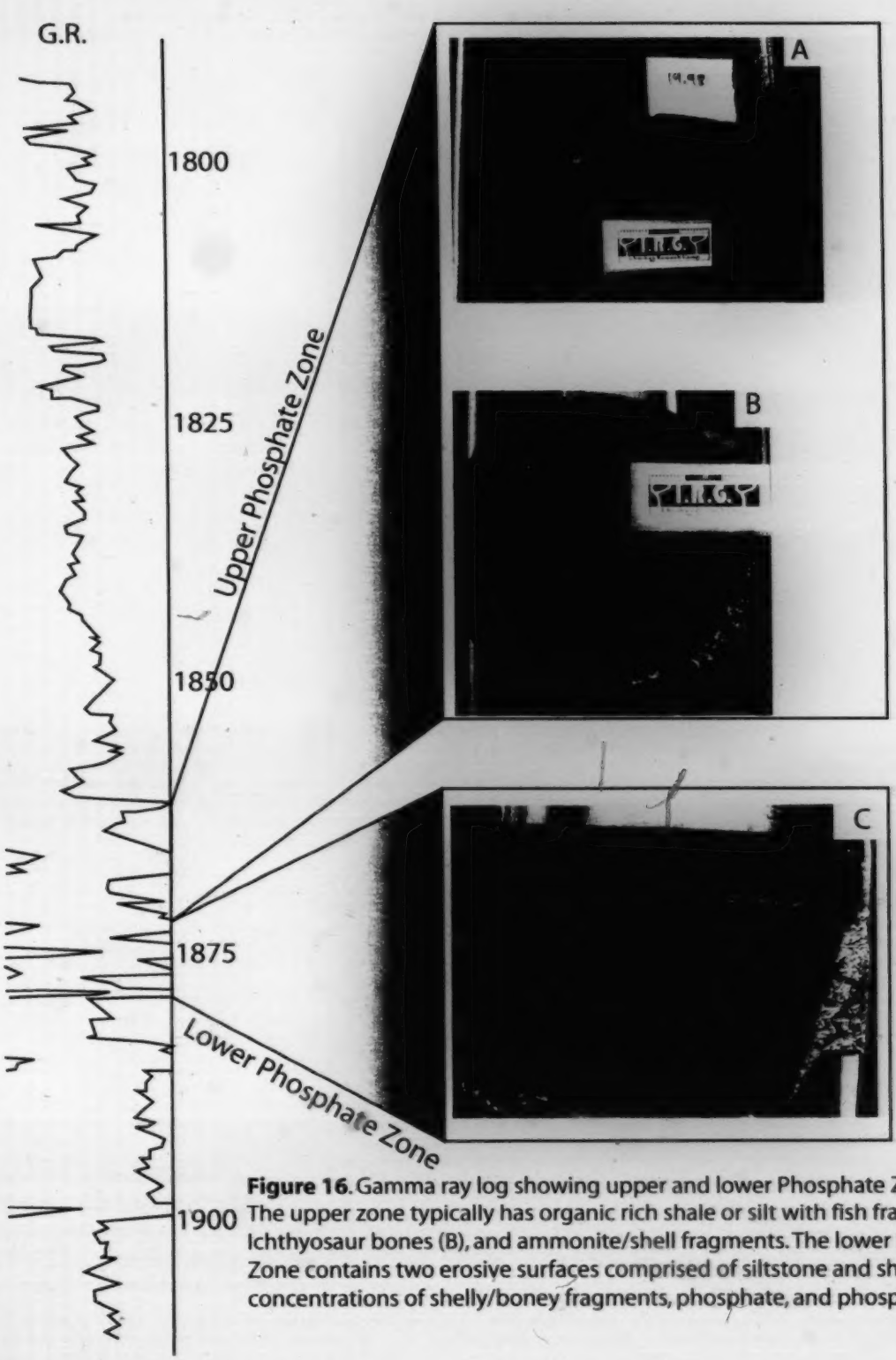


**Figure 16.** Gamma ray log showing upper and lower Phosphate Zone sediments. The upper zone typically has organic rich shale or silt with fish fragments (A), Ichthyosaur bones (B), and ammonite/shell fragments. The lower Doig Phosphate Zone contains two erosive surfaces comprised of siltstone and shale with high concentrations of shelly/boney fragments, phosphate, and phosphate nodules (C).

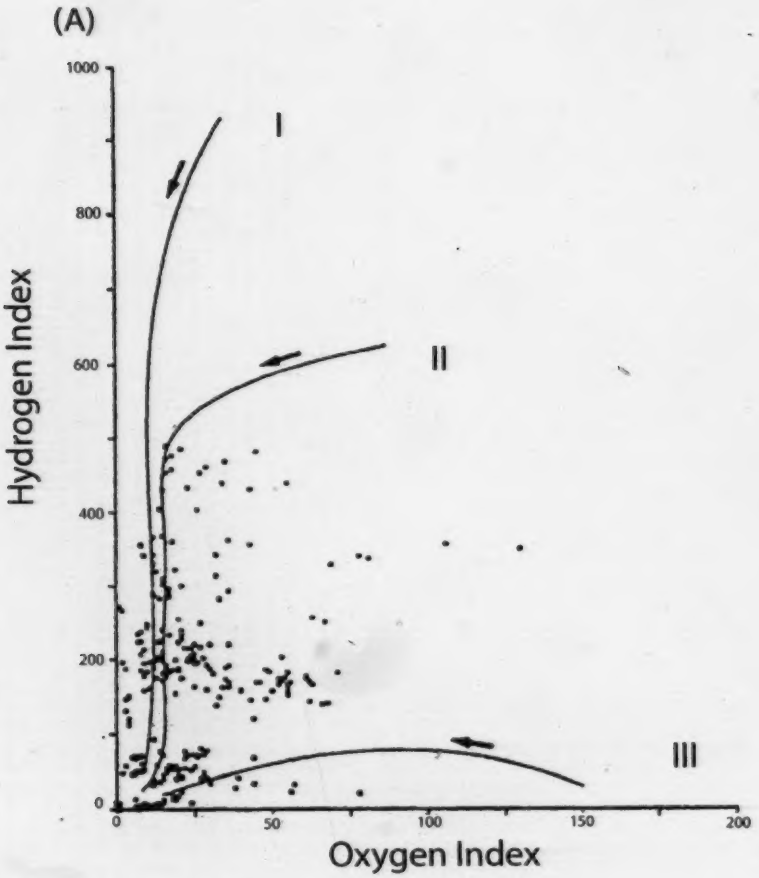


**Figure 17**. Hydrogen Index versus Oxygen Index from the Doig Phosphate Zone, indicating the dominance of type II and III organic matter. From Riediger et al. (1990a).

rocks. In the Triassic, upwelling of ocean currents occurred along the western shelf margins at mid latitudes (Figure 19), placing subsurface Doig strata in areas conducive to the formation of phosphates. Upwelling of cold bottom waters directly relates to offshore winds derived from trade wind belts, which force surface waters offshore. Cool waters upwelling from the deep replaced these surface waters (Wittenberg, 1992). Deeper, cooler waters rich in phosphate ions and organics subsequently cause the formation of phosphates in the typical forms of peloids, nodules, coated grains, and replaced skeletal material (Davies, 1997a).

Present day formation of phosphates occurs on the western facing continental shelves of Baja, Peru, Sahara, Atacama, and Namibia deserts (Wittenberg, 1992; Davies, 1997a; Figure 20). Onshore climatic arid conditions and seasonal winds are common traits for these locations, with the formation of phosphates occurring mostly around 100 m water depth; however, a large range of phosphates materialize in 30 – 500 m water depth (Blatt, 1982).

Both Davies (1997a) and Wittenberg (1992) noticed a less than abundant occurrence and distribution of trace fossils within the Phosphate Zone. Wittenberg (1992) believed that the presence of phosphate and low diversity/abundance of trace fossils directly correlates with an anoxic environment. Davies (1997a) shared in this interpretation but adds that coastal upwelling triggers phytoplanktonic blooms in mid latitude areas. He speculates that phytoplankton may create biogenic toxins, which when mixed with an already stressful anoxic environment, may have led to the demise of invertebrates, and likely even vertebrates like ichthyosaurs, living in shelf environments. Davies' supports this interpretation citing the lack of invertebrates, less than abundant traces, presence of bone beds, and present day phytoplanktonic blooms in mid latitudes.

In the Triassic, Doig phosphates represent an erosive submarine surface associated with a long periods of non-deposition (Wittenberg, 1992). These phosphates typify flooding surfaces, which help to designate parasequences to the formation. From a source

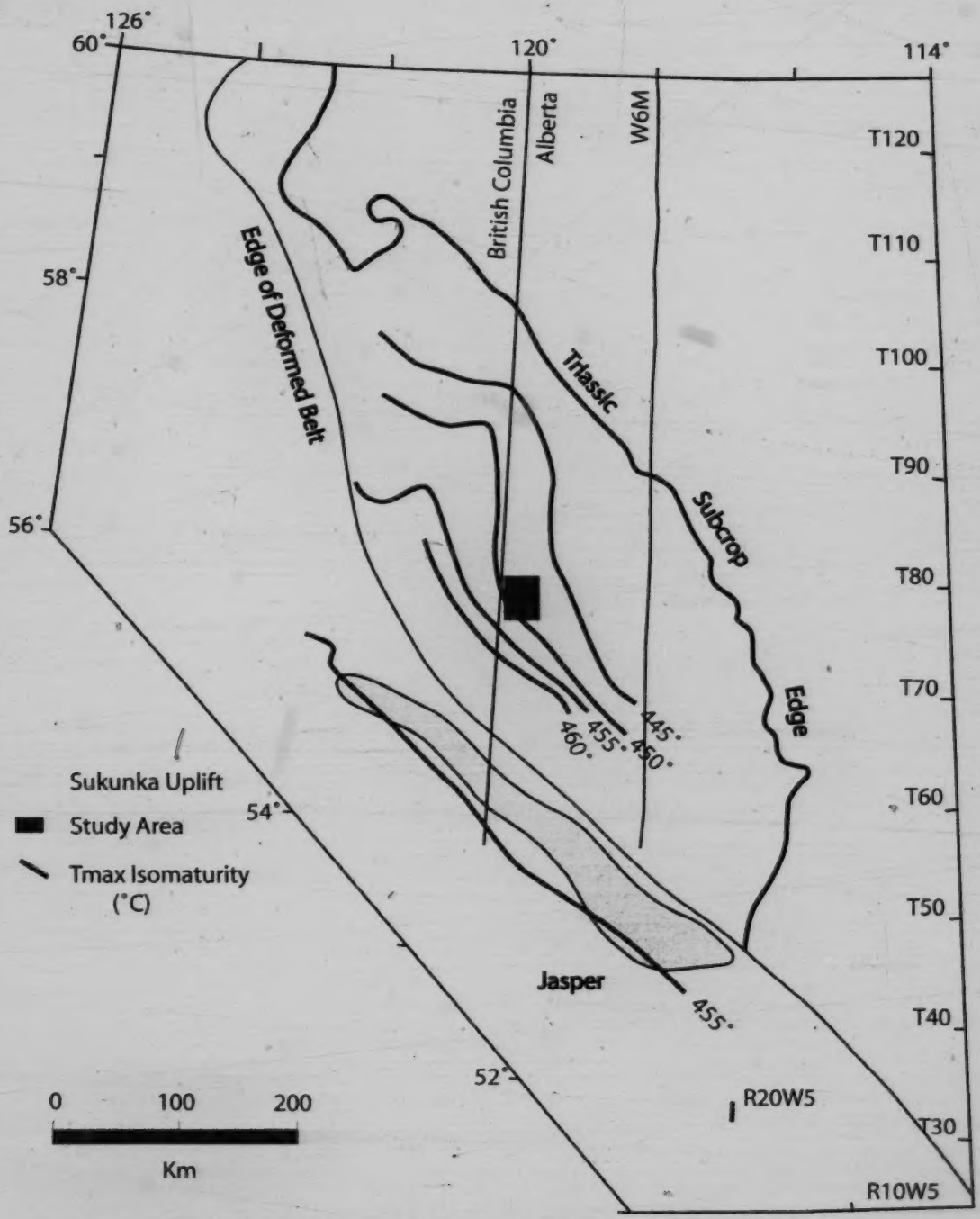


**Figure 18**. Map showing the study area in relation to Tmax thermal maturity based off Riedigers core and outcrop values (1997). Modified after Riediger (1997).

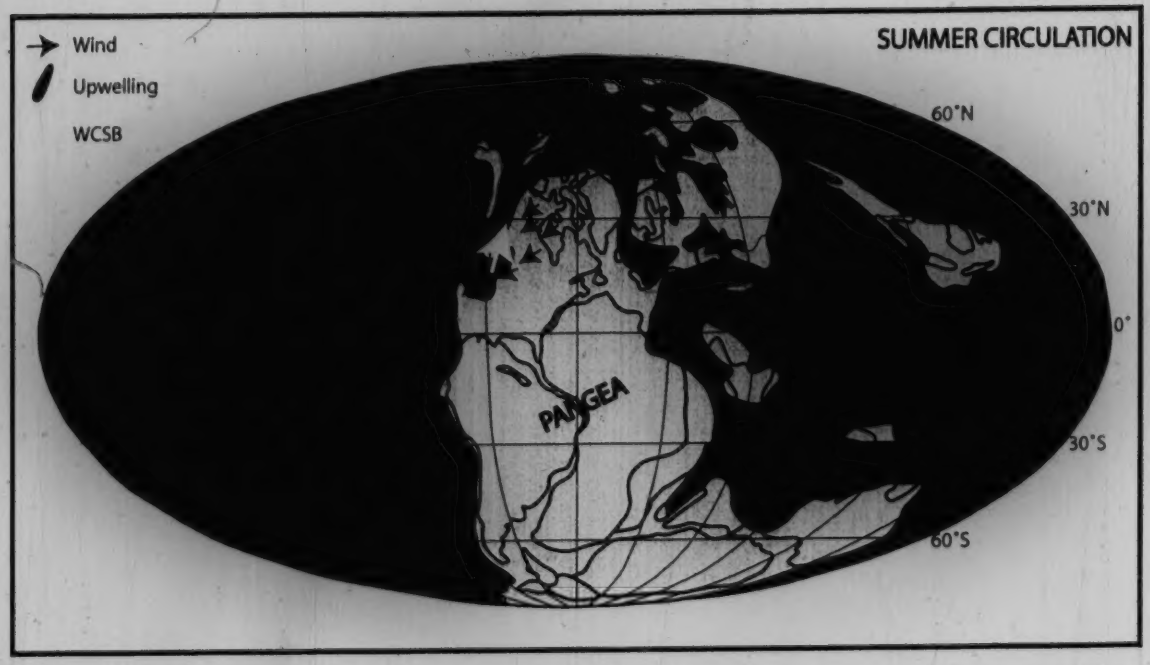


**Figure 19**: Early Triassic Paleogeography showing zones of upwelling in relation to wind direction and WCSB. Modified after Smith et al. (1995), Golonka et al. (1994), and Davies (1997a).

**Figure 20**. Modern analog of trade winds and coastal upwelling in relation to the formation of phosphate on western portions of coastal margins. Predominant phosphate formation is 30°N and 30°S latitudes, which would be similar latitude, and physical environment, to ancient Triassic of WCSB. Modified after numerous sources, including Sarnthein and Diester-Haass (1997) and Davies (1997a).

rock and correlative perspective, phosphate dispersion throughout sands can be both beneficial and problematic. If a significant amount of dispersed phosphates exist, the end result can be bypass of pay through misinterpretation (Davies, 1997a). Since phosphates require seawater for formation and seawater contains uranium, uranium is locked into the phosphates allowing the gamma ray log to interpret readings as shale as opposed to sand (Davies, 1997a).

## 1.10 METHODS AND OBJECTIVES

This project was undertaken in order to formulate a depositional model and stratigraphic history of the Triassic Moig Siltstone, Moig Sandstone, and Lower Doig Formation of northwestern Alberta. Interpretations will focus on sedimentary and ichnological analysis utilizing core from 16 wells at the Core Research Facility in Calgary. In order to arrive at depositional model, sedimentary structures and trace fossils will be placed into facies associations related to a depositional environment. In addition to this, geophysical well logs will be analyzed to develop maps and regional cross-sections. Where available core was used to define key stratigraphic surface that can be recognized on well logs.

These objectives are completed in chapters two and three. Chapter two resolves fifteen facies (F1-F11) constrained to three facies associations (SO, B, SS). Building off chapter two, chapter three reviews maps, cross-sections, stratigraphic history, and depositional models pertaining to well logs and core analysis. Finally, chapter four summarizes important aspects discussed in the previous chapters.

# CHAPTER TWO

## FACIES, FACIES ASSOCIATIONS, DISCRPTIONS AND INTERPRETATIONS

### 2.1 INTRODUCTION

Within the study area, cores were viewed and analyzed from the Moig Siltstone, Moig Sandstone and Lower Doig Formation. Lithology, sedimentology and ichnologic characteristics were documented. Based on observations of core, several different units were identified and separated into fifteen facies (Table 1). From these facies, three facies associations were derived: Facies Association SO (Facies 5a, 1, 2, 3 and 4) represents the Moig Siltstone structurally influenced offshore/shoreface transition to upper offshore deposits; Facies Association B (Facies 5b, 6, 7a and 7b) is characterized by the Moig Sandstone structurally controlled offshore/shoreface transition zone to proximal lower shoreface deposits; and Facies Association SS (Facies 5c, 5d, 8, 9, 10 and 11) contains the Lower Doig Formation shelf deposits. Facies associations can be described as genetically related strata (facies) grouped together to identify a depositional system. Further information on the three depositional models in relation to facies associations can be found in chapter three.

Davies et al (1997) had informally named the Gordondale Sandstone; however, to reduce confusion with the Jurassic Gordonale Member it will be referred to as the Moig Sandstone in this thesis. The following section discusses non-genetic and genetically related strata, my observations and possible depositional environments. All core logs can be found in appendix A.

| Facies Association | Facies | Lithofacies | Description | Ichnology | Interpretation | Sedimentary structures |
|---|---|---|---|---|---|---|
| SO | F1 | Tan to light brown siltstone and fg sand with light colored silty beds. | Burrows break planar to wavy bedded fg sands and silts with minor oscillation ripples. There are also some muds and organics. | Unrecognizable traces, Pl, Sc, Fu | Proximal offshore/ shoreface transition | Wavy beds, planar laminations, rhythmic beds, and rare oscillation ripples. |
| SO | F2 | Light black to dark grey siltstone with fg sand. | Massive appearing siltstone. | Ph | Distal offshore/ shoreface transition | Some planar laminations and massive bedding. |
| SO | F3 | Dark brown siltstone with fg sand. | Wavy to planar laminated siltstone with rhythmic beds. Very sparse bioturbation with some plant and animal material. | Pl, Lo, Sc, Fu | Storm dominated upper offshore | Wavy bedding, wave scours, pinch and swale planar laminations, and rhythmic bedding. |
| SO | F4 | Dark brown siltstone with fg sand. | Micro faulted and soft sediment deformed wavy to planar laminated siltstone with rhythmic beds. Very sparse bioturbation with some plant and animal material. | Pl, Lo, Sc, Fu | Strom and seismite dominated upper offshore | Wavy bedding, planar laminations, wave scours, pinch and swale, rhythmic bedding, micro faults, and convolute beds. |
| SO | F5a | Dark brown to black rudstone | Ooids, peloids, phosphate grains, minor bone fragments, fine-grained sands, silts, and mud. | Not seen | Transgressive surface of erosion | Lag deposit |
| B | F5b | Dark brown to black rudstone | Ooids, peloids, phosphate grains, minor bone fragments, fine-grained sands, silts, and mud. | *Glossifungites* surface with Rh, Sk, Th, Pl | Transgressive surface of erosion | Lag deposit |
| SS | F5c | Dark brown to black rudstone | Ooids, peloids, phosphate grains, minor bone fragments, fine-grained sands, silts, and mud. Sands and silts are preserved in relic beds. | Rh, Sc, Te in the sands | Transgressive surface of erosion | Lag deposit and thin relic sands. |
| SS | F5d | Dark brown to black rudstone | Ooids, peloids, phosphate grains, minor bone fragments, fine-grained sands, silts, and mud. Sands and silts are reserved in relic beds. | Rh, and Sc in the sands | Transgressive surface of erosion | Lag deposit and thin ribbon or relic sands. |
| B | F6 | Tan colored dolomitic lower fg sandstone | Mostly heavily horizontally burrowed fg sand with stylolites. Possibly once wavy bedding and deformed oscillation ripples. Can have a mottled look from cementation of burrows. | Te, He, Rh, Th, Ch, Ast, Pl, Pa, Ph, Sc | Proximal offshore/ shoreface transition | Stylolites, wavy bedding, and rare deformed oscillation ripples. |
| B | F7a | Grey to tan colored dolomitic lower fg sandstone | Heavily bioturbated sand by subvertical to horizontal mud lined burrows. Possible ripples, with stylolites. | Cy, Ast, Pa, Rh, Ch, Th, Pl, He, Ph, Te, Sc | Distal lower shoreface | Stylolites and deformed oscillation ripples. |

| | | | | | | |
|---|---|---|---|---|---|---|
| B | F7b | Grey to tan dolomitic lower fg sandstone | Heavily bioturbated sand with vertical to subvertical mud lined burrows with stylolites. | Di, Ro, Sk, Cy, Rh, Pl, Pa, He, Te | Proximal lower shoreface | Minor stylolites |
| SS | F8 | Black organic rich shale | Very black thin-bedded organic rich shale with pyrite. | Non seen | Anoxic sheltered shelf | Planar laminations |
| SS | F9 | Black Muddy siltstone (40% mud) | Massive to planar laminated black muddy siltstone. Moderately to heavily bioturbated. | Ph | Sheltered shelf with fluctuating oxygen levels. | Massive to planar laminated beds. Also some dish and pillar structures. |
| SS | F10 | Black muddy siltstone (30% mud) | Black muddy siltstone with deformed lenticular sandy/silty beds. Can have vertical anhydrite filled fractures. | Ph Th, Sc, Pl | Open shelf | Deformed lenticular bedding and sand ribbons. |
| SS | F11 | Black to dark grey sandy siltstone | Structures are deformed ripples with heavy bioturbation. There is also the presence of flame structures and dish and pillar. Can have vertical anhydrite filled fractures. | Ph, Th, Sc, Ph, Sk | Open shelf | Deformed ripples, flame structures, and dish and pillar. |

**Table 2.1** Facies and Facies Associations

## 2.2 FACIES DESCRIPTION AND INTERPRETATION

### 2.2.1 Facies F1: Heavily bioturbated silty sand

*Description:*

Facies F1 overlies Facies F5a and is overlain by Facies F2. When seen in core, thicknesses can be up to 4.08 meters. Tan to brown colored siltstone with rhythmic beds of alternating silt, minor very fine-grained sand and mud/organics represent Facies F1. Sand content can be up to 50 percent with the remainder of the grains comprised of silt and to a lesser extent mud. The silts tend to be white while mud/organics are black and when mixed by bioturbation this facies becomes tan to brown. The beds are deposited in rhythmites of mm to cm scale with wavy bedding, planar bedding and rare oscillation ripples. Found within this facies are minor organics, possibly both plant and animal. Rare occurrences include pyrite bands, which seem to follow the rhythmic beds.

About 70% of the beds have been broken by bioturbation with recognizable traces representing *Scolicia*, *Planolites* and cryptic bioturbation (Figure 2.1). It is possible that some of these traces are Fugicnia (escape structures) though the cryptic nature of these traces makes definitive identification difficult. *Scolicia*, *Planolites* and cryptic bioturbation resemble a stressed archetypal *Cruziana* ichnofacies.

*Interpretation:*

This particular facies was most likely deposited in a proximal offshore/shoreface transition zone. Similar to Facies F3, original deposition is from storm-derived sands that settled out of suspension as graded rhythmites. Bioturbation then destroyed original bedding in the transition zone so any possible wave generated structures were eradicated. A homogenous look at the transition zone can be seen in the Gulf of Gaeta where most of the original bedding is destroyed by *Scolicia* (Reineck and Singh, 1980). In the modern

**Figure 2.1. Facies F1**

**A)** Well 6-34-78-10W6 at a depth of 1835.9 m showing bioturbation of sediments by *Planolites* (Pl) and *Scolicia* (Sc). Notice the tan color once water is applied.

**B)** Well 15-31-77-11W6 at a depth of 2003.4 m showing bioturbation by *Scolicia* (Sc).

A
Pl
Sc
P.I.R.G.

B
P.I.R.G.
Sc

transition zone by the Yangtze subaqueous delta there are storm derived rhythmic units. Slightly proximal of these units are structureless fine-grained sediments that are heavily bioturbated (Zhanghua et al., 2005).

Since Facies F1 carries more sands than the overlying Facies F2 and F3 and it is part of a transgressive system and therefore deposition in a transition zone may be implied. As mentioned above this facies contains rhythmic beds from storm deposits, which have been recognized in other transition zones. Adding to this, a high degree of bioturbation by *Scolicia* was found to be common in the Gulf of Gaeta transition zone.

### 2.2.2 Facies F2: Dark grey massive sandy silt

*Description:*

Facies F2 is a light black to dark grey colored siltstone that overlays Facies F1 and underlies Facies F3. The thickness of this faces is on average .6 meters. Silt is the dominant sediment with up to 40% sand and minor mud. There are only spars planar laminations seen in this facies, other wise it has a massive appearance (Figure 2.2). In some situations small, vertical, sinuous mud lined burrows are present in large numbers.

It is likely that Facies F2 was completely bioturbated but due to the small size of the burrows and the homogeneous nature of the silts assessment can be difficult. The burrows as described above lend to the interpretation that these traces are of *Phycosiphon*. A stressed distal archetypal *Cruziana* ichnofacies may be represented by this singular trace.

*Interpretation:*

Facies F2 was deposited at the distal end of the offshore/shoreface transition zone. This interpretation is derived from the fact that there are less sand layers than seen in the underlying Facies F1, which contains proximal offshore/shoreface transition deposits.

**Figure 2.2. Facies F2**

**A)** Well 14-14-78-10W6 at a depth of 1848.4 m. Notice the homogenous massive appearance to this facies.

**B)** Once the image is zoomed in small sinuous mud lined burrows appear, which represents pervasive burrows of the traces *Phycosiphon* (Ph).

B
Pb
A
P.I.R.G.
Phinology Research Group

Furthermore, deposition in a distal transition zone can be inferred since it is part of a transgressive systems tract with F1 below and muddier F3 and F4 upper offshore deposits above.

One factor in generating the massive appearance results from deposition of a constant grain size through suspension fallout of hemipelagic sediments (Reineck and Singh, 1980). The massive appearance may also be caused by bioturbation destroying evidence of original bedding, or compaction, squeezing all the water out and in turn mixing the beds, or by a gas bubble moving through the layers (Forstner et al., 1968; Reineck and Singh, 1980). Core analysis revealed burrows, therefore it is possible that bioturbation by *Phycosiphon* has destroyed the original bedding. Even with the presence of traces dewatering still plays a role in this facies.

### 2.2.3 Facies F3: Rhythmic to wavy laminated sandy silt

*Description:*

Facies F3 in most cases overlies F1 and F2 and is interbedded with Facies F4. The thickness of this facies can range from cm scale up to 9.2 meters. Dark brown to black colored organic rich siltstone generally represents Facies F3. Most of F3 is comprised of silt and minor very fine-grained sands (up to 40%) that are white to light blue in coloration likely due to calcite cementation. Sedimentary structures are commonly rhythmic beds in mm to cm scale deposited in planar laminations, wavy laminations (hummocky cross-stratification) and low angle cross lamination (Figure 2.3). Also found in F3 are rare wave scours and erosional truncations. Similar to Facies F1, pyrite beds can be found following sands in rhythmic beds.

Bioturbation in F3 is rare with about 4% to 25% of the facies comprising bioturbated media. The only traces seen are: small sand filled burrows representing *Planolites*, *Lockeia*, fuzzy unrecognizable burrows of *Scolicia* and rare vertical escape

**Figure 2.3. Facies F3**

**A)** Well 3-22-78-10W6/4 at a depth of 1843.9 m. Here the Moig Siltstone unit shows rhythmic beds with low angle cross lamination (LA) and wavy bedding (WB).

**B)** Well 6-34-78-10W6 at a depth of 1828.9 m. This figure shows pyrite following rhythmic bedding, deformed beds (DF) and wavy bedding (WB).

**C)-D)** showing Rhythmic beds with erosional surfaces from wave scours (WS) and the occasional deformed bedding (DF). C) Well 6-34-78-10W6 at depth of 1829 m. D) Well 15-31-77-10W6 at a depth of 1994 m.

A
WB
LA
T.R.G.
Ichnology Research Group

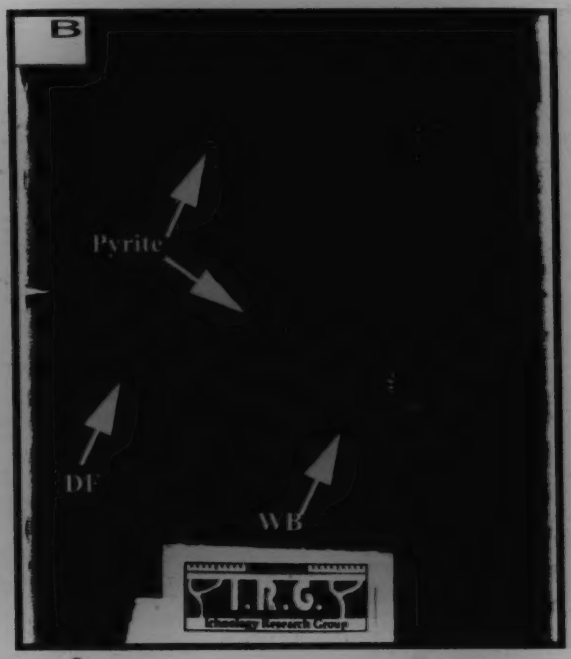
B
Pyrite
DF
WB
T.R.G.
Ichnology Research Group

C
WS
WS
T.R.G.
Ichnology Research Group

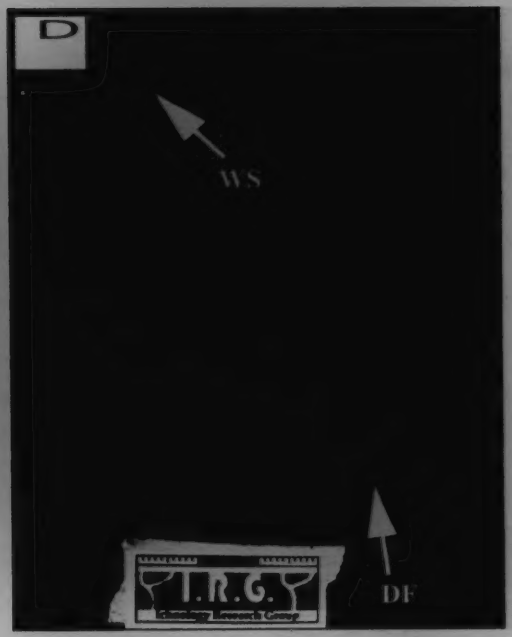
D
WS
DF
T.R.G.
Ichnology Research Group

traces (fugicnia). Burrows do not deeply penetrate and where mud has draped sandy beds bioturbation is not present. The overall bioturbation represents a stressed distal Cruziana ichnofacies.

*Interpretation:*

Facies F3 has ichnological and sedimentological features suggestive of storm deposit found in the upper offshore. Wave scours and rhythmic bedding preserved in planar and wavy laminations are common aspects of storm deposits (Reineck and Singh, 1980). Brenchley (1985) described storm beds forming below or around storm weather wave base (SWWB) as resembling parts A to D in the Bouma sequence; however, he states that storm deposits below SWWB are not as well organized as the Bouma A to D sequence of scoured base, plane parallel laminations, wavy laminations and laminated silts respectively. Facies F3 has disorganization of this sequence consistent with distal storm deposit.

When massive storms hit the study area large waves were generated causing the occasional scoured surface to form. Sands and silts were taken from nearshore regions and deposited in the offshore environment by retreating waves and ebb currents (Reineck and Singh, 1980; Dott, 1983). This offshore deposition occurs when there is a decrease in wave energy allowing sands to fall out of suspension creating laminated sands and silts, which settle atop the wave scour (Reineck and Singh, 1980; Johnston and Baldwin, 1986). Minor bioturbation occurs when there is a waning of the storm. Energy decreases and opportunistic feeding increases due to deposition of the food sources in the fine-grained low energy sediments (Pemberton et al, 2001). The stressed suite of distal *Cruziana* ichnofacies may represent either storm stresses or global/local anoxia at the time of colonization.

### 2.2.4 Facies F4: Deformed sandy silt

*Description:*

Facies F4 is found interbedded with Facies F3 and is overlain by Facies F5b. On average the thickness of Facies F4 in core is 1.5 meters with a maximum of 8.9 meters. The coloration, ichnology, organics, sediments and sedimentary structures are the same as the above-described Facies F3. The main distinguishing feature between the two facies is the presence of: convolute beds, disturbed laminations and microfaults throughout Facies F4, which are separated by nondisturbed beds of Facies F3 (Figure 2.4). There is also an increase in muds and silts moving up in the core until it culminates with Facies F5b.

*Interpretation:*

Similar to Facies F3, Facies F4 was deposited in a storm dominated upper offshore environment; however, there appears to be a significant amount of tectonic activity during deposition. This activity was preserved in syndepositional microfaults, convolute beds and disturbed laminations. These were preserved on beds with relatively shallow dip; therefore it is possible that slope instability was not a major generating factor.

Syndepositional and metadepositional microfaults, along with softsediment deformation features associated with tectonic activity, were described by Mazumder et al., (2006). In their study of the Chaibasa Formation it was recognized that: these seismites where deposited in discrete stratigraphic intervals, deformation structures persisted over a kilometer in distance, there was reoccurrence of deformation over time, and undeformed layers confined seismite layers. These same tectonically induced features have been described by Sims, 1975; Seilacher, 1984; Obermeier, 1996; and Jones and Omoto, 2000.

Facies F4 contains microfaults with angles of less than 45 degrees. This

**Figure 2.4. Facies F4**

**A)** This image shows seismites with convolute bedding (CB) and microfaults (MF). Well 6-34-78-10W6 at a depth of 1832.1 m.

**B)** Organics are a common element of facies F4. In well 6-34-78-10W6 at a depth of 1848.8 m there is a bone possibly an ichthyosaur vertibra.

**C)-D)** Facies F4 has isolated horizons of seismites containing semilithified fractures (SF), microfaults (MF) and wave scours (WS) from possible storm erosion. C) Well 15-31-77-10W6 at a depth of 1834.7 m. D) Well 15-31-77-10W6 at a depth of 1895.2 m.

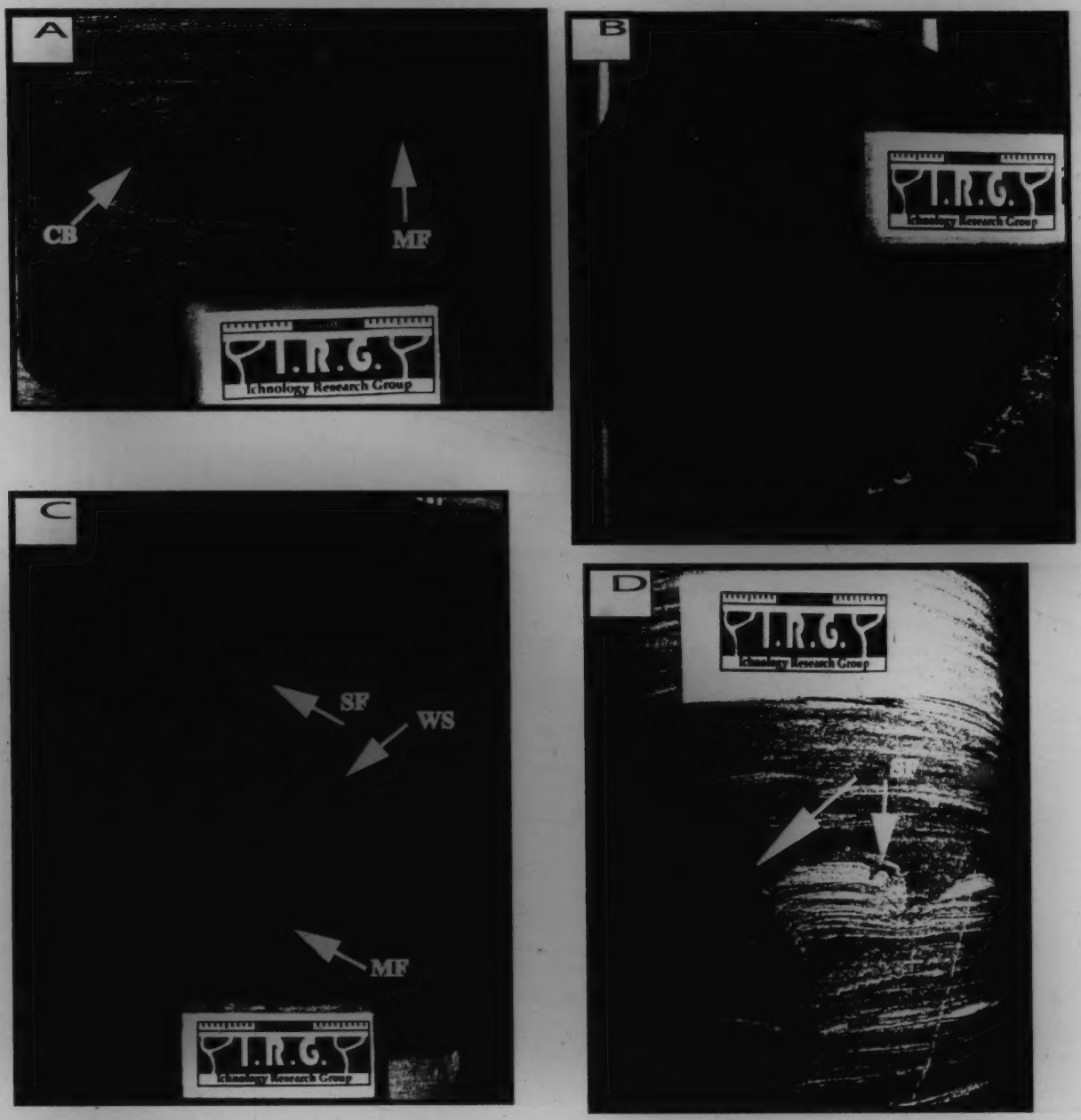
A
CB
MF
B
C
SF
WS
MF
D

microfaulted facies can be contained within the undeformed Facies F3. The reoccurrence of microfaults throughout depositional time over a large area also represents Facies F4. In some cases microfaults appear to have been broken or pulled apart and the overlying layers were unaffected. This would imply that there was some consolidation and semilithification of the sediments before faulting. A significant amount of force would be needed to break the semilithified beds. This suggests the microfaults are earthquake-induced. Microfaults also appear to be stacked in sets; this may reflect a series of seismic shocks related to earthquakes. These earthquakes would have been generated by reactivation of the Paleozoic structures. Soft-sediment deformation such as convolute beds and disturbed laminations may also be the result of semiliquified sediment disturbed by seismic events (Mazumder et al., 2006). These soft-sediment structures are also present in Facies F4.

### 2.2.5 Facies F5: Lag deposits

Facies F5 is representative of lag deposits relating to four transgressive events. The transgressive lag deposits of this facies type contain phosphatized bones, ooids and peloids. Adding to this, anhydrite, pyrite and calcite are the dominant minerals present in visible proportions. The formation of these surfaces/facies occurred in the same transgressive manner so only one interpretation for the four F5 facies types is needed.

### 2.2.5a Facies F5a: Lag deposit

*Description:*

Facies F5a has an average thickness of 6 cm. This particular facies rests atop very fine-grained hummocky cross stratified beds of the Montney Formation and is overlaid by Facies F1. The coloration is dark brown to black rudstone comprised of ooids, peloids,

phosphate grains, minor bone fragments, fine-grained sands, silts and mud (Figure 2.5a). There is no distinct sedimentary structures that can be described in this facies. Despite this a lag deposit is the closest sedimentary classification. The main minerals visible to the naked eye in Facies F5a are calcite, pyrite and anhydrite cements.

There is no bioturbation seen in this facies, nevertheless the presence of ichnotaxa cannot be ruled out.

*Interpretation:*

All Facies F5 types are transgressive surfaces of erosion that occur at the base of or within the transgressive systems tract. Erosional surfaces are created by wave erosion at the shoreface during times of sea level rise (Swift, 1968). This rise in sea level reworks old and newly deposited sediments only if there is moderate to high wave energy (Cattaneo and Steel, 2003). These wave energies are typically found at depths down to fair-weather wave base (~ 10 m). In some cases storm dominated areas may have significantly deeper erosional capabilities (Thorne and Swift, 1991). Overlying the erosional surfaces are lag deposits containing ooids and peloids representative of shallower water depositional environments (Prothero and Schwab, 2003). These were emplaced into the lag deposit upon transgression. The large regional extent of these surfaces coupled with the limited depth these surfaces can form on would imply a shallow topographic gradient across the study area.

### 2.2.5b Facies F5b: Lag deposit

*Description:*

Facies F5b is on average a 3 cm thick lag that rests atop F4 and is overlain by F6 (Figure 2.5b). The coloration is dark brown to black rudstone comprised of ooids, peloids, phosphate grains, minor bone fragments, fine-grained sands, silts and mud. It is

**Figure 2.5a. Facies F5a**

**A)-B)** Well 15-31-77-10W6 at a depth of 2006.55 m. This facies is transgressive lag deposit resting atop the Montney Formation and overlain by the Moig Siltstone. Notice the presence of ooids, peloids, and bone fragments.

A
B
S.I.R.G.S.

gradational with Facies F6 sands, which contain some organics distributed throughout the lower parts by bioturbation. There is a strong presence of calcite and anhydrite cements along with minor bands and blotches of pyrite.

The main distinguishing feature of F5b is the amount of bioturbation. F5b is heavily bioturbated by suspension feeders (SF) and deposit feeders (DF) such as *Skolithos* (SF), *Rhizocorallium* (DF), *Planolites* (DF) and *Thalassinoides* (DF). In some cores burrowing goes 10 cm below the base of the phosphate zone into the underlying Moig Siltstone facies. This is referred to as a *Glossifungites* ichnofacies (c.f. Pemberton et al., 2001).

*Interpretation:*

Found at the base of the Moig Sandstone is a lag deposit (Facies F5b) associated with a *Glossifungites* surface. The lag deposit consists of ooids, peloids, phosphate grains, and some bone fragments delineating a transgressive surface of erosion. Adding to this interpretation of a key stratal surface is the presence of a *Glossifungites* surface seen by *Skolithos*, *Rhizocorallium*, and *Thalassinoides*, penetrating to a depth of 10 cm through the underlying silty sands of the SO Facies Association. The burrows show no cross cutting of sedimentary grains so the interpretation of a frimground as apposed to a hardground substrate is derived. The burrows are infilled with very fine- grained sands, ooids, phosphate grains, peloids, and some bone fragments. This would imply that the lag deposit formed penecontemporaneous to the colonized surface and when the trace maker left, lag deposits and sands infilled the burrows.

Historically the *Glossifungites* ichnofacies is substrate controlled and represents a setting where a firm ground or palimpsest softground assemblage has been dewatered and compacted by erosional exhumation representing erosional discontinuities (Pemberton et al., 2001). Preceding this, colonization under marine conditions by dominantly vertical to subvertical suspension feeding and dwelling organisms typical

of *Diplocraterion*, *Skolithos*, *Psilonichnus*, *Arenicolites*, and *Gastrochaenolites* occurs (Pemberton and Frey, 1985). The presence of deposit feeding organisms can also be found in horizontal to subhorizontal dwelling structures commonly of *Rhizocorallium*, *Zoophycos*, *Thalassinoides*, *Taenidium*, and *Spongeliomorpha* (MacEachern and Burton, 2000). Typically traces are of low diversity and high abundance with robust (0.5-1cm in diameter), deep penetrating burrows (20-100cm) (Pemberton et al., 2004). Following colonization is passive infilling of the burrowed substrate by courser material. Presence of the colonization after erosion and exhumation represents a depositional hiatus followed by a later stage of sediment infill therefore representing a significant sequence stratigraphic surface (Pemberton et al., 2001).

There are a number of ways that the *Glossifungites* ichnofacies can be applied to depositional settings and stratigraphy. In a depositional context the *Glossifungites* surface can form wherever there is erosional exhumation of unlithified, firm or palimpsest softground assemblages available for colonization in marine conditions and later passive infill of sediments. This can occur in a number of environments represented by erosive shoreface retreat, coastal erosion, submarine channels, meandering tidal channels, channel migration, and valley incision (MacEachern and Pemberton 1992; Pemberton et al., 2001). In a stratigraphic context the *Glossifungites* surface may be found in regressive surfaces of erosion (RSE) below forced regressive shorefaces, sequence boundaries (SB) underlying lowstand shorefaces, SB for estuarine mouths of incised valleys prior to transgressive infill, SB for submarine canyon margins, and transgressive surfaces such as marine flooding surfaces and low relief transgressive surfaces of erosion (Pemberton et al., 2004). The most common manner of preserving this substrate controlled ichnofacies is through the formation of transgressive surfaces of erosion (Pemberton et al., 2004).

As described above this Facies F5b is created by erosional exhumation of unlithified, firm or palimpsest softground assemblages available for colonization in marine conditions and later passive infill of sediments thus creating a sequence boundary.

**Figure 2.5b. Facies F5b**
**A)-C)** This facies represents a transgressive surface of erosion with an associated lag deposit and *Glossifungites* surface. Notice the presence of pyrite, calcite plus anhydrite (white minerals). Typical traces are *Thalassinoides* (Th), *Skolithos* (Sk), *Planolites* (Pl), and *Rhizocorallium* (Rh). The base of this surface contains the Moig Siltstone, which is overlain by the Moig Sandstone. A) Well 4-2-79-10W6 at a depth of 1806.59 m. B) Well 6-34-78-10W6 at a depth of 1826.32 m. C) Well 6-16-78-10W6 at a depth of 1864.5 m.

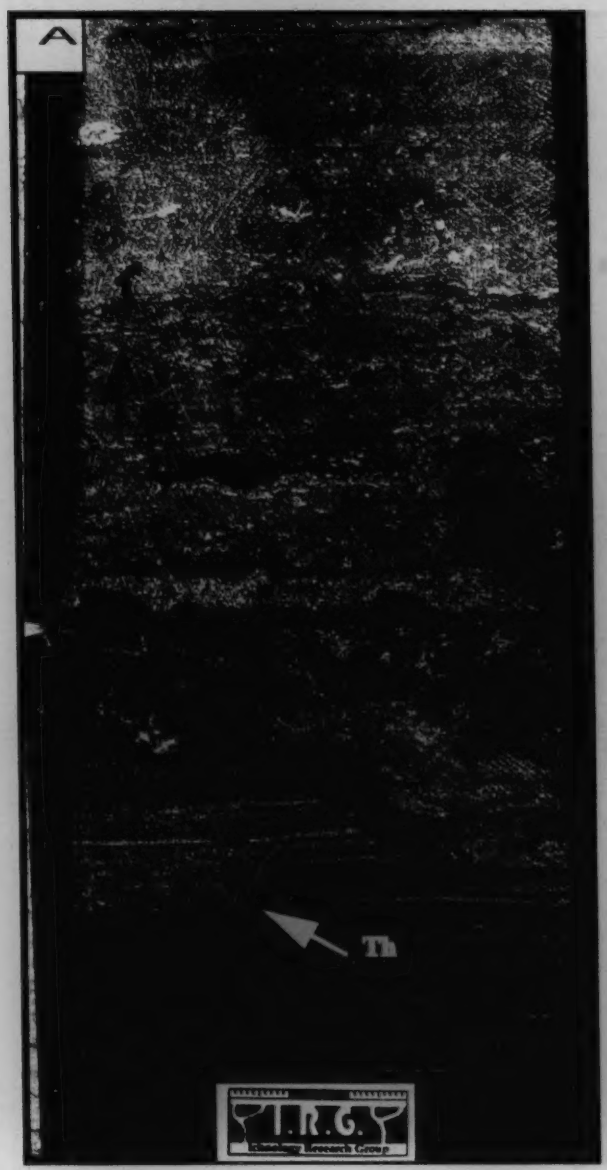
A
Th

B
Sk
Rh

C
Th
Pl
Rh

Here the *Glossifungites* surface formed in four steps; 1) deposition of Facies Association SO by transgression, 2) erosion by a commencing of the transgressive event (TSE), 3) depositional hiatus allowing the formation of lag deposits and colonization by *Skolithos*, *Rhizocorallium*, and *Thalassinoides*, and 4) progradation of the Moig Sandstone overtop of colonized surface consequently passively infilling the burrowed surface with sand and lag material.

### 2.2.5c Facies F5c: Lag deposits

*Description:*

Facies F5c found at the base of the Lower Doig Phosphate Zone overlies Facies F6, F7a, or F7b. Above Facies F5c is the Lower Doig Facies F8, F5d, or F9. The thickness is 6 cm to 30 cm with an average of 15.5 cm. Coloration is very dark black rudstone with large amounts of bone fragments, phosphate grains, ooids and more minor amounts of fine-grained sands and silts (Figure 2.5c). There is a large amount of calcite and anhydrite cements with pyritized materials. Like the other lag deposits there are no sedimentary structures and in most cores bioturbation is not present.

There are two cores where a thin 9 cm thick fine-grained sand is mixed with the top of F5C lag deposit. Here the sands are from scouring of the Moig Sandstone upon transgression. This sand is mixed into the lag deposit by intense bioturbation by *Rhizocorallium* and *Scolicia* ichnotaxa.

### 2.2.5d Facies F5d: Lag deposits

*Description:*

Facies F5d is a black rudstone lag deposit overlying Facies F5c, F8, or F9. Overlying facies F5d is facies F9 or F10. F5d is considerably thinner than F5c with

**Figure 2.5c. Facies F5c**

**A)** This image shows the erosional contact with the Moig Sandstone and facies F5c above. Notice the lag deposit containing bone and ooids (Oo). Well 4-2-79-10W6 at a depth of 1800.59 m.

**B)** Occasionally in facies F5c sands from the erosional scoured Moig Sandstone unit are incorporated into the lag deposit. These sands are heavily bioturbated by *Rhizocorallium* (Rh) and *Scolicia*. Also present are more bones and ooids (Oo). Well 6-34-78-10W6 at a depth of 1819.98 m.

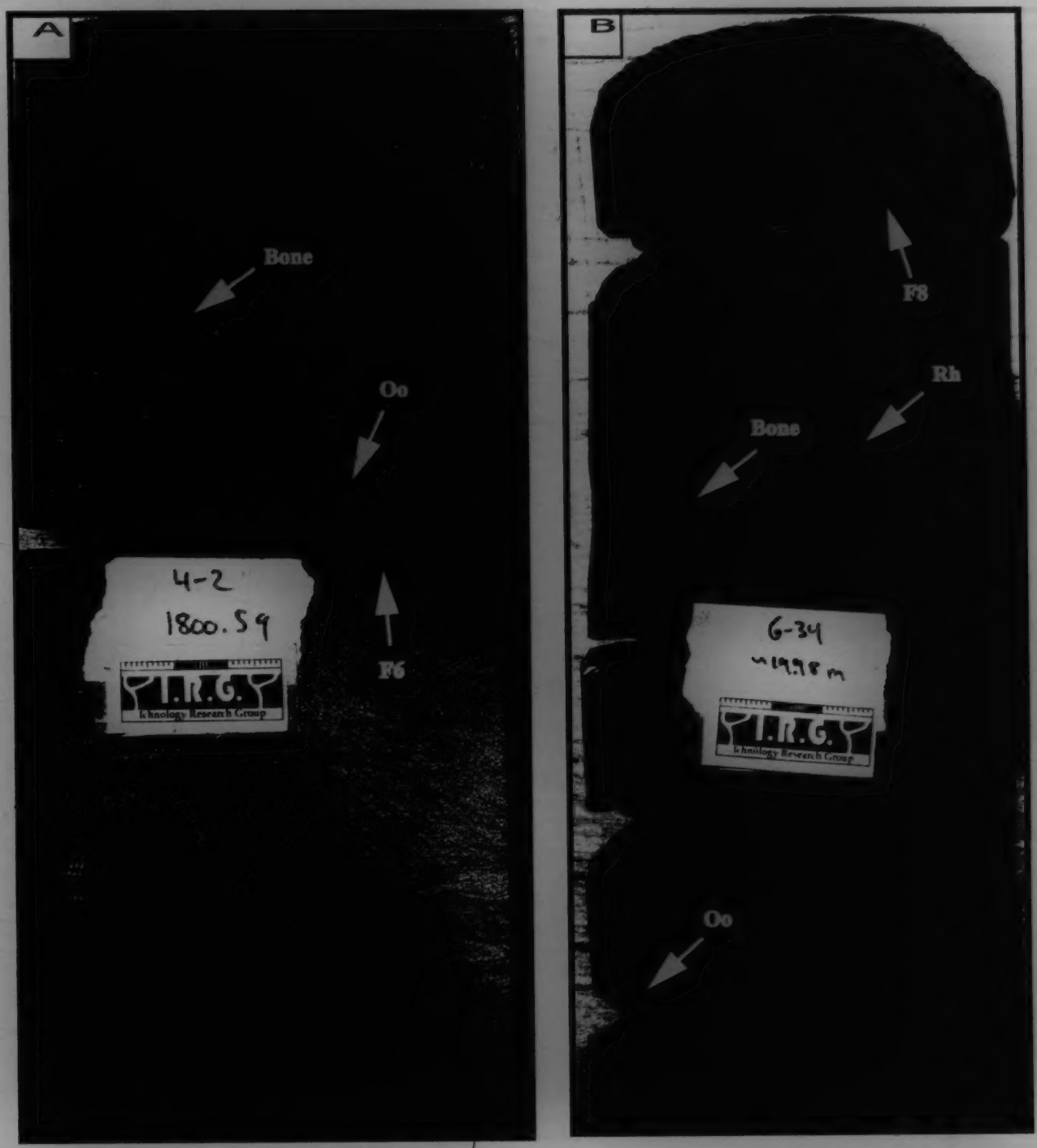
A
Bone
Oo
4-2
1800.59
F6
T.R.G.
Technology Research Group
B
F8
Rh
Bone
6-34
~19.98 m
T.R.G.
Technology Research Group
Oo

a thickness of 1 cm to 6 cm with an average of 3 cm. This Facies F5d rudstone is comprised of bone fragments, phosphate grains and peloids (Figure 2.5d). In some cores the occasional peloid has siderite or is coated in pyrite. Other visible minerals are calcite and anhydrite cements.

There is one core where a thin 15 cm thick fine-grained sand is mixed with the top of F5d lag deposit. Similar to Facies F5c, the sand is from scouring of the Moig Sandstone or reworked Upper Doig deposits. This sand is mixed into the lag deposit similar to F5c via intense bioturbation through *Rhizocorallium* and *Scolicia* ichnotaxa.

### 2.2.6 Facies F6: Heavily bioturbated mottled sandstone

*Description:*

The base of F6 is represented by F5b lag deposit and is overlain by F7a, F7b, or F5c. In core 6-16-78-10W6 the top of Facies F6 is represented by a .6 meter thick zone of muddy wavy beds with virtually no bioturbation. F6 thickness can range from 20 cm to 6.04 meters with an average of 2.46 meters. Generally Facies F6 is comprised of tan very fine-grained dolomitic sandstone. Mud represents up to 25% with an overall decrease in mud up through this facies. Sedimentary structures are extremely rare given that intense bioturbation eradicates original bedding. There is only minor preservation of stylolites and rare occurrences of what appear to be wavy bedding and deformed oscillation ripples. The mottled appearance of this facies is derived from calcite and anhydrite cements following bioturbated media (Figure 2.6).

From an ichnological perspective, almost all of the original bedding has been overprinted by fecal pellets and horizontal burrows from deposit feeders (DF), systematic grazers (SyG), and dwelling burrows (DS). The dominant ichnotaxa are *Scolicia* (DF), *Planolites* (DF), *Palaeophycus* (DS), *Thalassinoides* (DF), *Chondrites* (DF), *Helminthopsis* (SyG), *Phycosiphon* (SyG), *Teichichnus* (DF), *Rhizocorallium* (DF),

**Figure 2.5d. Facies F5d**

**A)** Core shot of facies F5d overlying facies F5c and F8 respectively. This is a phosphate rich zone with ooids (Oo). Well 6-16-78-10W6 at a depth of 1858.79 m.

**B)** This is one of the more significant erosional surfaces above facies F5c in the Lower Doig unit. Notice the presence of fine-grained sand, anhydrite cements (white), sideritised peloids (Pi) and phosphate (P). Well 2/7-26-78-10W6 at a depth of 1808.5 m.

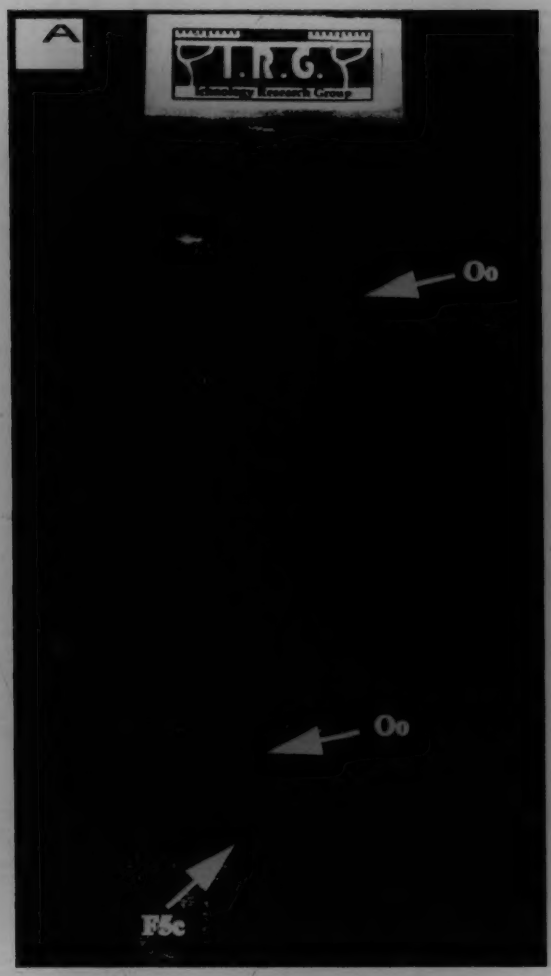
A
Oo
Oo
Fsc

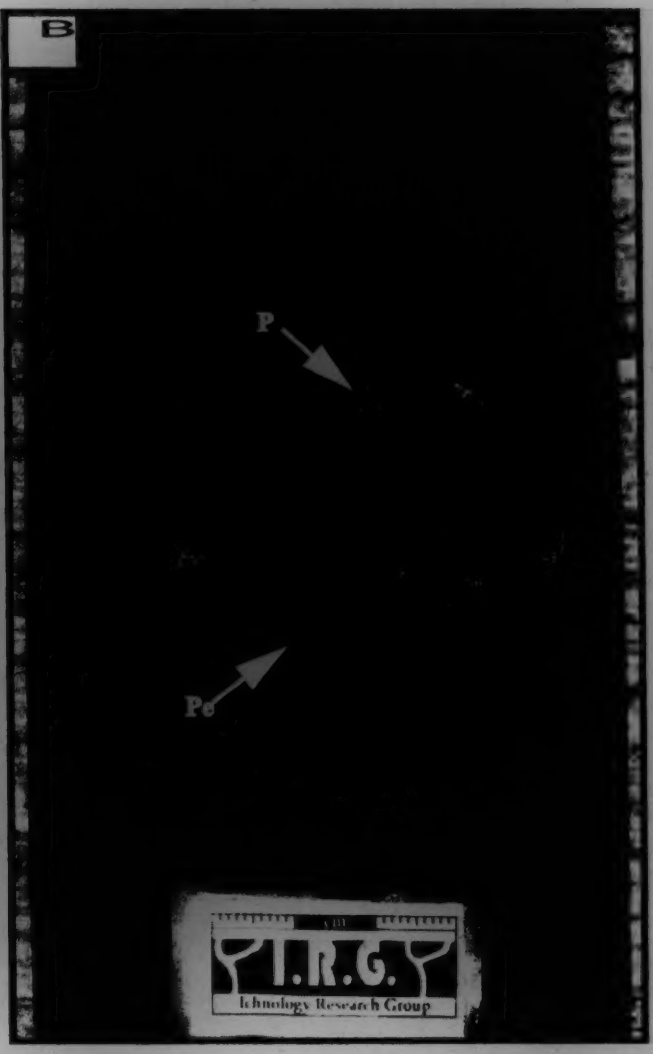
B
P
Pe

**Figure 2.6. Facies F6**

**A)** This image shows the contact with facies F5b and the Moig Sandstone (facies F6). Notice the heavily bioturbated sands with a mottled look from calcite cements following the bioturbated media. Well 14-15-78-10W6 at a depth of 1844 m.

**B)-D)** Typical high abundance high diversity suite of trace fossils erasing most of the sedimentary structures. Traces are typically *Rhizocorallium* (Rh), *Asterosoma* (As), *Helminthopsis* (He), *Chondrites* (Ch), *Scolicia* (Sc), *Planolites* (Pl), *Thalassinoides* (Th), and *Phycosiphon* (Ph). B) Well 2/7-26-78-10W6 at a depth of 1811.19 m. C) Well 6-34-78-10W6 at a depth of 1821.59 m. D) Well 4-2-79-10W6 at a depth of 1802.6 m.

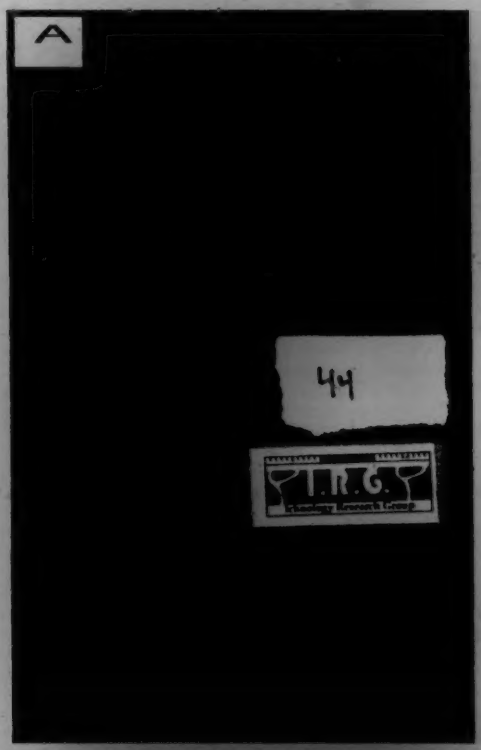
A
44
T.R.G.

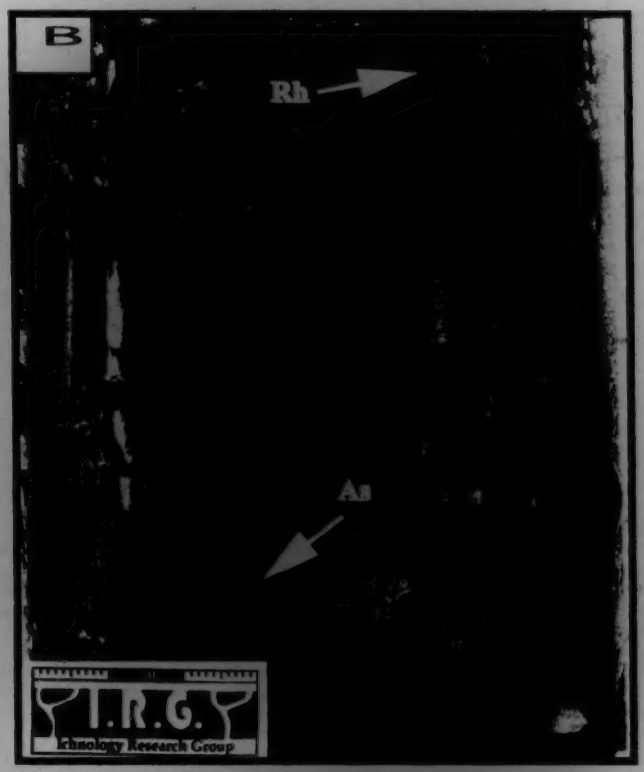
B
Rh
As
T.R.G.
Rhnology Research Group

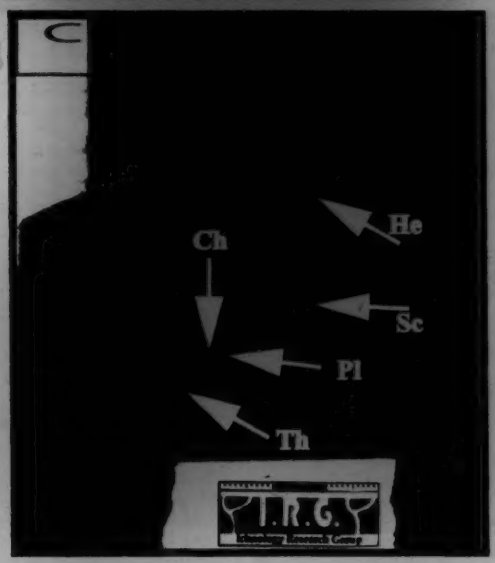
C
Ch
He
Sc
Pl
Th
T.R.G.

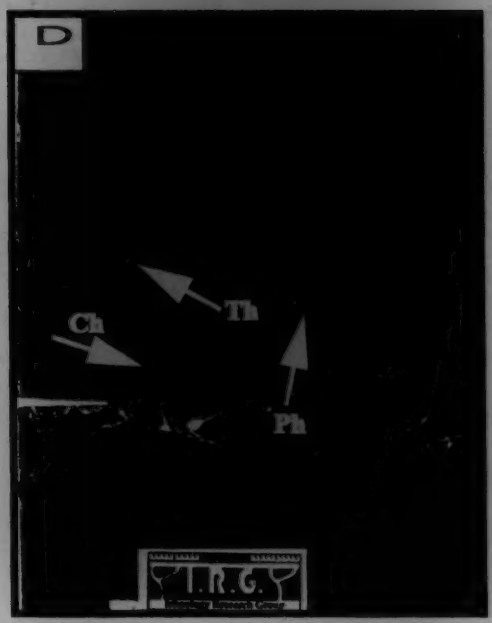
D
Ch
Th
Ph
T.R.G.

and *Asterosoma* (DF). All ichnotaxa represent a diverse suite of archetypal *Cruziana* ichnofacies.

*Interpretation:*

The diverse suit of traces associated with predominantly horizontal burrows of deposit feeding organisms suggests a community of archetypal *Cruziana* ichnofacies (Frey and Pemberton, 1985; MacEachern et al., 2007). The overall lack of sedimentary structures due to complete bioturbation of a high diversity and high abundance *Cruziana* ichnofacies suggests deposition in a location with uniform rates of sedimentation, bottom water conditions, and minimal turbidity currents (Moslow and Pemberton, 1988). These conditions are typical in shallower waters below daily wave base but above storm weather wave base or in deeper quieter waters (Frey and Pemberton, 1985). When sedimentary structures are preserved they represent wavy bedding and possible deformed wave ripples. These sedimentary structures may represent storm layers (Reineck and Singh, 1980). Considering the overall parameters deposition in an offshore/shoreface transition zone is possible.

### 2.2.7 Facies F7a: Heavily bioturbated very fine-grained sand

*Description:*

Facies F7a can be found atop Facies F6 and is overlain by Facies F7b or F5c. The thickness of Facies F7a ranges from 10 cm to 3.15 meters with a mean of 1.19 meters. Coloration is the same as F6 or F7b with a grey to tan color represented in the very fine-grained dolomitic sandstone. Mud comprises 20 % of Facies F7a with a decrease in composition upwards in this facies. Sedimentary structures are rarely preserved given that bioturbation is extreme leaving behind the occasional wavy parallel bedding along with some stylolites. Similar to Facies F6 and F7b there can be a mottled look to the interval,

**Figure 2.7a. Facies F7a**

**A)-D)** Facies F7a contains a diverse suite of trace fossils with the presence of some vertical and horizontal burrows. The dominant traces in the photos are *Rhizocorallium* (Rh), *Asterosoma* (As), *Helminthopsis* (He), *Chondrites* (Ch), *Scolicia* (Sc), *Planolites* (Pl), *Thalassinoides* (Th), *Cylindrichnus* (Cy), *Teichichnus* (Te), *Palaeophycus* (Pa) and *Phycosiphon* (Ph). A) Well 6-16-78-10W6 at a depth of 1863.8 m. B) Well 6-16-78-10W6 at a depth of 1861 m. C) Well 14-14-78-10W6 at a depth of 1838 m. D) Well 6-16-78-10W6 at a depth of 1863.8 m.

A
Rh
As

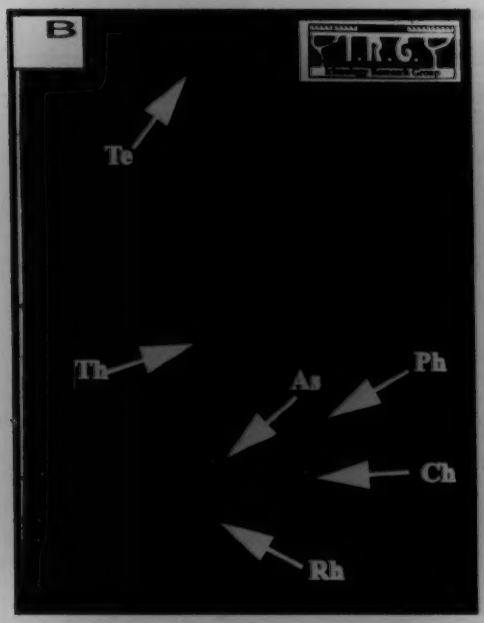
B
Te
Th
As
Ph
Ch
Rh

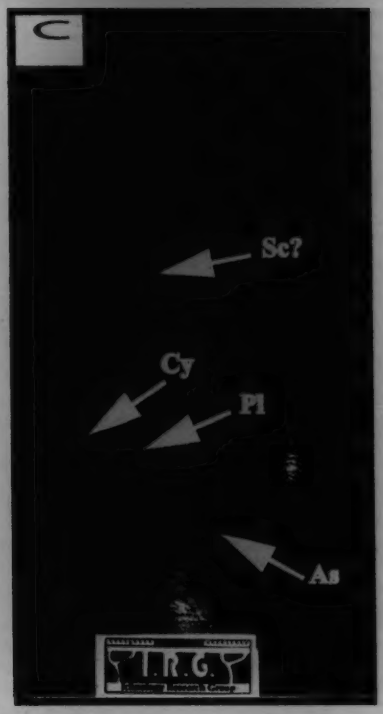
C
Sc?
Cy
Pl
As

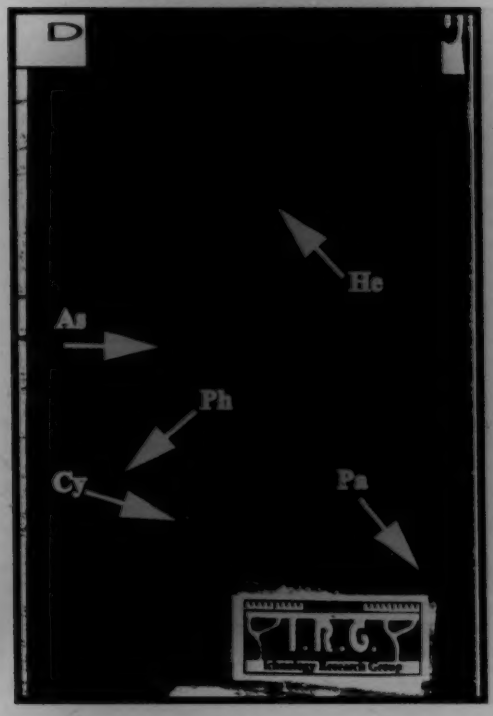
D
He
As
Ph
Cy
Pa

which represents calcite and anhydrite cements following bioturbated texture.

Dominant ichnotaxon of this facies are vertical to subvertical deposit feeding (DF) and suspension feeding (SF) traces representing a diverse array of archetypal *Cruziana* ichnofacies. Typical traces are *Teichichnus* (DF), *Cylindrichnus* (SF), *Rhizocorallium* (DF), as well as horizontal traces of deposit feeders (DF), systematic grazers (SyG), and dwelling burrows (DS) such as *Chondrites* (DF), *Planolites* (DF), *Palaeophycus* (DS), *Thalassinoides* (DF), *Asterosoma* (DF), *Helminthopsis* (SyG), and *Scolicia* (DF) (Figure 2.7a).

*Interpretation:*

Similar to Facies F6, Facies F7a has complete bioturbation removing previously deposited sedimentary structures. The presence of vertical, inclined, and horizontal structures as well as a diverse assemblage of trace fossils exemplifies the archetypal *Cruziana* ichnofacies (Frey and Pemberton 1985; MacEachern et al., 2007). The presence of some vertical to inclined *Cylindrichnus* and *Rhizocorallium* traces may be explained by a moderate increase in energy from shallowing of the overall depositional system. This shallower environment dominated by *Cruziana* ichnofacies may be found in a distal lower shoreface zone. Typically sedimentary structures found within the *Cruziana* ichnofacies are oscillation ripple laminated sands, and low angle, undulatory, parallel and subparallel laminations (Frey and Pemberton, 1985; Pemberton et al., 2001; MacEachern et al., 2007). In this facies only vary rare wavy or undulatory laminations are seen and may be interpreted as hummocky cross-stratification (HCS) and deformed wavy bedding. Brenchley (1985) described HCS as forming in a shallow marine storm dominated environment, which may equate in this unit to the distal lower shoreface.

### 2.2.8 Facies F7b: Heavily bioturbated with vertical and horizontal burrows

*Description:*

Facies F7b is only preserved in two cores. This facies is found atop and below Facies F6 and has a mean thickness of 1.77 meters. The presence between two F6 Facies possibly represents a shift back to deeper water facies or a reduction in wave energy. F7b is a grey to tan colored very fine-grained dolomitic sandstone with 10 % mud mostly preserved in burrows and stylolites. Like Facies F7a, all sedimentary structures have been over printed by intense bioturbation leaving only stylolites. Cementing is similar to the other facies in this association with a mottled look due to calcite and anhydrite cements.

Ichnology of Facies F7b is slightly different than Facies F7a. In Facies F7b, most of the ichnotaxa are vertical to subvertical mud lined burrows of *Rosselia* (DF), *Skolithos* (SF), *Cylindrichnus* (SF), and *Diplocraterion* (SF), with lesser amounts of *Teichichnus* (DF), *Rhizocorallium* (DF), *Palaeophycus* (DS), *Planolites* (DF) and possible *Helminthopsis* (SyG). This suite may represent an expression of the proximal *Cruziana* ichnofacies (Figure 2.7b).

*Interpretation:*

Facies F7b is the last prograding sand found within facies association B. Complete bioturbation of the sand yet again implies uniform rates of sedimentation, bottom water conditions, and very minor turbidity currents (Moslow and Pemberton, 1988). These conditions may also apply to a weekly storm influenced shoreface (Howard and Reineck, 1981). The presence of vertical suspension feeding organisms implies that there was a higher level of energy than F6 or F7a. Because of the higher energy levels organisms would have to burrow vertically to ensure stable life habits (Seilacher, 1964). Low diversity and high abundance of suspension feeding organisms (*Skolithos*, *Diplocraterion,* and *Cylindrichnus*) are typical of the *Skolithos* ichnofacies in shoreface

**Figure 2.7b. Facies F7b**

**A)-D)** Facies F7b is dominated by vertical traces with some cryptic horizontal traces. In these photos dominant traces are *Diplocraterion* (Di), *Cylindrichnus* (Cy), *Palaeophycus* (Pa), *Rosselia* (Ro) and *Cylindrichnus* (Cy). Plate C shows the bedding plane with vertical *Diplocraterion* (Di) and *Rosselia* (Ro). A) 6-16-78-10W6 at a depth of 1862.6 m. B) 6-16-78-10W6 at a depth of 1863.2 m. C) 6-16-78-10W6 at a depth of 1862.6 m. D) Well 3-22-78-10W6/4 at a depth of 1834.9 m.

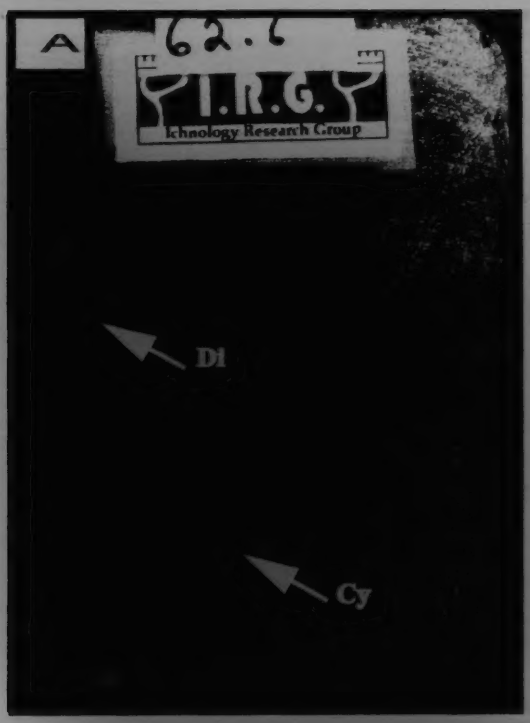
A
62.6
T.R.G.
Technology Research Group
Di
Cy

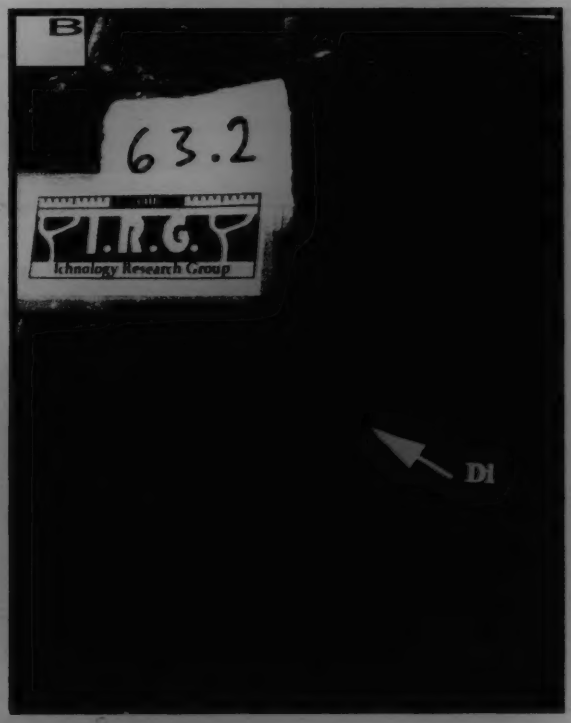
B
63.2
T.R.G.
Technology Research Group
Di

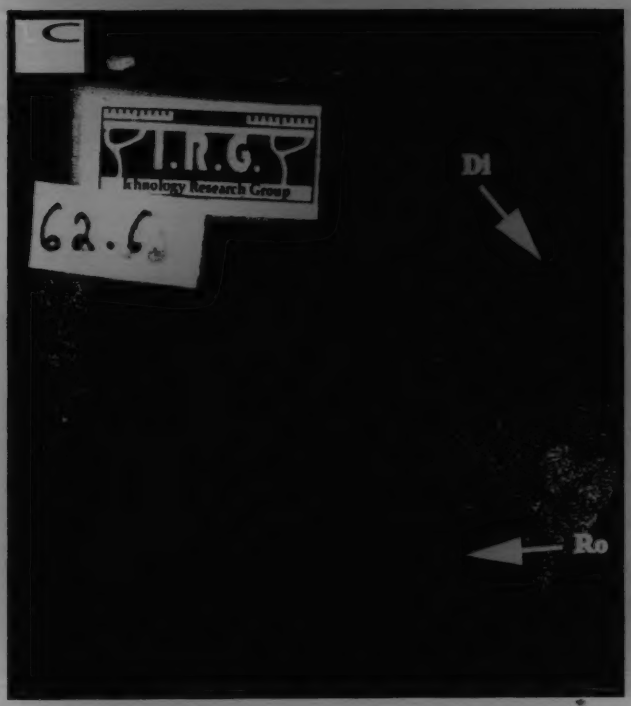
C
T.R.G.
Technology Research Group
62.6
Di
Ro

D
T.R.G.
Technology Research Group

to sheltered foreshore environments (Pemberton et al., 2001; MacEachern, 1994). However, the presence of mixed *Cruziana* ichnofacies (*Teichichnus*, *Rhizocorallium*, *Palaeophycus*, *Planolites*, and possible *Helminthopsis*) allows for the interpretation of proximal lower shoreface sands in a proximal *Cruziana* setting (Pemberton et al., 2001).

### 2.2.9 Facies F8: Organic rich black shale

*Description:*

Facies F8 is a highly organic vitrinite rich black fissile shale. Typically this facies overlays F5c and can be interbedded with F9. Facies F9 or F5d characteristically overlies Facies F8. The thickness can range from non-present to 1.6 meters with an average of 8 cm. Occasionally pyrite can form in nodules or bands due to replacement of organic matter, which appears to be very high in abundance (Figure 2.8). Some bedding planes show fish remains, ammonoidea, phosphate grains, and plant material. Sedimentary structures present are very thin planar laminated beds. There is a complete lack of ichnotaxa present in this facies.

*Interpretation:*

Shales of marine origin are deposited in many different depositional settings. This creates great difficulty in interpreting a depositional environment. Prothero and Schwab (2003) describe marine shales as being deposited by suspension fall out of pelagic materials, terrigenous materials deposited by density currents, windblown materials from continents, transportation and deposition by contour currents, fluvial transported shales that fall out of suspension in nearshore zones, and deposition of muds in tidal flats.

Where present above F5c, Facies F8 is interpreted as shelf muds representing a flooding surface relating to a major transgression. When F8 is interbedded with F9 this facies lends to the interpretation of minor fluctuations in oxygen and sea levels.

**Figure 2.8. Facies F8**

Facies F8 is a maximum flooding surface with organic rich shale.

**A)** Often pyrite is a major component of this facies. Well 14-15-78-10W6 at a depth of 1836 m.

**B)** Organics and bone fragments can be seen on bedding plains. Well 2/7-26-78-10W6 at a depth of 1810.52 m.

**C)** Facies F8 in some cores can be found between facies F5c and F5d. Well 6-16-78-10W6 at a depth of 1858.79 m.

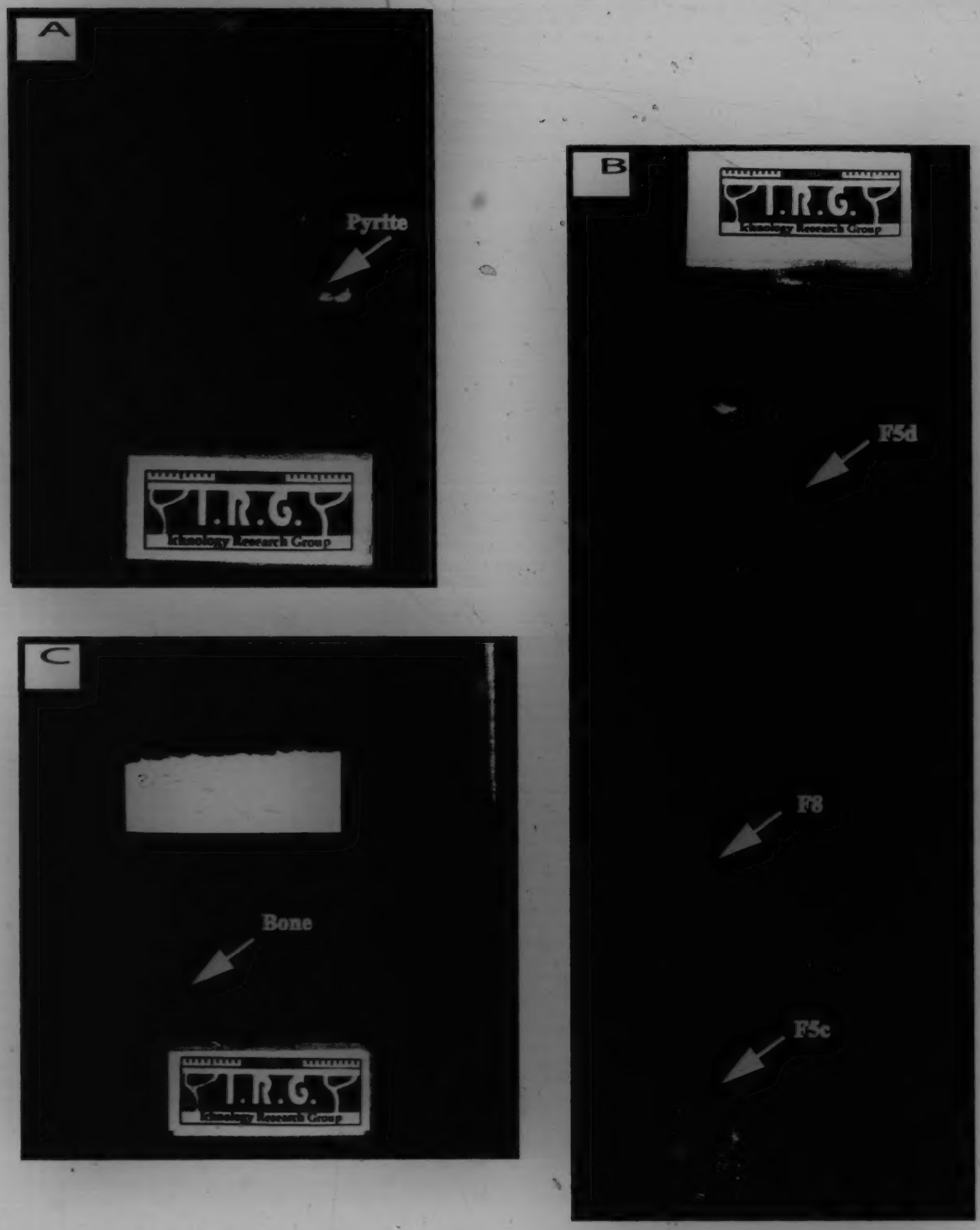
A
Pyrite
B
F5d
F8
F5c
C
Bone

Deposition of shale may be from muds settling out of suspension in a protected environment with oxygen levels of less than 0.1 ml of oxygen per liter of water (anoxic) (Prothero and Schwab, 2003). Levels in this range give little to no bioturbation as well as good preservation of animals when buried on the sea floor. Since there is no evidence of current or storm action, which could remove or break up organics and bioturbation is not present, a depositional setting in a deep anoxic shelf environment is suggested.

### 2.2.10 Facies F9: Muddy siltstone

*Description:*

Facies F9 is a black colored muddy siltstone interbedded with F8, F10, and F11. Mud content is a significant component representing up to 50% with the other grain sizes comprising of silt. Thickness can range from 7 cm to 3.6 m. Facies F9 is found in close contact with Facies F8, F10, and F11 from interbedding in some locations. The mineralogy of this facies can show pyrite and anhydrite nodules. Also found within this facies can be a significant amount of organic material, and possible phosphatic grains. Sedimentary structures are represented in massive beds, minor dish and pillar structures, as well as planar laminations (Figure 2.9).

*Phycosiphon* is the only ichnotaxon present within this facies, which heavily bioturbated some sections of this facies. Detailed examination must be made when analyzing bioturbation in this facies to make sure such burrows are not confused with dish and pillar structures.

*Interpretation:*

Facies F9 is possibly part of a system of minor sea level changes along with changes in oxygen levels in a sheltered shelf environment. It is underlain by deep shelf muds of Facies F8 and overlain by shelf sands in Facies F10. This pattern may represent one of three things: First, a shallowing upward sequence; Second, changes in oxygen as

**Figure 2.9. Facies F9**

**A)** A typical box shot of facies F9 showing an organic rich muddy siltstone with planar laminations. Well 14-11-77-10W6 at a depth of 1943.59-1946.07 m.

A
3
15 centimeters

mentioned above; and Third, shifts in sediment supplied by storms.

Massive appearing beds can have many different generating factors described in Facies F2. Facies F9 shows a combination of massive beds and planar laminated beds from suspension fall out. Massive beds show heavy bioturbation by *Phycosiphon*, which destroys the original planar laminations. Where planar laminations are present oxygen, levels may be unfavorable therefore organisms do not disturb the sediments. Similar to facies F8, this facies was deposited in a sheltered shelf environment with varying oxygen levels. A sheltered shelf environment is implied because there are no storm derived sands and silts similar to those in Facies F10 and F11. Varying levels of oxygen can be inferred by the presence of bioturbated and unbioturbated zones. Zones of bioturbated and unbioturbated media relating to oxygen fluctuations have been described in northern Italy by Twitchett and Wignall (1996).

### 2.2.11 Facies F10: Muddy silt with deformed lenticular sands

*Description:*

Facies F10 can be found interbedded with Facies F11 and F9. Coloration of this facies tends to be dark grey to black and where thin sands are present there is a tan coloration to the sands. The dominant sediments are 70% sandy silt and 30% mud. Where minor amounts of sands are present sizes range from lower fine to upper fine. Thickness of the sand beds can range from ¼ cm to 6 cm thick. Anhydrite and pyrite nodules can be present within this unit along with large rare vertical fractures filled with anhydrite (Figure 2.10). Dominant sedimentary structures are deformed lenticular sands and thin bioturbated silty beds.

A stressed suite of distal *Cruziana* ichnofacies dominates the bioturbated sediments. Ichnotaxa include abundant traces of *Phycosiphon* and *Scolicia*, with minimal colonization of *Thalassinoides* and *Planolites*. Traces are very difficult to see because of the coloration and homogenous nature of the sediment grain size.

**Figure 2.10. Facies F10**

**A)** This image shows a fine-grained sand from storm deposition or reworking of relic sediments. Notice the deformed lenticular beds (LB) and anhydrite nodules. Well 2/7-26-78-10W6 at a depth of 1807.8 m.

**B)** Facies F8 is dominated by deformed lenticular beds (LB) with sporadic traces of *Phycosiphon* (Ph) and *Scolicia* (Sc). Well 6-16-78-10W6 at a depth of 1856.5 m.

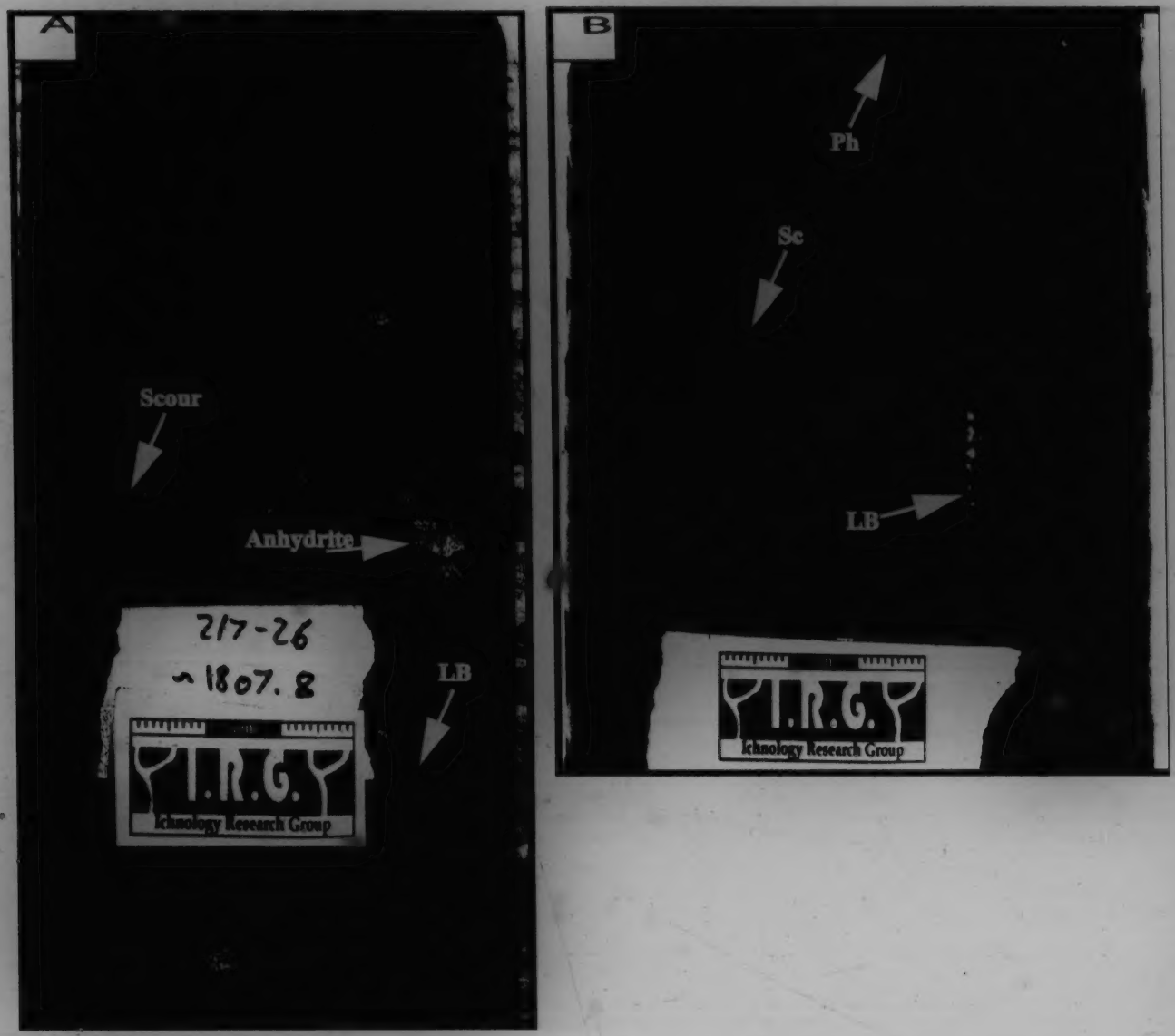
A
Scour
Anhydrite
217-26
~1807.8
LB
PIRGY
Ichnology Research Group
B
Ph
Sc
LB
PIRGY
Ichnology Research Group

*Interpretation:*

Facies F10 is interpreted as sands deposited in a shelf environment. Similar to Facies F11, beds have undergone a significant degree of deformation from liquefaction, loading, and dewatering. This facies has coarser and more distinct sand content than F11. There are two interpretations for this: One, sands are thicker and more distinct here because deposition is more proximal to the coastline. These proximal sands were possibly deposited by storm events, which soon underwent deformation due to liquefied sediments lying underneath. Sedimentary structures have mostly been deformed, therefore they are of no help. Two, these are relic sediments from a previous coastal environment that has been submerged and reworked upon transgression. The thicker sand layers (5 to 6 cm) may be the result of deposition of sand ribbons or patches, which formed by reworking of preexisting sediments related to the transgression or reworking of storm sands (Cattaneo and Steel, 2003). These sand ribbons or patches then underwent bioturbation dominantly by *Scolicia* and *Phycosiphon,* which in turn overprinted the internal structure. Either interpretation may be applied to this facies.

*Scolicia* typically occurs in silty and fine grained sands of deeper water settings with bottom currents and higher sedimentation rates (Fu and Werner, 2000). Bottom currents can produce sand ribbons or patches while high sedimentation rates are related to storms. Accordingly, *Scolicia* may be a good indicator of these conditions (Fu and Werner, 2000). In most cases, the backfill in the burrows are not preserved owing to relatively little change in grain size and lithology of the sediment units because of this *Scolicia* ends up looking like a small fuzzy golf ball.

### 2.2.12 Facies F11: Silty sand with flame structures

*Description:*

Facies F11 is interbedded with F10 and F9. The diagnostic coloration found within this facies is dark black to brown with some white coloration to the thin sandy beds. Sediments are for the most part muddy silt with up to 35% lower fine-grained sand. Like Facies F10 there can be anhydrite and pyrite nodules. Large vertical fractures filled with anhydrite are also commonly present. Frequent occurrences of pyrite in bands are another distinguishing feature. Sedimentary structures formed in this facies are deformed beds of lower fine-grained sands. Structures appear to be small cuspate (dish and pillar) shapes relating to deformation structures or even possibly flame structures; however, deformation does not allow for a definite identification of original bedding which may have been rhythmic (Figure 2.11). Individual sandstone beds are not as thick as F10. The average thicknesses of the sandy/silty beds are estimated to be less than ¼ of a cm.

The dominating ichnotaxa are *Phycosiphon* and *Scolicia* with minor amounts of *Thalassinoides*, *Planolites*, and small 1 cm high *Skolithos*. For this depositional setting the traces are grouped into a stressed distal *Cruziana* ichnofacies.

*Interpretation:*

Facies F11, similar to other Lower Doig facies, suggest sands deposited in a shelf environment. Sand deposition may originally have been laid down in rhythmic beds from storms. Syndepostionally or slightly after deposition sands may have undergone deformation from deposition atop hemipelagic liquefied muds and silts creating small dish and pillar structures from fluid escape (Lowe, 1975). Intense bioturbation by subhorizontal *Phycosiphon*, *Scolicia*, *Thalassinoides*, *Planolites*, and small 1 cm high *Skolithos* add to the chaos. These traces are representative of a stressed distal *Cruziana* ichnofacies. Furthermore distal *Cruziana* ichnofacies have been recognized overprinting

**Figure 2.11. Facies F11**

**A)-C)** Facies F11 containing flame structures (FS), anhydrite and pyrite. Typical traces in this facies are *Skolithos* (Sk), and *Phycosiphon* (Ph). A) Well 3-22-78-10W6/4 at a depth of 1833.9 m. B) Well 4-2-79-10W6 at a depth of 1798.2 m. C) Well 2/7-26-78-10W6 at a depth of 1808.6 m.

**D)** Possible dish and pillar structures seen in facies F11. Well 6-16-78-10W6 at a depth of 1858.7 m.

A
Anhydrite
FS
B
FS
C
FS
Ph
Sk
Pyrite
D

storm deposits in the Cretaceous (MacEachern, 1994; Pemberton et al., 2001). Both *Anconichnus* now called *Phycosiphon* and *Scolicia* are the dominant traces and have been described in shelf settings by Wetzel and Bromley (1994) and Fu and Werner (2000) respectively. On the other hand *Skolithos* is typically found in shallower depositional environments with higher energy; however, there may have been enough energy and sediments from storms to allow opportunistic suspension feeding by rare *Skolithos* in deeper depositional systems (Pemberton and Frey, 1984; Vossler and Pemberton, 1989; MacEachern and Pemberton, 1992; MacEachern 1994).

## 2.3 FACIES ASSOCIATIONS

### 2.3.1 Facies Association SO (Moig Siltstone)

Facies Association SO contains deposits relating to offshore/shoreface transition zone grading into a tectonically influenced storm dominated upper offshore. The particular facies found within these two environments are Facies F1, which is overlain by Facies F2, F3 and F4. There is an interbedded nature to the latter three facies. Facies F1 and F2 are described as a storm dominated offshore/shoreface transition zone representing a highly bioturbated zone with some graded rhythmites. Facies F3 and F4 are storm dominated upper offshore deposits showing graded rhythmites, planar lamination, wave scours, wavy bedding, minor bioturbation, and tectonically influenced seismites. The main difference between F3 and F4 is the presence of seismites found in F4 possibly from reactivation of the underlying Paleozoic structure. The base of this facies association contains a transgressive surface of erosion (F5a) and associated bones, peloids, ooids, and phosphates representing a lag deposit. This wedge of sediment is an overall transgressive deposit with gradational contacts between all facies except for the transgressive surface of erosion (F5a). For the purpose of this study, Facies Association

SO has been renamed the Moig Siltstone.

### 2.3.2 Facies Association B (Moig Sandstone)

Facies Association B is highly bioturbated relating to offshore/shoreface transition deposits overlain by distal to proximal lower shoreface deposits with more vertical suspension feeding traces. The transition zone (F6) contains highly bioturbated media dominated by archetypal *Cruziana* ichnofacies. Moving up core there is a gradational contact with the distal lower shoreface (F7a) archetypal *Cruziana* ichnofacies. This distal lower shoreface zone has the presence of some vertical to subvertical suspension and deposit feeding structures implying an increase in energy. Continued shallowing of the system gives rise to another gradational contact with the proximal lower shoreface (F7b), which shows a more proximal *Cruziana* ichnofacies character relating to continued shallowing and therefore an increase in energy. For the purpose of this paper the entirety of Facies Association B has been named the Moig Sandstone. The base of this association is represented by a transgressive lag deposit (Facies F5b) and capped by a major transgressive ravinement surface and associated lag deposit (Facies F5c). This sandy package is a prograding system with a minor fluctuation in sea level depositing a thin wavy bedded dark silt followed by more bioturbated sands (2 prograding sands). In core this gradational unit is found at the top of Facies F5b.

### 2.3.3 Facies Association SS (Lower Doig)

Facies Association SS pertains to a shelfal environment with varying degrees of bioturbation. It has been speculated that these varying levels are from fluctuating oxygen and energy levels. The base of this association starts with a transgressive surface of erosion (F5c) followed by an organic rich condensed section (F8). Atop Facies F8

are interbedded Facies F9 to F11 with varying amounts of deformation, bioturbation, and storm plus erosion derived sands and silts. Within Facies F9 to F11 other minor transgressive surfaces of erosion can be seen with the most dominant one relating to Facies F5d. This overall association can be considered a transgressive unit mixed with distal portions of the Upper Doig stillstand deposits. Stillstand deposits similar to these have been described in the Cretaceous Viking Formation in central Alberta (Walker and Davies, 1991; MacEachern, 1994).

# CHAPTER THREE

# STRATIGRAPHY, DEPOSITIONAL ENVIRONMENTS, AND DISTRIBUTION OF THE MOIG AND DOIG UNITS

## 3.1 INTRODUCTION

Available core for the three studied units is primarily concentrated within the southeast portion of the study area (see chapter 1 Figure 4). Since there is poor distribution of core, depositional models described herein are based on a combination of facies, facies associations, structure maps, isopach maps and cross-sections.

The complexity of the structural and stratigraphic relationships requires each unit in this study to be described with a separate depositional model. The Moig Siltstone lies unconformably atop the Montney Formation and is represented by a structurally controlled offshore/shoreface to proximal upper offshore transgressive Facies Association SO. Unconformibly overlying the Moig Siltstone is the Moig Sandstone, which is a structurally controlled offshore/shoreface to proximal lower shoreface Association (B). The third model describes the Lower Doig Formation, which unconformably overlies the Moig Sandstone. The Lower Doig is an overall transgressive unit deposited in a structurally controlled shelf environment characterized by Facies Association SS.

## 3.2 MAPS

Mapping of the Moig Siltstone reveals a morphology not characteristic to any depositional setting (Figure 3.1). The western and southern edges of the study area exhibit the thickest isopach values, as well as a couple of small isolated thicks toward the

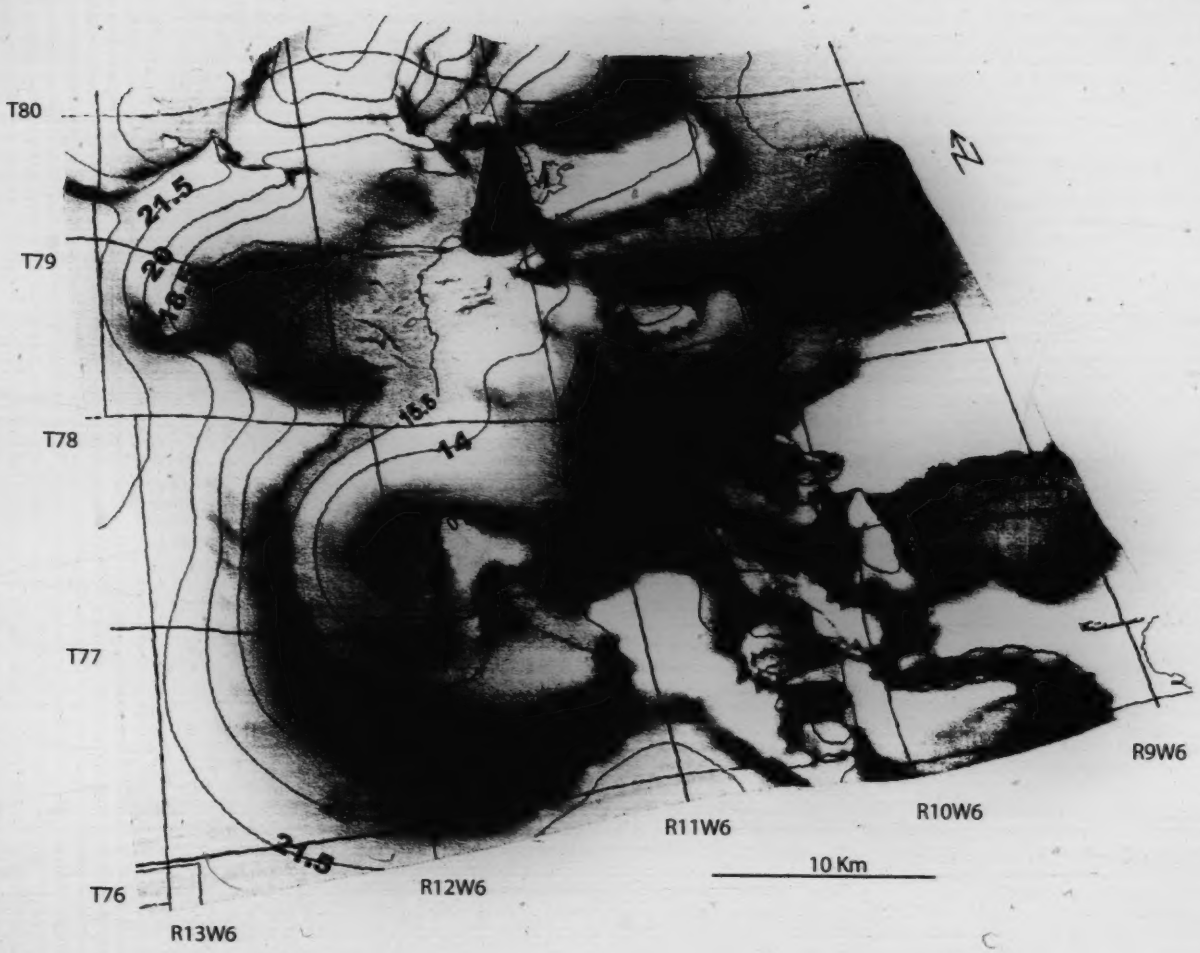


**Figure 3.1.** Gross thickness map of the Moig Siltstone unit with a contour interval of 1.5 m.

north and southeast. Structural analysis of the underlying Paleozoic Belloy Formation reveals a series of faults (Figure 3.2 and 3.3). These Paleozoic structures influenced deposition of the Montney Formation and the Moig Siltstone (Figure 3.3). Sediments of the Moig Siltstone can be seen draping over the Farmington Fault in T79 R12W6. An overall thinning of the unit over the faulted area represents this sediment drape. Reactivation of these basement structures caused the formation of graben structures, which increased accommodation space and allowed for thicker isolated bodies to form (Figure 3.3 T79R12W6). Evidence of basement structure reactivation is also observed in core in the form of seismites (see Facies F4 Chapter 2). Also affecting the morphology of the Moig Siltstone is the transgressive surface of erosion (HE FS 2, F5b) at the base of the overlying Moig Sandstone. Based on figures 3.1 and 3.4, it is evident that the Moig Siltstone is thinnest where the Moig Sandstone was deposited. The thinning of the siltstone unit is a result of scouring during transgressive ravinement (HE FS 2, F5b) that occurs as the shoreface profile attempts to maintain equilibrium (Swift, 1975; Demarest and Kraft, 1987).

Mapping of the Moig Sandstone confirms a lobate shape for the unit. If mapping was the only tool used to interpret Facies Association B, a deltaic depositional model would probably be the end result (Figure 3.4). However, complete bioturbation of these sands by a diverse and abundant assemblage of trace fossils corresponds to shoreface deposition (Moslow and Pemberton, 1988; Bann and Fielding, 2004). On closer examination of the core and structure maps, there are two explanations for the similarities to deltaic morphology. Deposition of the sand was controlled by the Paleozoic structure (Figure 3.2). Examining the Belloy structure map revealed a series of faults, in which two were previously named the Farmington Fault and the Gordondale Fault (Richards et al., 1994). These faults affected sand deposition by increasing or decreasing accommodation space as well as by changing the depositional gradient causing draping of sediments over the faults (Figure 3.7). Examples of draping of sediments over the fault can be

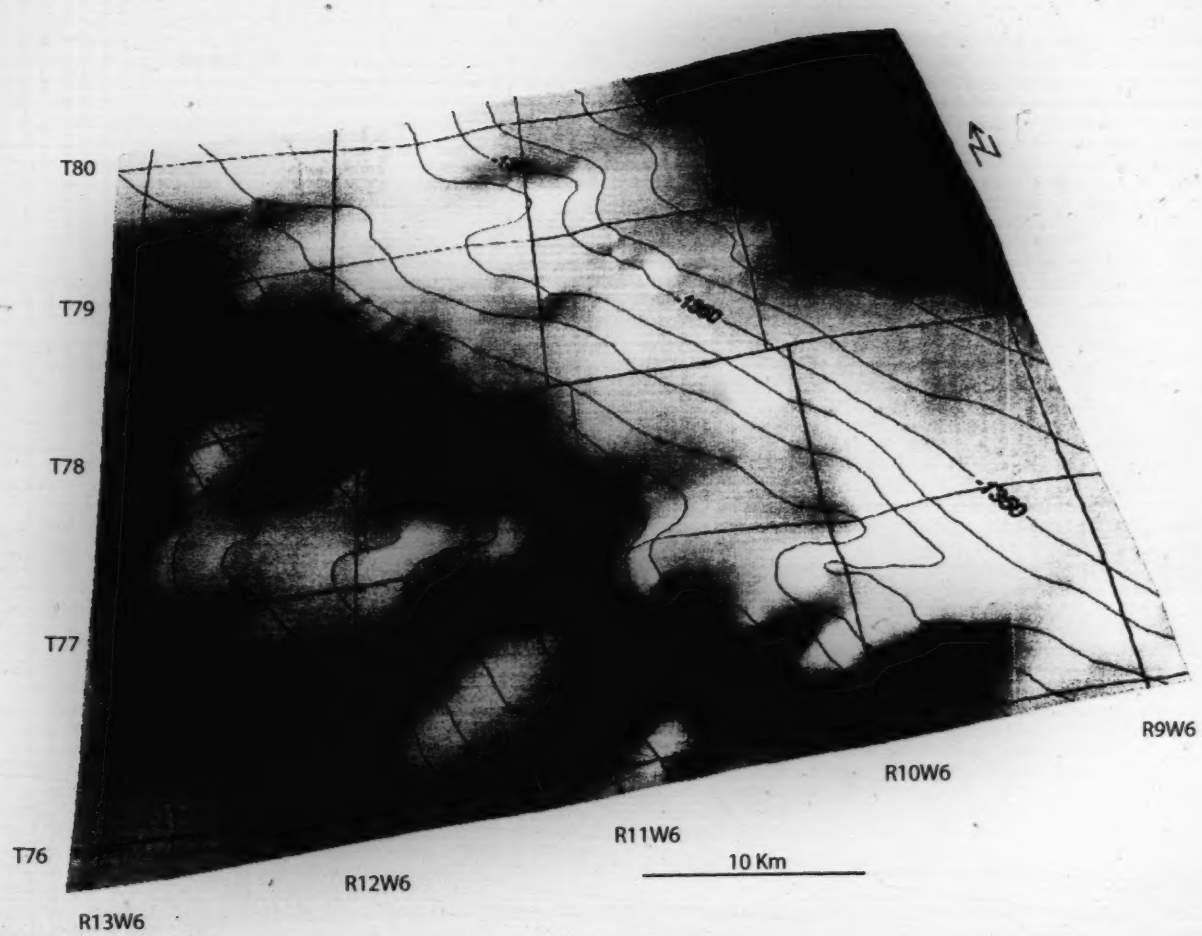


**Figure 3.2.** Structure map of the Paleozoic Belloy Formation with a contour interval of 30 m..

**Figure 3.3.** Gross thickness map of the Moig Siltstone unit with a contour interval of 2 m. Wells present on the map are all the control points used in the study. The upper faults in red are the Farmington Fault and the Gordondale Fault from north to south (After Richards et al., 1994). Blue faults are possible faults discovered in this study from the Belloy structure map. Wells present on the map are all the control points used in the study.

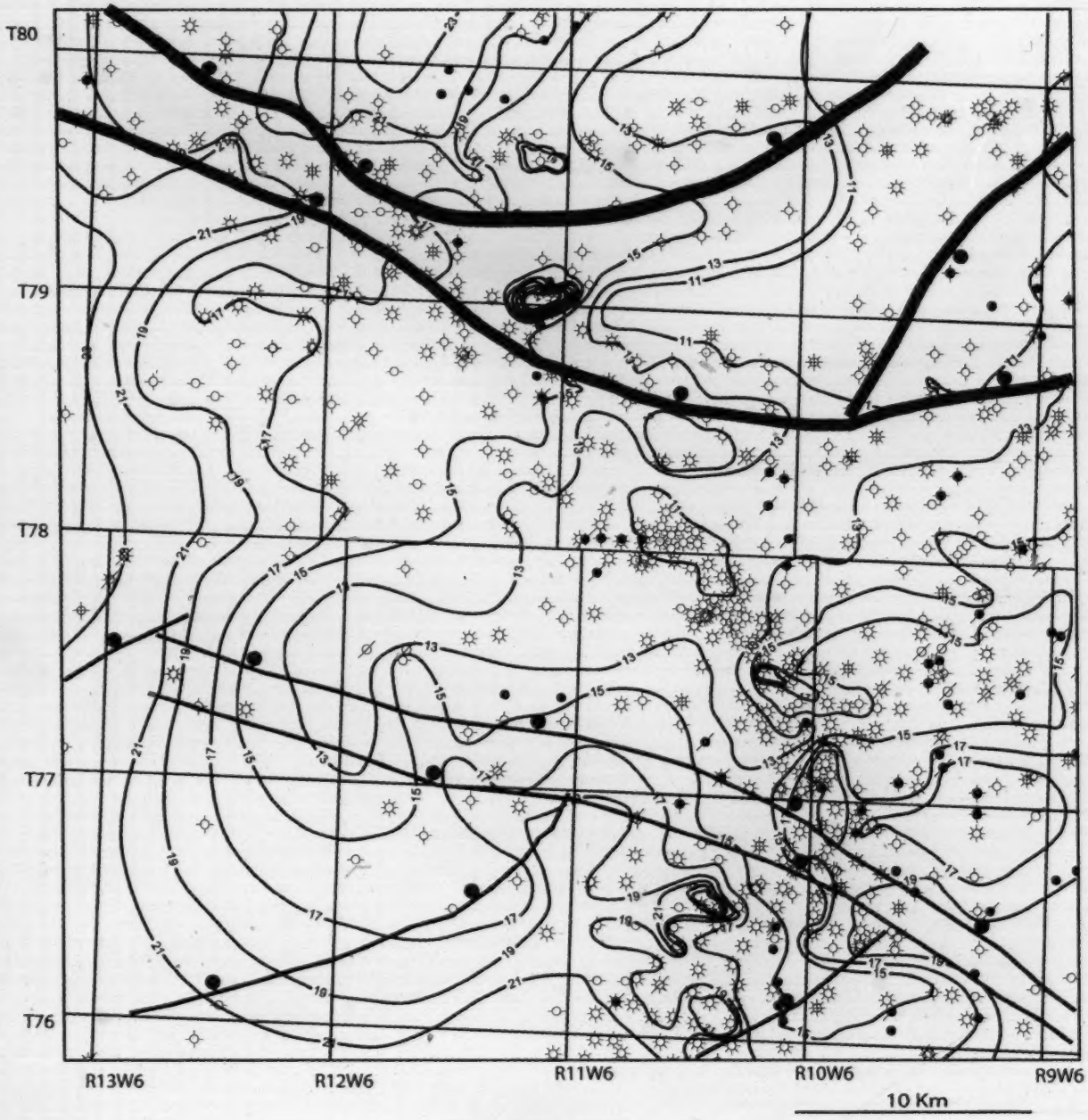
T80
T79
T78
T77
T76
R13W6
R12W6
R11W6
R10W6
R9W6
10 Km
Faults from Richards et al., 1994
Gas
Abandoned
Faults from this study
Suspended
Oil
N

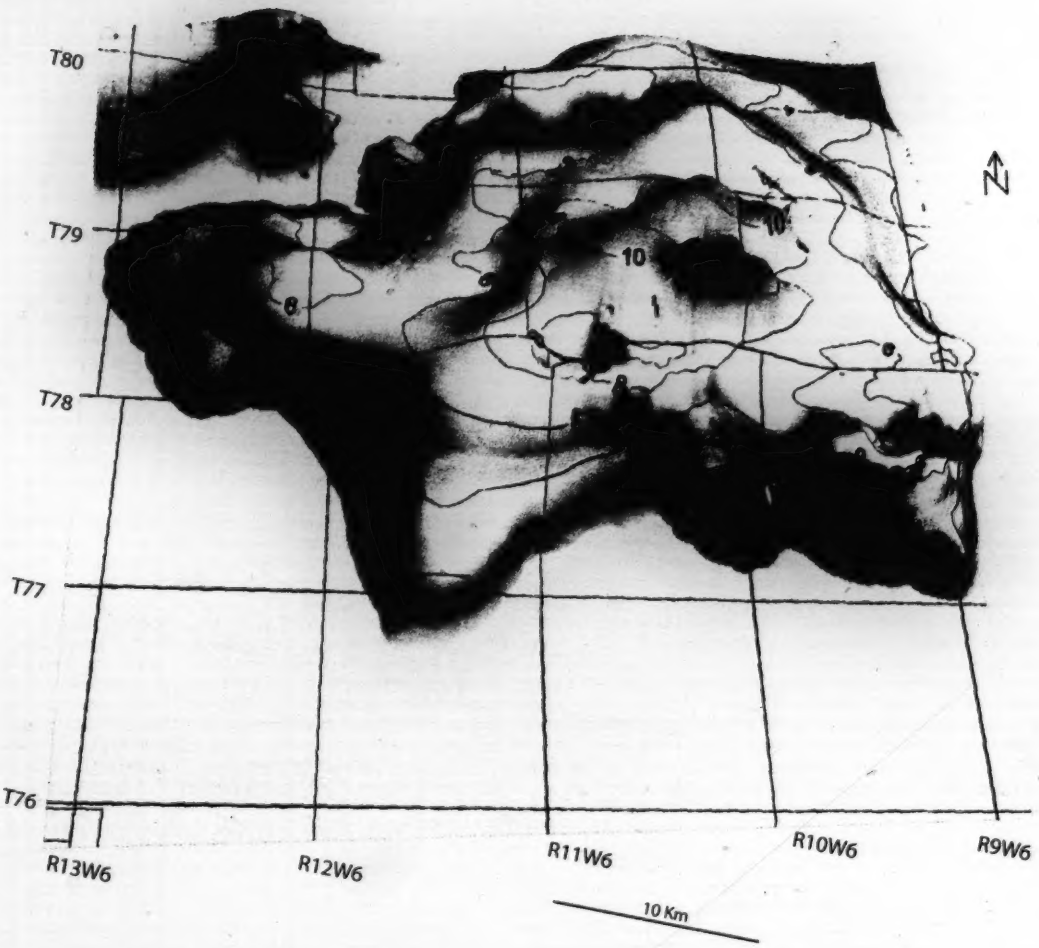


**Figure 3.4.** Net sand isopach of the Moig Sandstone unit with a contour interval of 2 m. Net sand values were obtained by using a combination on gamma ray, resistivity, neutron, and density logs since phosphates may give a false shale reading.

**Figure 3.5.** Paleozoic faults overlain on the net sand isopach of the Moig Sandstone. The upper faults in red are the Farmington Fault and the Gordondale Fault from north to south (After Richards et al., 1994). Blue faults are possible faults discovered in this study from the Belloy structure map. Wells present on the map are all the control points used in the study. Contour interval: 2 m

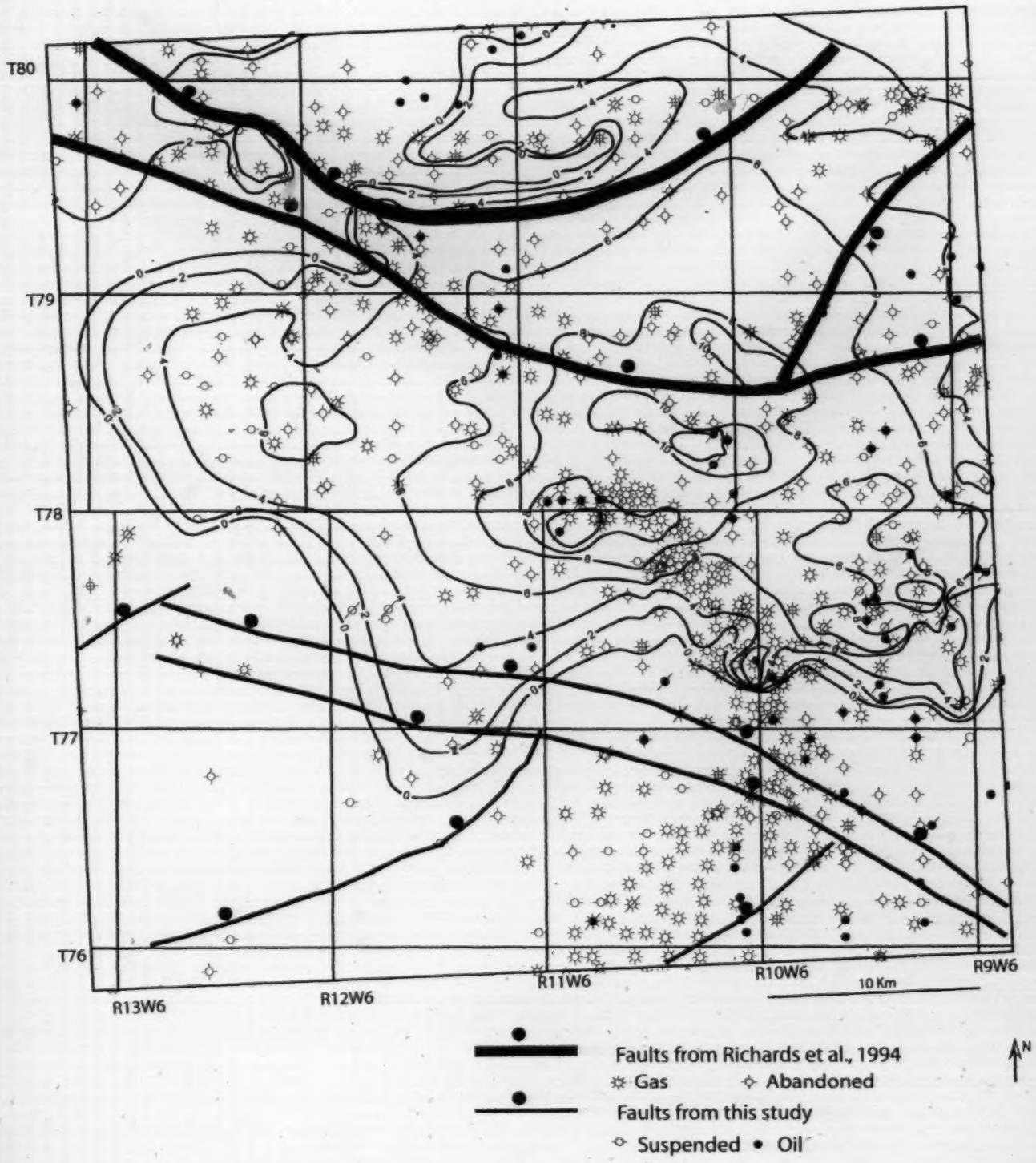
T80
T79
T78
T77
T76
R13W6
R12W6
R11W6
R10W6
R9W6
10 Km
N
Faults from Richards et al., 1994
Gas
Abandoned
Faults from this study
Suspended
Oil

found on all three of the isopach maps. In the Moig Sandstone sediment draping over the Farmington Fault is represented by the thinning of sediments in northern sections of the study area (T79R11-13). The second factor affecting the morphology of the Moig Sandstone isopach map is the presence of unconformities below and above the sand (HE FS 2 and HE FS 3). The primary influence is the transgressive surface of erosion (HE FS 3 and Facies F5c) that overlies the Moig Sandstone. This surface may have removed as much as 20 meters of the substrate in an attempt to maintain the shoreface profile (Swift, 1975; Demarest and Kraft, 1987). It can be speculated that tectonics resulted in more severe erosion to the east by a reduction in slope, which created a more extensive erosional surface. This degree of erosion may account for the paucity of middle to upper shoreface deposits (Catuneanu, 2006). The shoreline at the time of deposition was also oriented northwest – southeast such that land was to the northeast, which suggests that dominant erosion would have been in that direction.

The Lower Doig shelf deposits exhibit similar thickness trends as the Moig Siltstone and Moig Sandstone (Figure 3.6). Paleozoic structures (faults), where present, influenced shelf deposition (Figure 3.7). In the northern section of the isopach map, the Farmington and Gordondale faults controlled deposition. In between the two faults there seems to have been an increase in accommodation space, which allowed for thicker Lower Doig deposits to accumulate. Directly overlying the faults there is a reduction in thickness implying that these faults may have reduced accommodation space in these areas. Toward the south, a similar but less pronounced trend in thickness is influenced by the unnamed faults of this study. In general, Facies Association SS thickens to the east and thins to the west, with the exception of a lobate shape in the southwest corner of the study area. The thickening to the east can be explained by the proximity to the shoreface (source), which would supply sands and silts deposited by stillstand progradation, gravity flows, and storms. The lobate shape to the southwest may be explained by structurally controlled debris flows. However, core is required from this location to provide further

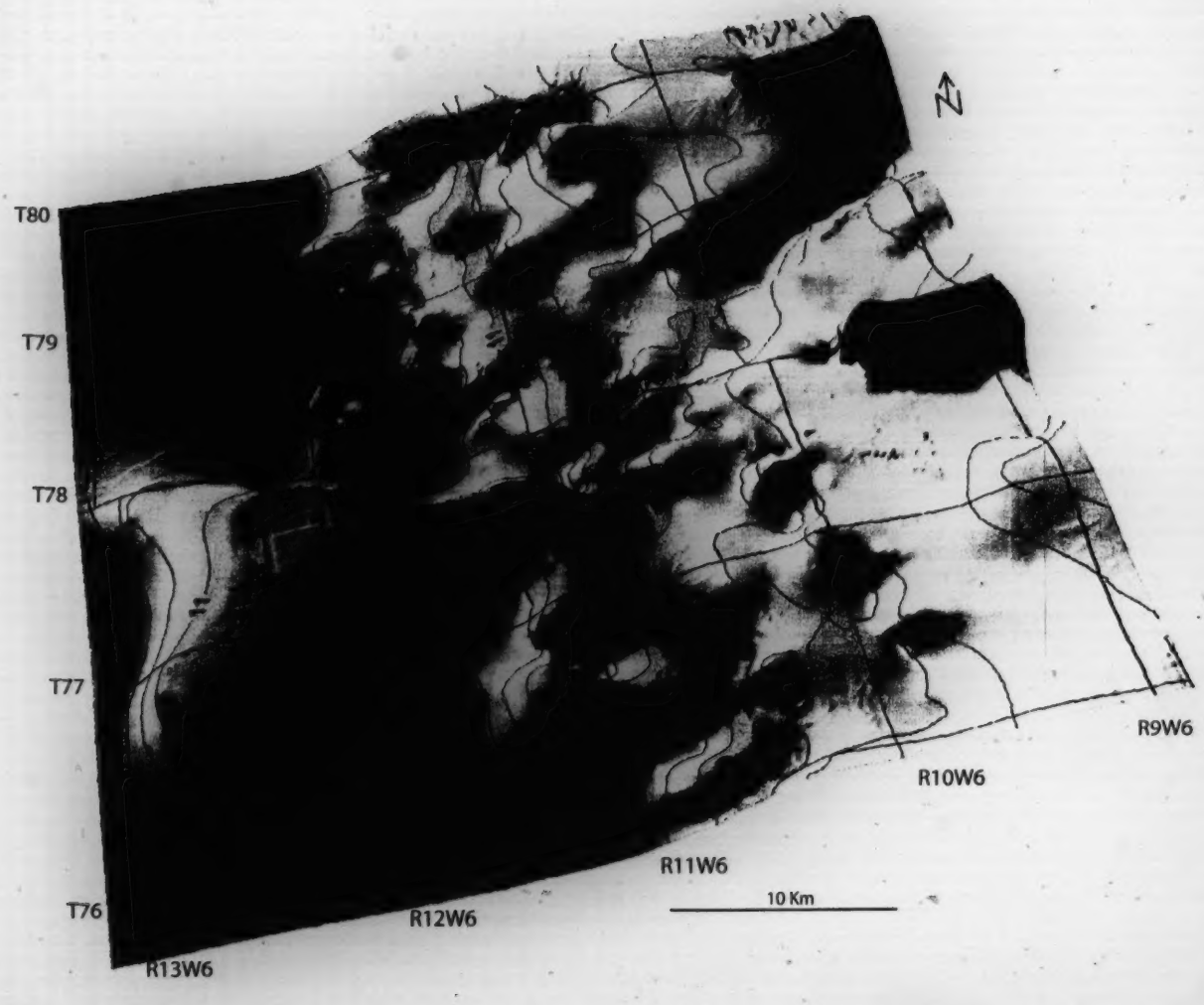


**Figure 3.6.** Gross thickness map of the Lower Doig Formation. Contour interval: 2 m

**Figure 3.7.** Gross thickness map of the Lower Doig Formation with Paleozoic faults overlain. The upper faults in red are the Farmington Fault and the Gordondale Fault from north to south (After Richards et al., 1994). Blue faults are possible faults discovered in this study from the Belloy structure map. Wells present on the map are all the control points used in the study. Contour interval: 2 m

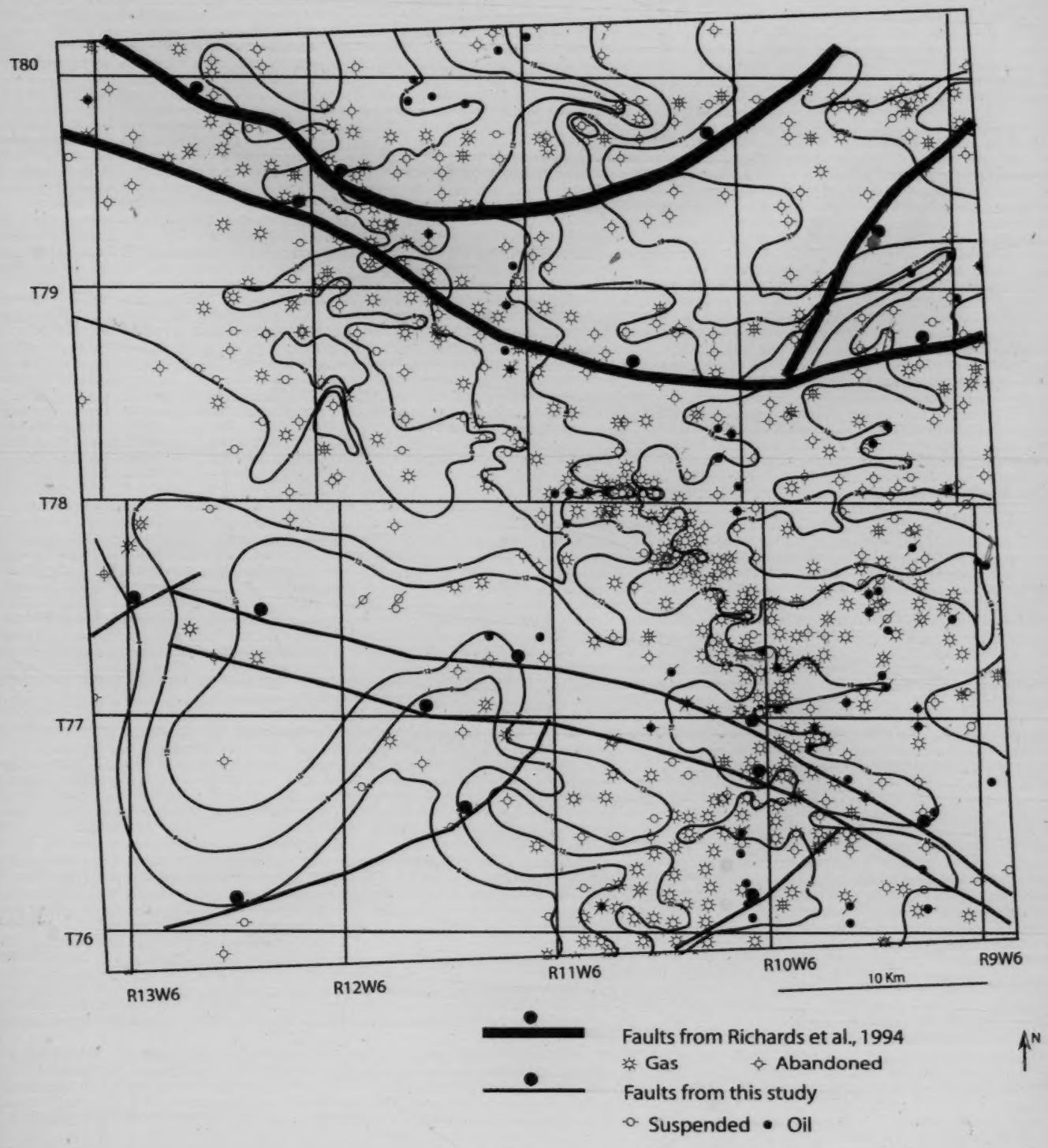
T80
T79
T78
T77
T76
R13W6
R12W6
R11W6
R10W6
R9W6
10 Km
Faults from Richards et al., 1994
Gas
Abandoned
Faults from this study
Suspended
Oil
N

evidence of this interpretation, as phosphates may give a false shale reading.

## 3.4 STRATIGRAPHIC EVOLUTION

The overall succession of the Moig to Lower Doig represents a transgressive package influenced by higher frequency periods of regression during stillstand conditions (Figure 3.8). The base of the Moig Siltstone is marked by a flooding surface/sequence boundary (FS/SB1 Facies F5a) where a low energy flooding surface (LE FS 1) forms below the FWWB and a high energy flooding surface (HE FS 1) above due to the erosional nature of shoreface retreat. This surface overlies the Smithian highstand systems tract (HST) of the Montney Formation, which may have an attached lowstand systems tract (LST) (Kendall, 1999). It is possible that the Swan and Dawson fields on the B.C. /Alberta boarder represents the LST that is overlain by transgressive deposits of the Moig Siltstone. After deposition of the transgressive Moig Siltstone is the Moig Sandstone, which is a stillstand shoreface deposit. The base of the Moig Sandstone contains an amalgamated SB/FS 2 with a low energy flooding surface (LE FS 2) below the FWWB and a high energy flooding surface (HE FS 2) above the FWWB. In order for shoreface deposits of the Moig Siltstone to be removed the Moig Sandstone must have started as a forced regressive deposit prograding over the transition zone to offshore deposits of the Moig Siltstone. Renewed transgression reworked the forced regressive surface and left the transition zone to offshore deposits of the Moig Siltstone overlain by an amalgamated FS/SB 2. Sediments of the Moig Sandstone directly overlying FS/SB 2 (Facies F6) are deposits below FWWB and therefore must have been deposited during a transgression through reworking of the sediment starved Moig Siltstone shoreface. If the Moig Siltstone shoreface was not thin and sediment starved there would be remnants of this shoreface left behind. Subsequently, a period of stillstand lead to the deposition of

the Moig Sandstone atop the FS/SB 2 surface. The Moig Sandstone is a transgressively incised stillstand shoreface deposited during a time of basinward shift. The base of the Moig Sandstone reflects a FS/SB 2 (TSE) with an associated *Glossifungites* Ichnofacies and lag deposit (Facies F5b) while the top represents another high energy FS/SB 3 and lag deposit (Facies F5c) from resumed transgression.

Following deposition of the Moig Sandstone is another sea level rise FS/SB 3 and associated lag deposit (Facies F5c) marking the beginning of the Lower Doig Stillstand deposits. Kendall, 1999 described this FS/SB 3 as a type one sequence boundary. It is agreed upon here since there is a drastic facies change from proximal lower shoreface (F7b) to shelf (F8-F11) and the sea level change was controlled by tectono-eustasy events (c.f. Pitman, 1978). The FS/SB 3 surface contains a low energy flooding surface (LE FS 3) below the FWWB and a high energy flooding surface (HE FS 3) above due to the erosional nature of the transgression. As transgression continued there was cannibalization of the Moig Sandstone from a reduction in structural relief to the east and the HE FS 3 surface, which can be confirmed in the cross-sections, maps and core. These Lower Doig deposits contain a series of TSE formed through continued stages of transgression. Each of these surfaces (FS/SB 3-5) contain low energy flooding surfaces (LE FS 3-5) below the FWWB and a high energy flooding surfaces (HE FS 3-5) above the FWWB from the erosional nature of shoreface retreat. These flooding surfaces and associated lag deposits (Facies F5c and F5d) may mark the distal extent of the prograding Upper Doig deposits (Wittenberg, 1992). Evidence for progradation is represented in stacked FS/SB in the Lower Doig. Since erosional surfaces (TSE) are cut only as deep as the FWWB these surfaces would lie progressively landward of one another unless there was a fall in sea level followed by a transgressive ravinement surface. Overall, proximal facies of the Moig Siltstone to the Lower Doig lie progressively landward of one another. This landward movement coupled with clastic wedges bounded by TSE and lag deposits representing retrogradational parasequences constituting a transgressive systems tract.

**Figure 3.8.** Graphical representation of the stratigraphic evolution for the Moig Siltstone, Moig Sandstone, and Lower Doig. **(1)** Relative sea level fall, possibly induced by tectonic events, produces a widespread subaerial exposure surface. Wave scouring occurs as deep as the fairweather wave base (FWWB) at the shoreline. In a basinward direction, the correlative conformity (CC) is developed and correlates to the sequence boundary (SB). A shoreface progrades over the SB and is called the lowstand systems tract (LST). It is possible that this LST characterizes the Swan and Dawson fields on the B.C. Alberta boarder. **(2)** A period of transgression occurs forming a low energy flooding surface (LE FS) below the FWWB and a high energy flooding surface (HE FS) above due to the erosional nature of shoreface retreat. The HE FS truncates the top of the LST forming a merged flooding surface and sequence boundary landward (FS/SB, Facies F5a). There is no preservation of the exposure surface due to the HE FS. A relative short stall in transgression allows for minor stillstand progradation over the FS/SB. **(3)** A period of regression allows for a drop in sea level and progradation of a sediment starved shoreface over top stage 2. Resumed transgression reworks the regressive deposits and forms another HE FS (Facies F5b) and a LE FS. The HE FS removes all of the thin stillstand shoreface deposits leaving behind only the transgressive deposits (The Moig Siltstone). These deposits represent a parasequence. A longer period of stillstand forms a prograding shoreface (The Moig Sandstone) deposited on top of the FS/SB. **(4)** A period of regression followed by resumed transgression from sea level rise and possible tectonic events causes a large transgressive episode that scours the top of the previous stillstand shoreface leaving behind a FS/SB (Facies F5c). This continued transgression forms the Lower Doig, which has a series of distal stillstand deposits and HE FS's.

Overall the nature of this succession from Moig Siltstone to Lower Doig represents a transgressive systems tract with deposits below FWWB being preserved on the FS/SB. This preservation of deposits below FWWB is what differentiates forced regressive shorefaces from stillstand shorefaces. Modified after MacEachern, 1994.

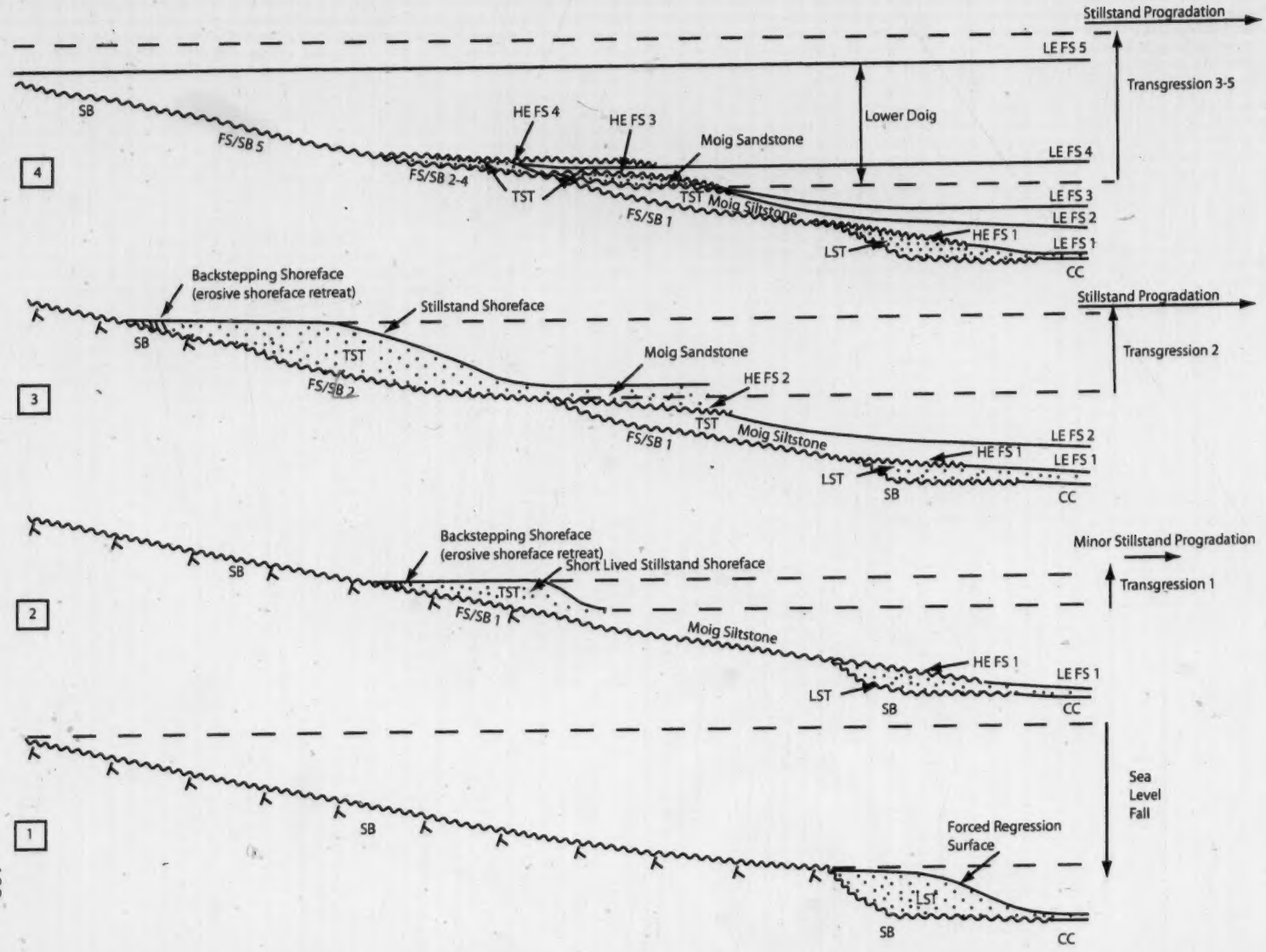
Stillstand Progradation
LE FS 5
Transgression 3-5
Lower Doig
SB
FS/SB 5
HE FS 4
HE FS 3
Moig Sandstone
LE FS 4
4
FS/SB 2-4
TST
TST
Moig Siltstone
LE FS 3
LE FS 2
FS/SB 1
HE FS 1
LE FS 1
LST
CC
Backstepping Shoreface
(erosive shoreface retreat)
Stillstand Shoreface
Stillstand Progradation
SB
TST
Moig Sandstone
Transgression 2
HE FS 2
3
FS/SB 2
TST
Moig Siltstone
LE FS 2
FS/SB 1
HE FS 1
LE FS 1
LST
SB
CC
Backstepping Shoreface
(erosive shoreface retreat)
Minor Stillstand Progradation
Short Lived Stillstand Shoreface
SB
TST
Transgression 1
2
FS/SB 1
Moig Siltstone
HE FS 1
LE FS 1
LST
SB
CC
Sea
Level
Fall
SB
Forced Regression
Surface
1
LST
SB
CC

## 3.3 CROSS-SECTIONS

Four cross-sections were constructed comprising of two dip and two strike sections (Figure 3.9). Core and gamma ray on the left, and resistivity on the right were used to elucidate the stratigraphic and depositional history. The crucial part of constructing the cross-sections was selecting a datum not of an erosional nature. Since most of the regional markers are erosional surfaces, the top of the Lower Doig was used as a datum. This regionally extensive surface was viewed in core and found to be a conformable surface. Since the depositional setting is transgressive in nature, there is minor distortion of the stratigraphy toward the east (landward). Therefore, trends seen in the cross-sections correspond as close as possible, to the original depositional architecture.

Cross-section S1-S1' is oriented parallel to depositional strike, and shows two silty units, the Moig Siltstone and the Lower Doig, and one sandy unit called the Moig Sandstone (Figure 3.10). Both the Moig Siltstone and Moig Sandstone produce gas across the study area. The base of the Moig Siltstone erosionally (FS/SB 1) overlies the highstand deposits of the Montney shoreface described by Kendall (1999). This contact is a HE FS 1 with an associated lag deposit (Facies F5a). Depositionaly, the Moig siltstone contains a transgressive fining upwards sequence of transition zone to upper offshore facies. This fining upward sequence is represented in core 4-2-79-10W6, which contains upper offshore transgressive Facies Association SO cut by a transgressive surface of erosion HE FS 2 (Facies F5b). Directly overlying this TSE is the sharp base of the Moig Sandstone. Presence of a *Glossifungites* Ichnofacies, a lag deposit, and a facies (F6) deposited below fairweather wave base implies that the Moig Sandstone was deposited by stillstand progradation after transgressive shoreface incision HE FS 2 (c.f. MacEachern et al., 1992). In this cross-section there is minor thinning to the east in the

Moig Sandstone shoreface deposits, which is from erosion by the overlying Lower Doig high-energy flooding surface HE FS 3 with an associated lag (Facies F5c). To the east the HE FS 3 may have had more erosive energy due to tectonic readjustments in the Spathian - Anisian aged Triassic (Kendall, 1999) decreasing the gradient of the shoreface profile. In the northwest the Moig Sandstone pinches out as it reaches its depositional limit of stillstand. The Lower Doig shows a thickening to the east in the strike sections. This thickening may be explained by proximity to thick Doig sands in the Mirage Field. Sands from the Upper Doig in this field were carried westward to the eastern edges of the Lower Doig in the study area. Overall the strike section contains little variability of Moig units other than a slight undulatory nature. This undulatory nature is interpreted to be the result of erosional surfaces and Paleozoic structures. Paleozoic faults are present between 6-21 and 14-09 (Farmington Fault) and 11-25 and 6-17 (Gordondale Fault). The high energy flooding surfaces contain lag deposits. These lag deposits and high energy flooding surfaces (HE FS 3-5) are present throughout the Lower Doig; however, these lags and associated flooding surfaces are not identifiable on the logs due to the high gamma from the presence of uranium and apatite. The Moig Siltstone also shows a radioactive nature of the gamma-ray log from uranium and apatite.

Cross-section S2-S2' is oriented with depositional strike, and resembles that of cross-section S1-S1' (Figure 3.11). Similarly HE FS 1 can be found above the HST deposits of the Montney Formation. In core 8-33-79-13W6 the lag (Facies F5a) associated with the HE FS 1 can be seen. The Moig siltstone in this cross-section and core 6-16-78-10W6/2 can be seen scoured by the HE FS 2 surface and associated lag (Facies F5b). Present in the stillstand Moig Sandstone deposits is a *Glossifungites* ichnofacies at the base (HE FS 2) and a high frequency period of sea level rise in the middle of the unit. This high frequency rise can be seen in well 7-32-78-12W6, 6-16-78-10W6/2, and 11-10-78-10W6/2 where the middle of the Sandstone unit contains a higher gamma signature. In core 6-16-78-10W6/2 this flooding period is preserved as

offshore deposits encased by shoreface deposits of the Moig Sandstone. To the southeast the Moig Sandstone has reached the depositional limit and is no longer present in 8-2-78-10W6. However, the Lower Doig overlying the sandstone is thickest in 8-2-78-10W6. Therefore, it is likely that the Moig Sandstone was deposited farther than can be mapped and was subsequently cannibalized by the overlying erosional event HE FS 3. Similar to cross-section S1-S1' the Lower Doig is thickest to the east due to more silts and sands deposited by stillstand Doig sands from the Mirage Field.

Cross-section D1-D1' is oriented parallel to depositional dip, and shows the three units of interest (Figure 3.12). In the dip section, a slight thinning of the transgressive Moig Siltstone as well as thinning of the stillstand Moig Sandstone in a landward direction (N.E.) is evident. Towards the northeast, the base of each of these units is demarcated by a transgressive surface of erosion HE FS 1 and HE FS 2 respectively and can be seen in core 6-16-78-10W6/2, 6-34-78-10W6, and 4-2-79-10W6. The erosive surface underlying the Moig Siltstone should pass basinward into a correlative conformity/LE FS 1 west of the study area. Southwest of 6-5-78-10W6 the Moig Sandstone is not present. Deposition of this unit may have changed to offshore deposits because of Paleozoic faulting which caused a deepening of the depositional system. The underlying erosional surface HE FS 2 may grade into a correlative conformity LE FS 2 in wells 6-3-77-11W6 and 15-3-77-11W6. If new cores are taken in 77-11W6 this LE FS 2 may be discovered. On the other hand, there is a thickening of the Lower Doig in a landward direction. The HE FS 3 and associated lag deposit (Facies F5c) at the base of the Lower Doig is a regional marker and is present across the entire study area. The extensive nature of the HE FS in the three units represents a relative shallow depositional gradient (Cattaneo and Steel, 2002). If the gradient was steeper, erosional surfaces would be less extensive, the Moig Sandstone would not have prograded as far during stillstand, and the sandstone would be much thicker. It is possible that in a basinward direction the Lower Doig Formation reflects a condensed section with minor stillstand sands from the

Middle and Upper Doig Formation. In a landward direction, the Lower Doig received more sands and silts from erosion of the Moig units, as well as sands from prograding stillstand Doig deposits. Adding to this variation in thickness may be compactional factors. When more sand is incorporated into the system there is less compaction and a thicker package forms nearer to the shoreline (Powers, 1967). This thicker package can be seen on the eastern sections of the study area and northeast of 6-5-78-10W6 in the cross-section.

Cross-section D2-D2' oriented parallel to depositional dip possesses similar characteristics to those of cross-section D1-D1' (Figure 3.13). The base of the Moig Siltstone contains the HE FS 1 overlain by a lag deposit (Facies F5a) and transgressive Facies Association S0. There is an overall thinning of the Moig Siltstone in a landward direction from a decrease in slope gradient, which caused greater erosion by the HE FS 2. Similarly, the stillstand Moig Sandstone deposits are eroded in a northeast direction by the HE FS 3 surface. The main difference in D2-D2' is the presence of two Paleozoic faults that affected deposition. These are the unnamed faults of the study between wells 15-28-77-13W6 and 7-32-78-12W6 and the Gordondale Fault between wells 10-18-79-11W6 and 2/11-25-79-11W6 (Figure 3.9). The most significant fault is the first mentioned where the Moig Siltstone is thickened in 15-28-77-13W6 compared to the northeastern wells. This may be from an increase in accommodation space resulting from the unnamed fault or from distal deposits of the Moig Sandstone, which are not resolvable on logs. If the later were the case there would be a LE FS 2 present in 15-28-77-13W6; however, more core is needed to prove this. In the southwestern well 15-28-77-13W6 the Lower Doig is more than double the thickness than in 7-32-78-12W6. The thickening of the Lower Doig is interpreted to be the result of increased accommodation space created by the underlying unnamed fault coupled with silt and sand deposition from distal storm deposits, debris flows, or prograding Upper Doig sands.

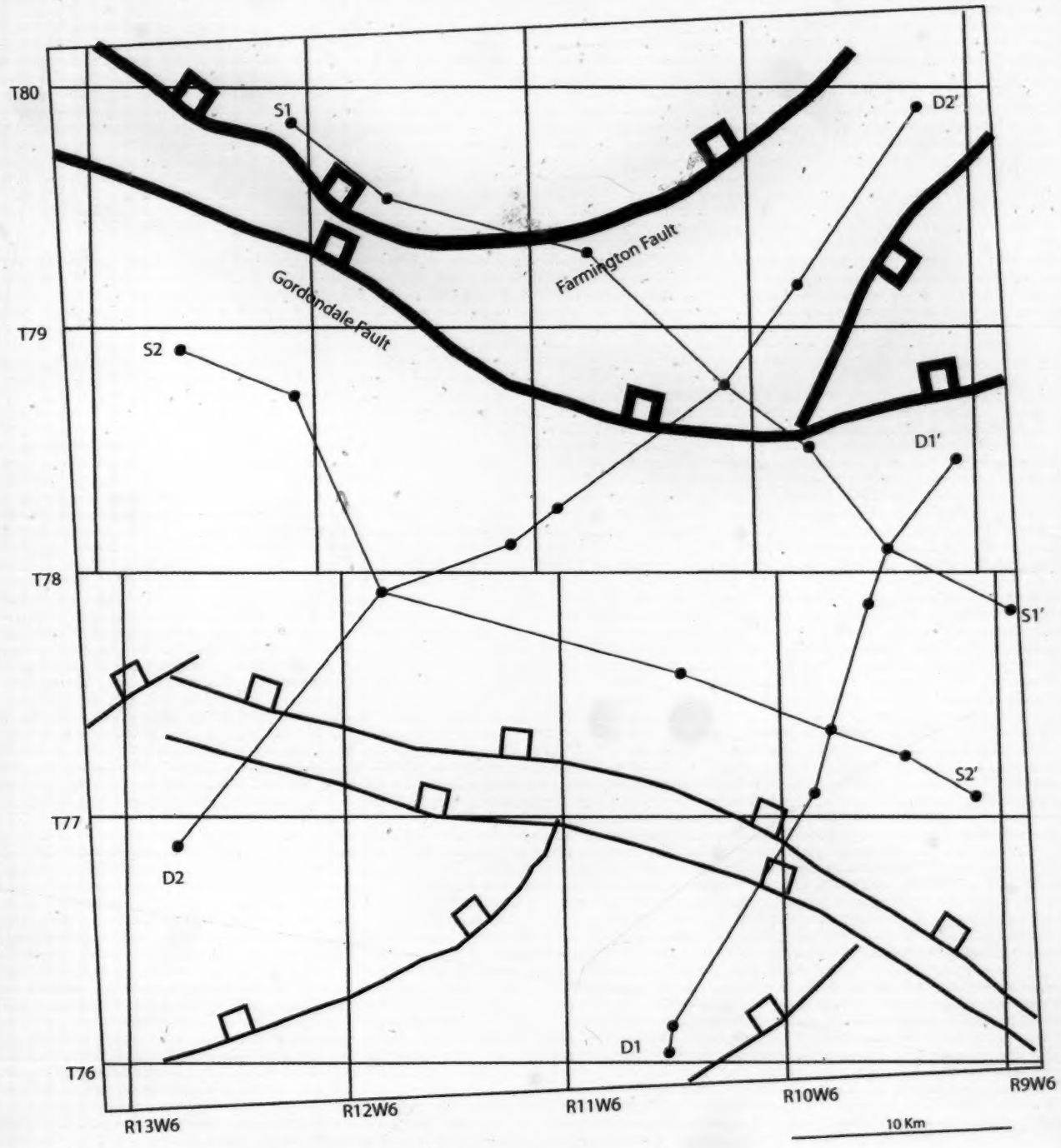


**Figure 3.9.** Base map illustrating cross-section placement and fault location. Modified after Richards et al., (1994).

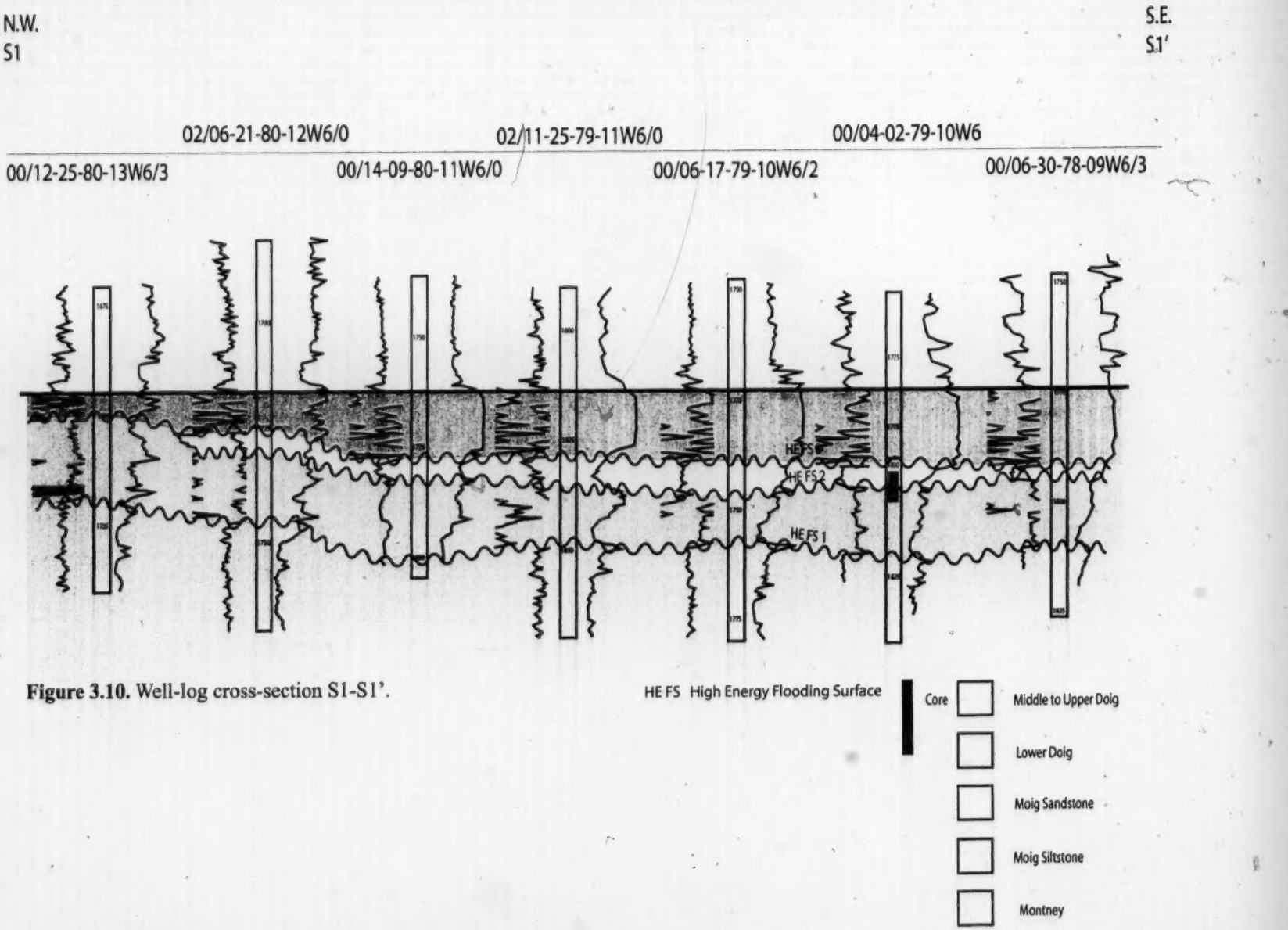


**Figure 3.10.** Well-log cross-section S1-S1'.

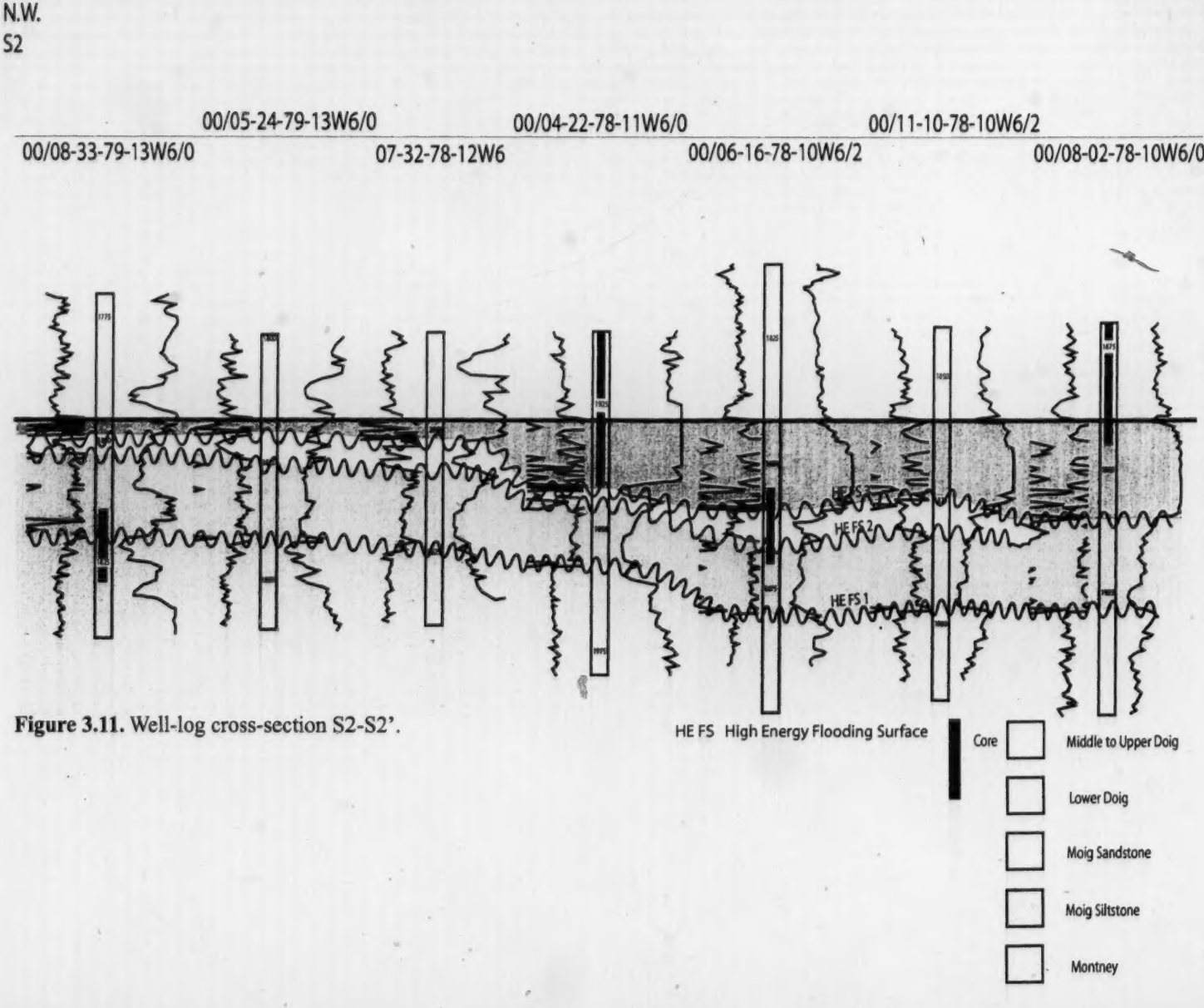


**Figure 3.11.** Well-log cross-section S2-S2'.

S.W.
D1

N.E.
D1'

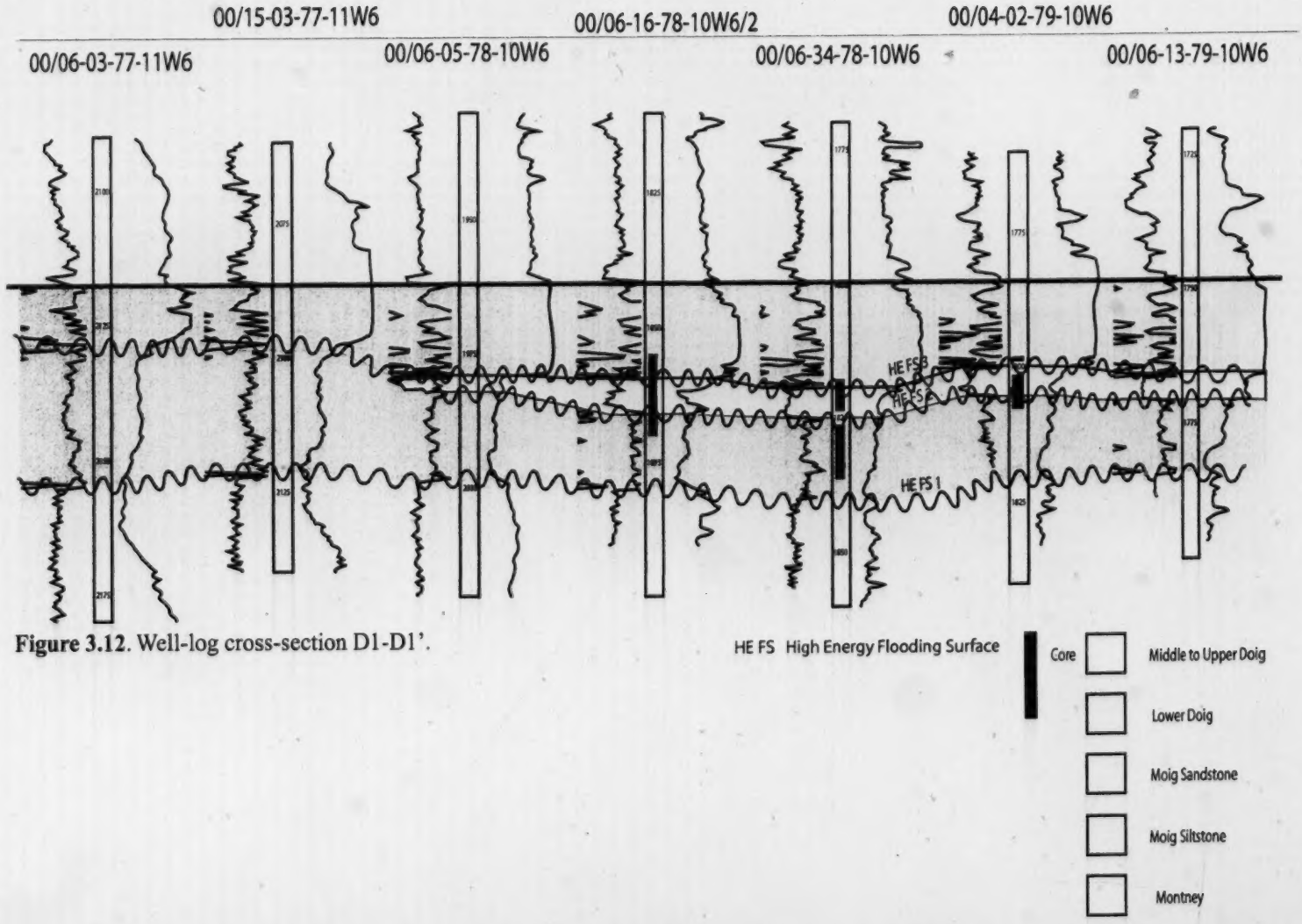


**Figure 3.12**. Well-log cross-section D1-D1'.

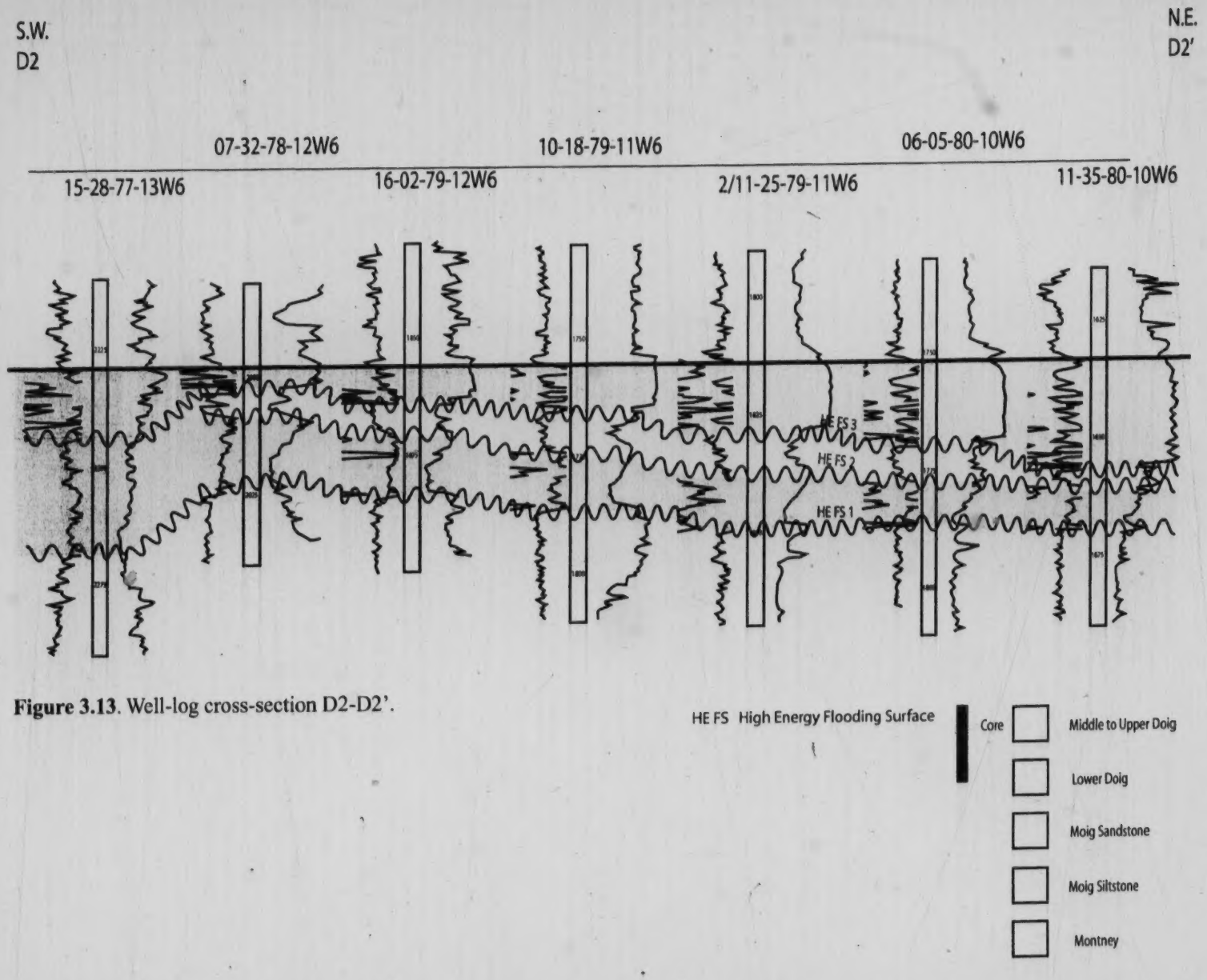


**Figure 3.13**. Well-log cross-section D2-D2'.

## 3.5 DEPOSITIONAL MODEL

Facies analysis for the Moig Siltstone, Moig Sandstone, and Lower Doig Formation convey deposition from shelf to lower shoreface (Figure 3.14). Core analysis based on sedimentology and ichnology exposed a three stage depositional system reflecting three facies associations. The three facies associations are found to be transgressive transition zone to proximal upper offshore deposits, stillstand transition zone to proximal lower shoreface deposits, and stillstand shelfal deposits with storm sands, relic sands, and distal debris flows. These depositional systems are interpreted to reflect a transgressive systems tract that was structurally controlled by underlying Paleozoic faults (see maps).

### *3.5.1 Depositional model 1 Moig Siltstone*: Transgressive Transition Zone to Proximal Upper Offshore.

The Moig Siltstone is a storm-dominated, structurally controlled facies association encompassing transition zone facies (F1 and F2), which are overlain by proximal upper offshore deposits (F3 and F4). The base of this association is characterized by a ravinement surface (HE FS 1) and associated lag deposit (F5a). The top of this association was eroded by a transgressive surface of erosion (HE FS 2 Facies F5b) overlain by the Moig Sandstone. For the most part, the Moig Siltstone displays an overall deepening of facies representing a transgressive event.

In the transition zone, virtually all sedimentary bedding has been cannibalized by *Scolicia*. As mention previously in chapter two, the transition zone in the Moig Siltstone is similar to the transition zone in the Gulf of Gaeta where most of the original bedding has been destroyed by *Scolicia* creating a homogenous appearance to the fine-grained sands (Reineck and Singh, 1980).

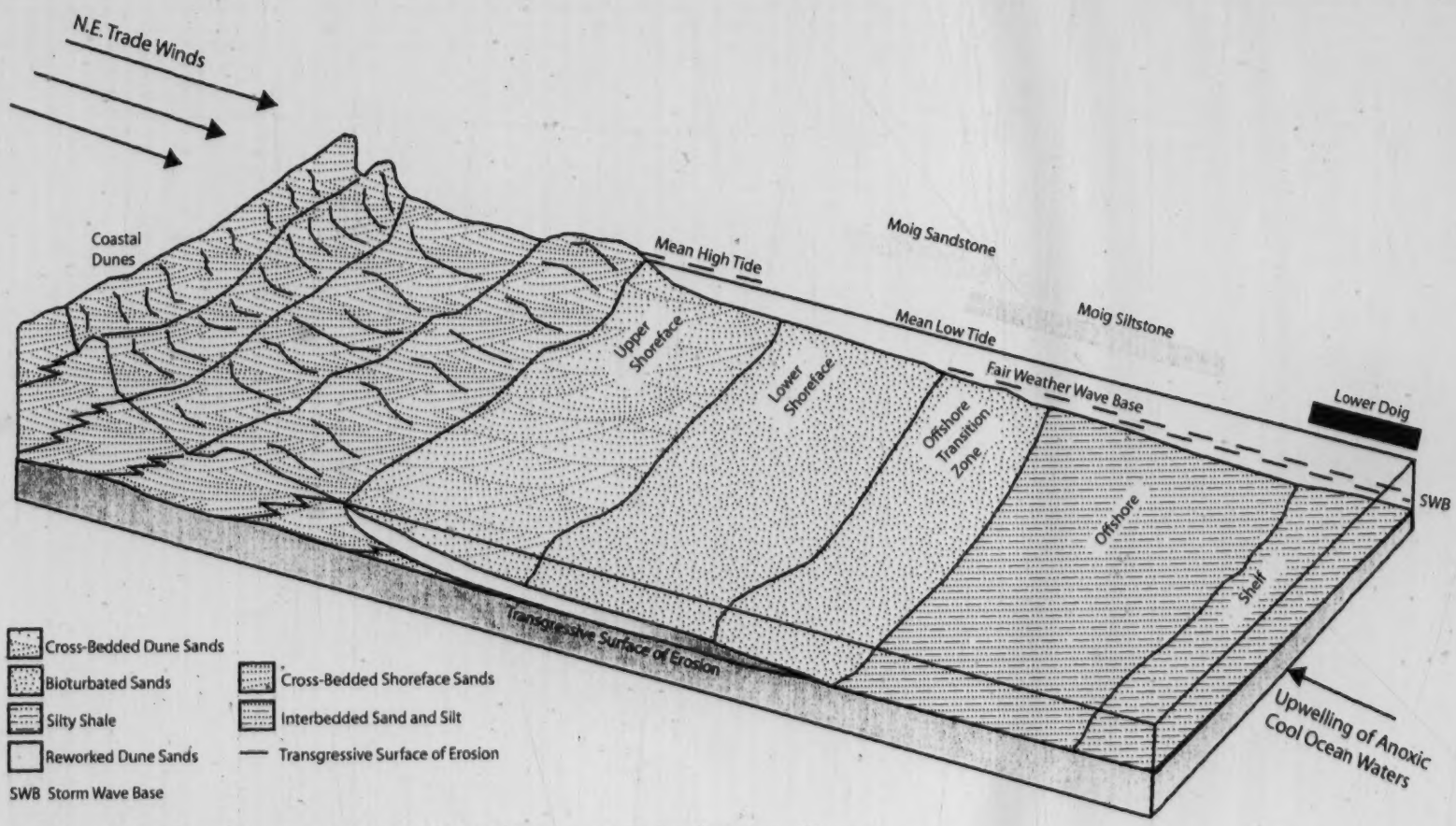


**Figure 3.14.** Depositional model for the Moig Siltstone, Moig Sandstone, and Lower Doig. Modified after Howell (2005).

In the upper offshore, bioturbation is reduced in comparison to a typical fair-weather offshore model characterized by a high diversity and uniform distribution of ichnogenera (Pemberton et al., 2001). Some examples of the typical fair-weather upper offshore models with high diversity and uniform distribution of ichnogenera come from the Doe Creek Member (Reid, 2005) and the Viking Formation (MacEachern and Pemberton, 1992; MacEachern, 1994; Pemberton et al., 2001) of the WCSB. Even in storm-dominated settings, bioturbation occurs when wave energy decrease and fairweather deposition of the food sources increases allowing for favorable opportunistic feeding (Pemberton et al, 2001). The settling of fine sediments can be attributed to waning of the storm followed by minor bioturbation. In most storm-dominated scenarios, such as the Cardium Formation of the WCSB (Pemberton et al., 2001) or the Blackhawk Formation in Utah (Pemberton et al., 1992), bioturbation occurs at the top of the storm unit.

Conversely, in the storm dominated Moig Siltstone upper offshore facies (F3 and F4), there is a low diversity of ichnogenera, localized distribution of ichnogenera, and rare burrowing of the top of storm beds. *Scolicia*, fugichnia, *Phycosiphon*, *Lockeia*, and *Planolites*, as well as cryptic traces are observed in this unit. This low-diversity, stressed expression of the *Cruziana* ichnofacies can be attributed to an aeolian sourced, anoxic, storm-dominated environment with high sedimentation rates. Howard (1975) noted that larger successions of rhythmically laminated beds (HCS) with minor amounts of bioturbation at the top of the event beds resemble an environment where there is a high rate of deposition and or anoxic events. These characteristics noted by Howard (1975) closely parallel the depositional setting, sedimentary structures, and ichnological signatures of the Moig Siltstone.

### 3.5.2 *Depositional model 2 Moig Sandstone:* Stillstand Transition Zone to Proximal Lower Shoreface.

The Moig Sandstone is a highly bioturbated, structurally controlled association, which includes transition zone (F6) deposits overlain by distal to proximal lower shoreface (F7a, F7b) deposits. The Moig Sandstone reflects a transgressively incised stillstand shoreface with minor fluctuations in sea level preserved as thin beds of muddy wavy parallel lamination. The base of this association is represented by a transgressive lag deposit (Facies F5b) infilling traces characterizing a *Glossifungites* ichnofacies on the FS/SB 2 surface. The Moig sands are capped by another transgressive lag deposit (Facies F5c) that is not associated with a *Glossifungites* ichnofacies in this case (FS/SB 3 and FS/SB 4).

The depositional model proposed herein for the Moig Sandstone is a transgressively incised low energy stillstand shoreface sourced from dune silt and sands. Ichnological signatures confirm a relatively unstressed transition zone to a proximal lower shoreface environment as the sediments have been highly reworked (c.f. Moslow and Pemberton, 1988).

The Moig Sandstone has characteristics similar to the low energy shoreface succession of the Albian Viking Formation in the Chigwell Field described by Raychaudhuri et al. (1992). In their interpretation the low energy shoreface deposits of the Viking Formation are sandwiched between two local erosional surfaces. The Viking Facies 3 directly overlies the first erosional surface consisting of vFU to upper fine (FU) sandstone. In this facies a high degree of bioturbation occurs by a mixed assemblage of *Cruziana* and *Skolithos* ichnofacies, which erases all previous sedimentary structures (Raychaudhuri et al., 1992). The only sediments resembling the formation of structures are wispy laminations interpreted to be horizontal *Ophiomorpha* burrows (Raychaudhuri et al., 1992). Directly overlying the Viking Formation Facies 3 is Faces 4 represented

by bioturbated and cross bedded medium grained sandstones representing the middle and upper shoreface deposits. Facies 3 of the Viking Formation closely resembles the Moig Sandstone unit with complete bioturbation by dominant *Cruziana* ichnofacies and less common *Skolithos* ichnofacies (Facies F7a and F7b). The Moig Sandstone is also sandwiched between two erosional surfaces (HE FS 2 and HE FS 3). In contrast to the Viking Formation the base of the Moig Sandstone can contain wavy bedded structure with moderate bioturbation (Facies 6) representing deposition in a transition zone. These transition zone facies possibly resemble once thin reworked regressive shoreface deposits. In the Moig Sandstone there are no deposits representing the middle and upper shoreface since the HE FS 3 has eroded all these deposits. Since this was the case the middle to upper shoreface deposits of the Moig Sandstone we no thicker than the FWWB (5-15 m).

Both the Moig Sandstone and the Viking Formation of the Chigwell Field represent a low energy shoreface. This interpretation is derived from lack of sedimentary structures and a diverse and abundant trace fossil suite. The lack of sedimentary structures would imply that there was a slow deposition of sediments in thin beds allowing for complete churning of sediments by organisms; therefore, large storms, salinity fluctuations, anoxia and other environmental factors were not significant factors during deposition.

It is possible that the Moig Sandstone is derived from reworked dune deposits upon transgression. Evidence for an aeolian source includes grain sizes no larger than fine-grained sand, which is easily transported by west flowing jetstream similar to northwest Africa at present day. The Montney Formation, which underlies the Moig units also contains silts and fine-grained sands derived from a desert source (Davies, 1997b). Furthermore Davies (1997b) also found the presence of frosted or pitted sand grains present in the Montney Formation, and the author speculated that this was also the case in distal settings of the Doig Formation. These distal settings in the Doig are probably the

Lower Doig stillstand and the Moig Siltstone deposits. Possible analogs are the Brushy Canyon, San Andres, and basal Grayburg formations found in the Permian Delaware Basin. In the Brushy Canyon dunes supplied sediment to the shallow and deep marine environments by sheet floods and wind blown deposits where they were populated by organisms (Fischer and Sarnthein, 1987). In the San Andes and basal Grayburg sand dunes were incorporated into the depositional system by transgression (Meissner, 1982). Its is speculated that the Moig Sandstone was in fact sourced by dunes similar to those seen in the Permian and Pleistocene and cannibalized by the preceding transgressive event.

### 3.5.3 *Depositional model 3 Lower Doig Formation:* Stillstand Shelfal Deposits with Storm Sands and Distal Debris Flows.

The Lower Doig is an overall transgressive package containing distal stillstand deposits. The base of this association is demarcated by a major transgressive surface of erosion (FS/SB 3) and associated lag deposits (F5c). Sand from the Upper Doig may be present in a thin (15 cm or less) bed overlying this erosive surface, which is generally subjected to opportunistic feeding by *Rhizocorallium* and *Scolicia*. Sharply overlying the erosive surface is Facies F8, which is a highly organic-rich shale. The facies overlying F8 can be quite variable in the degree of sand, silt, and mud content. These overlying facies (F9, F10, and F11) contain flame structures, planar laminations, dish and pillar structures, and some deformed lenticular bedding. These structures likely may be storm-derived or related to distal expressions of debris flows (Wittenberg, 1992). Also present are a series of erosive surfaces (FS/SB 3-5) with associated lag deposits. The most pronounced in core of the erosive surfaces with a lag deposit (F5c) is HE FS 3. In a landward direction this association may correlate with the Doig parasequences described by Wittenberg (1992). Wittenberg (1992) recognized that each progradational cycle in

the Doig is capped or bounded by phosphatic shale interpreted as a condensed section associated with transgression. These phosphatic shales with varying sand and silt content are associated with deposition in a shelf environment (Gibson and Barclay, 1989), and characterize the Lower Doig Formation.

Another significant factor in relation to sedimentological and ichnological expressions in this depositional setting is fluctuating oxygen levels. Typically, shelf deposits are anoxic and contain pyrite, phosphates, organic material, and unbioturbated sediments (Hallam, 1994; Martin, 2004). Anoxia has been recognized to effect the diversity and distribution of traces (Twitchett and Wignall, 2003). Isozaki (1994) called the time between Permian to Middle Triassic the "superanoxia" time, which created great stress on organisms by reducing available oxygen levels. This "superanoxia" event resulted in mass extinction at the Permo-Triassic boundary and concordantly greatly reduced trace fossil diversity (Twitchett and Wignall, 1996). Davies (1997a) speculated that during Triassic time, ocean waters were depleted in oxygen and there were seasonal phytoplankton blooms. The phytoplankton consumed large amounts of oxygen, which created an anoxic event insuring a stressed suite of traces. Robertson (1984) also proposed that an increase in organic mater sourced from black shales of the Cretaceous aged Atlantic Ocean Basin could have resulted in a decrease in oxygen levels therefore creating an anoxic event. In the Lower Doig some sediments are bioturbated, there is less pyrite, as well as a slight decrease in phosphate content. The presence of bioturbation, lack of pyrite, and lack of phosphate represents fluctuations in oxygen levels. As mentioned previously some of these sediments are probably sourced by wind blown dune deposits (Davies, 1997b).

## 3.6 FUTURE WORK

Limited amounts of core through all three units within the study allows for

constant speculation of paleogeography, stratigraphy, and depositional settings. More core should be introduced into the study area to further back up interpretations discussed in the chapters. With an increase in core a good study of digenesis may be completed with the aid of thin sections, XRD and SEM. This may help to resolve the varying amounts of anhydrite, calcite and dolomite cements seen in core and not study in detail in this thesis.

Branching the study area out into B.C. would be highly beneficial to see how the Moig units and Lower Doig Formation change in a depositional and stratigraphic nature. This would have huge implications to the oil and gas industry since there is now a large emphasis for drilling and completing Upper Montney zones, which may correlate to any of the three units studied herein. Some of these Upper Montney completions can be found in the Swan and Dawson Fields on the edge of the B.C./Alberta boundary.

# CHAPTER FOUR

## CONCLUSIONS

1. The Moig Siltstone, Moig Sandstone, and Lower Doig Formation were deposited in northwestern Alberta during the early (Spathian) Triassic time. Both the Moig Siltstone and Moig Sandstone are clastic wedges bound by high energy flooding surfaces (HE FS 1 – HE FS 3). The overall succession of the three units studied demonstrates deposition during a time in transgression with retrogradational/ stillstand events characterizing the Moig Sandstone and the Lower Doig deposits.

2. Facies analysis revealed fifteen facies based on detailed sedimentological and ichnological descriptions. These fifteen facies were limited to three facies associations represented by transgressive transition zone to proximal upper offshore deposits (FA SO, Moig Siltstone), stillstand transition zone to proximal lower shoreface deposits (FA B, Moig Sandstone), and stillstand shelf deposits with storm sands and distal debris flows (FA SS, Lower Doig).

3. Mapping and cross-sections revealed unusual morphologies not characteristic of typical clastic depositional packages. Two main reasons for varying morphologies are the influence from the underlying Paleozoic faults and scouring by high energy flooding surfaces attempting to maintain the shoreface profile.

## REFERENCES


Amati, L., Feldmann, R.M. and Zonneveld, J-P. 2004. A new family of Triassic Lobsters (Decapoda: Astacidea) from British Columbia and a cladistic analysis of the infraorders Astacidea and Palinura: Journal of Paleontology, v. 78, p. 150-168.

Armitage, J.H. 1962. Triassic oil and gas occurrences in northeastern British Columbia, Canada. Journal of Alberta Society of Petroleum Geologists, v. 10, p. 35-56.

Aukes, P.G. and Webb, T.K. 1986. Triassic Spirit River Pool, northwestern Alberta. In: Canadian Society of Petroleum Geologists, 1986 Core Conference, Calgary, Alberta, Canada. N.C. Meijer Drees (ed.). p. 3.1-3.34.

Bann, K.L. and Fielding, C.R. 2004. An integrated ichnological and sedimentological comparison of non-deltaic shoreface and subaqueous delta deposits in Permian reservoir units of Australia, in McIlroy, D. (ed), The Application of Ichnology to Palaeoenvironmental and Stratigraphic Analysis, Lyell Meeting 2003, The Geological Society of London, v. 228, p. 273-307.

Barss, D.L., Best, E.W. and Meyers, N. 1964. Triassic, Chapter 9. In: Geological History of Western Canada. R.G. McCrossan and R.P. Glaister (eds.). Calgary, Alberta Society of Petroleum Geologists, p. 113-136.

Blatt, H. 1982. Phosphorites (Ch. 16). In: Sedimentary Petrology. W.H. Freeman and Company, San Francisco, p. 424-443.

Brack, L., Abbott, G.M., Noble, I.A. and Tang, R.C.W. 1989. Chapter 7 - Triassic/ Jurassic Fields. In: Geophysical Atlas of Western Canadian Hydrocarbon Pools. N.L. Anderson, L.V. Hills, and D.A. Cederwall (eds.). The Canadian Society of Exploration Geophysicists and The Canadian Society of Petroleum Geologists, p. 187-215.

Barclay, J.E., Krause, F.F., Campbell, R.I. and Utting, J. 1990. Dynamic casting and growth faulting of the Dawson Creek Graben Complex: Carboniferous-Permian Peace River Embayment, Western Canada. In: Geology of the Peace River Arch. S.C. O'Connell and J.S. Bell (eds.). Bulletin of Canadian Petroleum Geology, v. 38A, p. 115-145.

Barclay, J.E. and Leckie, D.A. 1986. Tidal inlet reservoirs of the Triassic Halfway Formation, Wembley Region, Alberta. In: 1986 Core Conference. N.C. Meijer Drees (ed.). Canadian Society of Petroleum Geologists, Calgary, Alberta, p. 4.1-4.6.

Bird, T.D., Barclay, J.E., Campbell, R.I. and Lee, P.J. 1994. Triassic gas resources of the Western Canada Sedimentary Basin, Interior Plains. Geological Survey of Canada

Bulletin 483, p.1-66.

Brenchley, P.J. 1985. Storm Influenced Sandstone Beds. Modern Geology, v. 9, p. 369-396.

Brenchley, P.J. and Williams, B.P.J. 1985. Sedimentology: recent developments and applied aspects. Blackwell Scientific Publications, Boston, 342p.

Buatois, L.M., Mangano, G., Gingras, M.K., MacEachern, J.A., Martin, A., Netto, R., Pemberton, S.G. and Zonneveld, J-P. in press. Colonization of brackish-water systems through time: evidence from the trace fossil record. Palaios, v. 20, No. 4, p. 321-347.

Callaway, J.M. and Brinkman, D.B. 1989. Ichthyosaurs (Reptilia, *Ichthyosauria*) from the Lower and Middle Triassic Sulphur Mountain Formation Wapiti lake area, British Columbia, Canada. Canadian Journal of Earth Sciences, v. 26, p. 1491-1500.

Campbell, C.V. and Horne, J.C. 1986. Depositional facies of the Middle Triassic Halfway Formation, Western Canada Sedimentary Basin. In: Modern and ancient shelf clastics: a core workshop. T.F. Moslow and E.G. Rhodes (eds.). Society of Economic Paleontologists and Mineralogists, core workshop No. 9, Atlanta, June 15, 1986, p. 413-459.

Campbell, C.V. and Hassler, G. 1989. Stratigraphy and facies of the Triassic Halfway and Doig Formations in west-central Alberta. C.S.P.G. Reservoir, Abstract, v.16, p. 2.

Campbell, C.V., Dixon, R.J. and Forbes, D.M. 1989. Updip erosional truncation of Halfway and Doig shoreline sequences: a new model for exploration in west central Alberta (Abstract). In: Exploration Update 1989 - Integration of Technologies, Program and Abstracts. Canadian Society of Petroleum Geologists Convention, Calgary, Alberta, p. 138.

Cant, D.J. 1984. Possible syn-sedimentary tectonic controls on Triassic reservoirs, Halfway, Doig, Charlie Lake formations, west-central Alberta (Abstract). In: Exploration Update '84 - Interaction for Success Through the 80's, Program and Abstracts, Canadian Society of Petroleum Geologists National Convention, Calgary, p. 45.

Cant, D.J. 1986. Hydrocarbon trapping in the Halfway Formation (Triassic), Wembley Field, Alberta. Bulletin of Canadian Petroleum Geology, v. 34, p. 329-338.

Cant, D.J. 1988. Regional structure and development of the Peace River Arch, Alberta: a Paleozoic failed-rift system? Bulletin of Canadian Petroleum Geology, v. 36, p. 284-295.

Caplan, M.L. and Moslow, T.F.1999. Depositional origin and facies variability of a Middle Triassic barrier island complex, Peejay Field, northeastern British Columbia. American Association of Petroleum Geologists Bulletin, v. 83, p. 128-154.

Cattaneo, A. and Steel, R. 2003. Transgressive Deposits: a review of their variability. Earth-Science Reviews, v. 62, p. 187-228.

Catuneanu, O., 2006. Principles of sequence stratigraphy. Elservier, Amsterdam, Netherlands. 375p.

Creaney S. and Allan J. (1990) Hydrocarbon generation and migration in the Western Canadian Sedimentary Basin. In Classical Petroleum Provinces (ed. J. Brooks); Geological Society Special Publication. 50,189-202.

Davies, G.R. 1997a. The Triassic of the Western Canadian Sedimentary Basin: tectonic and stratigraphic framework, paleogeography, paleoclimate and biota. Bulletin of Canadian Petroleum Geology, v.45, p.434-460.

Davies, G.R. 1997b. Aeolian sedimentation and bypass ,Triassic of Western Canada. Bulletin of Canadian Petroleum Geology, v.45, p.624-642.

Davies, G.R. 1997c. The Upper Triassic Baldonnel and Pardonet formations, Western Canadian Sedimentary Basin. Bulletin of Canadian Petroleum Geology, V. 45, p. 643-674.

Davies, G.R., Moslow, T.F. and Sherwin, M.D. 1997a. The Lower Triassic Montney Formation, west-central Albert. Bulletin of Canadian Petroleum Geology, v.45, p. 474-505.

Davies, G.R., Moslow, T.F. and Sherwin, M.D. 1997b. Ganoid fish *Albertonia sp.* from the Lower Triassic Montney Formation, Western Canadian Sedimentary Basin. Bulletin of Canadian Petroleum Geology, v.45, p. 715-718.

Dawson, G. M. 1881. Report on a exploration from Port Simpson on the Pacific Coast to Edmonton on the Saskatchewan, embracing a portion of the Northern part of British Columbia and the Peace River Country. Geol. Nat. Hist. Surv., Canada, Report of Progress 1879-80, part B, p. 1-177.

Demarest, J.M. and Kraft, J.C. 1987. Stratigraphic record of Quaternary sea levels: implications for more ancient strata. In sea level fluctuation and coastal evolution (D. Nummedal, O.H. Pilkey and J.D. Howard, Eds.), SEPM Special Publication 41. P. 223-239.

Dickins, J.M. 1993. Climate of the Late Devonian to Triassic. Palaeogeography,

Palaeoclimate, Palaeoecology, v.100, p. 89-94.

Dilek, Y. 1994. The model and nature of continental rifting along the northwestern periphery of Gondwanaland during the break-up of Pangea. In: Pangea: Global Environments and Resources. A.F. Embry and B. Beauchamp (eds.). Canadian Society of Petroleum Geologists, Memoir 17, p. 113-121.

Dixon, J. 1999. Isopach maps of Triassic units in the Trutch (94-G) map area (Central Forelands Natmap). Geological Survey of Canada Open File 3765.

Dixon, J. 2002a. A modification of Wittenberg's model for the deposition of thick sandstone bodies in the Triassic Doig Formation, Wembley area, west-central Alberta. Bulletin of Canadian Petroleum Geology, v.50, p. 393-406.

Dixon, J. 2002b. Triassic stratigraphy in the subsurface of the Trutch (94-G) map-sheet, northeast British Columbia, Central Foreland Natmap Project. Geological Survey of Canada Open File 3465.

Dixon, J. 2005. A major unconformity at the base of the Upper Triassic Charlie Lake Formation in the Western Canada Sedimentary Basin. Bulletin of Canadian Petroleum Geology, v. 53, p. 432-453.

Dott, H.R. 1983. 1982 SEPM Presidential Adress: Episodic Sedimentation - How Normal is Average? How Rare is Rare? Does it Matter? Journal of Sedimentary Petrology 53, p. 5-23.

Edwards, D.E., Barclay, J.E., Gibson, D.W., Kvill, G.E. and Halton, E. 1994. Triassic strata of the Western Canadian Sedimentary Basin. In: Geological Atlas of the Western Canadian Sedimentary Basin. G.D. Mossop and I. Shetson (comps.). Canadian Society of Petroleum Geologists and Alberta Research Council, p. 257-275.

Embry, A.F. and Gibson, D.W. 1995. T-R sequence analysis of the Triassic succession of the Western Canadian Sedimentary Basin. In: Proceedings of the Oil and Gas Forum '95 – Energy from Sediments. J.S. Bell, T.D. Bird, T.L. Hillier and P.L. Greener (eds.). Geological Survey of Canada, Open File 3058, p. 25-28.

Embry, A.F. 1997. Global sequence boundarys of the Triassic and their identification in the Western Canada Sedimentary Basin. Bulletin of Canadian Petroleum Geology, v.45, p. 415-433.

Evoy, R.W. 1995. The Role of Sediment Bypassing In Siliclastic Facies Variability on the Continental Shelf: Examples from the Fraser River delta foreslope and the Middle Triassic Doig Formation. Ph.D thesis, University of Alberta, Edmonton, Alberta, 452 p.

Evoy, R.W. and Moslow, T.F. 1995. Lithofacies associations and depositional environments in the Middle Triassic Doig Formation, Buick Creek Field, northeastern British Columbia. Bulletin of Canadian Petroleum Geology, v. 43, p. 461-475.

Evoy, R.W. 1997. Lowstand shorefaces in the Middle Triassic Doig Formation: implications for hydrocarbon exploration in the Fort St. John area, northeastern British Columbia. Bulletin of Canadian Petroleum Geology, v. 45, p. 537-552.

Faraj, B. 2003. Shale gas potential of selected formations from the WCSB of Western Canada. In: 5th Annual Unconventional Gas and Coalbed Methane Conference Procedings, 2003, Calgary.

Fischer, A.G. and Samthein, M. 1987. Airborne silts and dune-derived sands in the Permian of the Delaware Basin. Journal of Sedimentary Petrology, v. 58, no 4, p. 637-643.

Forstner, U. and Muller, G., Reineck, H. E. 1968. Sedimente und Sedimentgefuge des Rheindeltas im Bodensee. Neues Jahrb. Mineral, Abhandl, v. 109, p. 33-62.

Frey, R.W. and Pemberton, S.G. 1985. Biogenic structures in outcrops and cores I—approaches to ichnology: Bulletin of Canadian Petroleum Geology, v. 33, p. 72–115.

Frey, R.W. 1990. Trace fossils and hummocky cross-stratification, Upper Cretaceous of Utah: Palaios, v. 5, p. 203–218.

Fu, S. and Werner, F. 2000. Distribution, ecology and taphonomy of the organism trace, *Scolicia*, in northeast Atlantic deep-sea sediments: Paleogeography, Paleoclimatology, Paleoecology, v. 156, p. 289-300.

Gibson, D.W. 1968a. Triassic stratigraphy between the Athabasca and Smoky rivers of Alberta. Geological Survey of Canada, Paper 67-65.

Gibson, D.W. 1968b. Triassic stratigraphy between Athabasca and Brazeau rivers of Alberta. Geological Survey of Canada, Paper 68-11.

Gibson, D.W. 1969. Triassic stratigraphy of the Bow River-Crowsnest Pass region, Rocky Mountains of Alberta and British Columbia. Geological Survey of Canada, Paper 68-29.

Gibson, D.W. 1970. Triassic stratigraphy, Pine Pass area, northeastern British Columbia. *In*: Peace River-Pine Pass-Yellowhead, Field Conference Guidebook. G.L. Bush and J. Dooge (eds.). Edmonton Geological Society, p. 23-38.

Gibson, D.W. 1971a. Triassic stratigraphy of the Sikanni Chief River-Pine Pass region, Rocky Mountain Foothills, northeastern British Columbia. Geological Survey of Canada, Paper 70-31.

Gibson, D.W. 1971b. Triassic petrology of Athabasca-Smoky River region, Alberta. Geological Survey of Canada, Bulletin 194.

Gibson, D.W. 1972. Triassic stratigraphy of the Pine Pass-Smoky River area. Rocky Mountain Foothills and Front Ranges of British Columbia and Alberta. Geological Survey of Canada, Paper 71-30, 108 p.

Gibson, D.W. 1974. Triassic rocks of the southern Canadian Rocky Mountains. Geological Survey of Canada, Bulletin 230.

Gibson, D.W. 1975. Triassic rocks of the Rocky Mountain Foothills and Front Ranges of northeastern British Columbia and west-central Alberta. Geological Survey of Canada, Bulletin 247.

Gibson, D.W. and Barclay, J.E. 1989. Middle Absaroka Sequence: The Triassic stable craton. *In*: The Western Canada Sedimentary Basin - A Case History. B.D. Ricketts (ed.). Calgary, Canadian Society of Petroleum Geologists, Special Publication no. 30, p. 219-232.

Gibson, D.W. and Edwards, D.E. 1990a. Triassic stratigraphy and sedimentary environments of the Williston Lake area and adjacent subsurface Plains, northeastern British Columbia. Field Trip Guidebook No. 6, Canadian Society of Petroleum Geologists, Basin Perspectives Conference, May 27-30, 1990, Calgary, Alberta.

Gibson, D.W. and Edwards D.E. 1990b. An overview of Triassic stratigraphy and depositional environments in the Rocky Mountain Foothills and Western Interior Plains, Peace River Arch area, northeastern British Columbia. Bulletin of Canadian Petroleum Geology, v. 38A, p. 146-158.

Golonka, J., Ross, M.I. and Scotese, C.R. 1994. Phanerozoic paleogeographic and paleoclimatic modeling maps. In: Pangea: Global Environments and Resources. A.F. Embry, B. Beauchamp and D. Glass (eds.). Canadian Society of Petroleum Geologists, Memoir 17, p. 1-47.

Habicht, J.K.A. 1979. Paleoclimate, paleomagnetiam, and continental drift. AAPG Studies in Geology No. 9, American Association of Petroleum Geologists, Tulsa, Oklahoma, U.S.A., 31 p.

Hallam, A. 1994. The earliest Triassic as an anoxic event, and its relationship to the end-Paleozoic mass extinction. In: Pangea: Global Environments and Resources.

A.F. Embry and B. Beauchamp (eds.). Canadian Society of Petroleum Geologists, Memoir 17, p. 797-804.

Harris, R.G. 2000. Triassic Doig Formation Sand bodies in the Peace River Area of Western Canada: Depositional and Structural Models, and the Impact of Diagenesis on Reservoir Properties. Unpublished M.Sc. Thesis. University of British Columbia, Vancouver, British Columbia, 205 p.

Harris, R.G. and Bustin, M.R. 2000. Diagenesis, reservoir quality, and production trends of the Doig Formation sand bodies in the Peace River area of Western Canada. Bulletin of Canadian Petroleum Geology, v. 48, p. 339-359.

Henderson, C.M. 1989. Absaroka Sequence - The Lower Absaroka Sequence: Upper Carboniferous and Permian. In: Western Canada Sedimentary Basin - A Case History. B.D. Ricketts (ed.). Canadian Society of Petroleum Geologists, Special Publication No. 30, Calgary, Alberta, p. 203-217.

Higgs, R.Y. 1990. Sedimentology and petroleum geology of the Artex Member (Charlie Lake Formation), northeast British Columbia (Abstract). In: Bulletin of Canadian Petroleum Geology, v. 38, p. 166.

Hitchon, B., Bachu, S. and Underschultz, J.R. 1990. Regional subsurface hydrogeology, Peace River Arch area, Alberta and British Columbia. Bulletin of Canadian Petroleum Geology, v. 38A, p. 196-217.

Howard, J.D. 1975. The sedimentological significance of trace fossils. *In*: R.W. Frey, ed., The Study of Trace Fossils, p. 131-146, Springer-Verlag, New York.

Howard, J.D. and Reineck, H.E. 1981. Depositional facies of high energy beach-to-offshore sequence: comparison with low energy sequence. American Association of Petroleum Geologists, Bulletin 65: p. 807-830.

Hunt, A.D. and Ratcliffe, J.D. 1959. Triassic stratigraphy, Peace River area, Alberta and British Columbia, Canada. American Association of Petroleum Geologists, Bulletin, v. 43, p. 563-589.

Isozaki, Y. 1994. Superanoxia across the Permo-Triassic boundary: Record in accreted deep-sea pelagic chert in Japan. In Embry, A.F., B. Beauchamp, and D.J. Glass (eds.) Pangea: Global Environments and Resources. Mem. Canad. Soc. Petrol. Geol. 17, 805–812.

Johnston, H.D. and Baldwin, C.T. 1986. Shallow siliclastic seas. *In*: Reading, H.G., eds., Sedimentary Facies and Environments (2nd edition), p. 229-282.

Jones, A.P. and Omoto, K. 2000. Towards establishing criteria for identifying trigger

mechanisms for soft-sediment deformation: a case study of Late Pleistocene lacustrine sands and clays, Onokibe and Nakayamadaira Basins, northeastern Japan. Sedimentology, v. 47, p. 1211-1226.

Kendall, D.R. 1999. Sedimentology and Stratigraphy of the Lower Triassic Montney Formation, Peace River Basin, subsurface of northwestern Alberta. M.Sc. thesis, University of Calgary, Calgary, Alberta, 293 p.

Kindle, E.D. 1944. Geological reconnaissance along Fort Nelson, Liard and Beaver rivers, northeastern British Columbia and southeastern Yukon: Canada. Geological Survey of Canada, Paper 44-16.

Kirste, D., Desrocher, S., Spence, B., Hoyne, B., Tsang, B. and Hutcheon, I. 1997. Fluid flow, water chemistry, gas chemistry and diagenesis in the subsurface Triassic in Alberta and British Columbia. Bulletin of Canadian Petroleum Geology, v. 45, p. 742-764.

Lowe, D.R. 1975. Water-escape structures in coarse-grained sediments. Sedimentology, v. 22, p. 157-204.

Macauley, G., Procter, R.M. and Tisdall, W.H. 1964. Carboniferous In: Geological History of Western Canada, R.G. McCrossan and R.P. Glaister (eds.). Alberta Society of Petroleum Geologists, Calgary, Alberta, p. 89-102.

MacEachern, J.A. and Burton, J. 2000. Firm Ground *Zoophycos* in the Lower Cretaceous Viking Formation, Alberta: a distal expression of the *Glossifungites* ichnofacies. *Palaios*, **15**, p. 387-398.

MacEachern, J.A. and Pemberton, G.S. 1992. Ichnological aspects of Cretaceous shoreface successions and shoreface variability in the Western Interior Seaway of North America. *In*: Pemberton, S.G. eds, Applications of ichnology to petroleum exploration, a core workshop 17, p. 57-84.

MacEachern, J.A., Raychaudhuri, I. and Pemberton, S.G.1992. Stratigraphic applications of the *Glossifungites* ichnofacies: delineating discontinuities in the rock record, *in* S.G. Pemberton, ed., Applications of ichnology to petroleum exploration, a core workshop: SEPM Core Workshop 17, p. 169–198.

MacEachern, J.A. 1994. Integrated Ichnological-Sedimentological Models: Applications to the Sequence Stratigraphic and Paleoenvironmental Interpretation of the Viking and Peace River Formations, West-Central Alberta. [Ph.D. Thesis]: University of Alberta, Edmonton, Alberta, 612p.

MacEachern, J.A., Pemberton, G. S., Gingras, M.K. and Bann, K.L. 2007. The Ichnofacies Paradigm: Fifty-Year Retrospective. In Miller, W. III (ed), Trace Fossils:

Concepts, Problems, Prospects, p. 52-77.

Martin, K.D. 2004. Are-evaluation of the relationship between trace fossils and dysoxia, *In:* McIlroy, D., ed., The Application of Ichnology to Paleoenvironmental and Stratigraphic Analysis: Geological Society of London, Special Publication **228**, p. 141-156.

Mazumder, R., van Loon, A.J. and Arima, M., 2006. Soft-sediment deformation structures in the Earth's oldest seismites. Sedimentary Geology, v 186., p. 19-26.

McConnell, R.G. 1891. Report on a proportion of the District of Athabaska comprising the country between Peace River and Athabaska River North of Lesser Slave Lake. Geological Survey of Canada, Annual Report. V. V, part I, part D.

McLearn, F.H. and Kindle, E.D. 1950. Geology of northeast British Columbia. Geological Survey of Canada, Memoir 259.

Meissner, F.G., 1982. Cyclic sedimentation in the Middle Permian strata of the Permian Basin, *In*: Elam, J.G., and Chuber, S., eds., Cyclic Sedimentation in the Permian Basin: West Texas Geological Society, p. 203-232.

Miall, A.D. 1976. The Triassic Sediments of Sturgeon Lake South and surrounding areas. *In*: The Sedimentology of Selected Clastic Oil and Gas Reservoirs in Alberta. M. Lerand (ed.). Canadian Society of Petroleum Geology, p. 25-43.

Moslow, T.F. and Davies, G.R. 1992. Triassic Reservoir Facies and exploration Trends: Western Canadian Sedimentary Basin. Canadian Society of Petroleum Geologists, Short Course Number 7 notes, Canadian Society of Petroleum Geologists-American Association of Petroleum Geologists Conference: June 25-26, 1992, Calgary, Alberta, 166 p.

Moslow, T.F. and Davies, G.R. 1993. Triassic reservoir facies and exploration trends: Western Canada Sedimentary Basin. Canadian Society of Petroleum Geologists, Short Course #4 notes.

Moslow, T.F., and Davies, G.R. 1997. Turbidite reservoir facies in the Lower Triassic Montney Formation, west-central Alberta. Bulletin of Canadian Petroleum Geology, v. 45, p. 507-536.

Moslow, T.F. and Pemberton, S.G. 1988. An integrated approach to the sedimentologic analysis of some Lower Cretaceous shoreface and delta front sandstone sequences, in James, D.P., and Leckie, D.A., eds., Sequences, Sedimentology: Surface and Subsurface: CSPG, Memoir 15. p. 373-386.

Moslow, T.F., Willis, A., Wittenberg, J., Caplan, M. and Evoy, R. 2003. Is there a basin-

wide unconformity associated with the Triassic Doig to Charlie Lake succession? No! Canadian Society of Petroleum Geologists, Reservoir, v. 30, Issue 3, p. 28-30.

Munroe, H.D. and Moslow, T.F. 1990. Depositional models for the Doig Formation of northeastern British Columbia. Opportunities for the Nineties, Program and Abstracts, 1991 Canadian Society of Petroleum Geologists Convention, Calgary, Alberta, p. 105.

Munroe, H.D. 1991. Depositional models for the Doig Formation of northeastern British Columbia, Abstract, Bulletin of Canadian Petroleum Geology, v. 39, p. 220.

Obermeier, S.F. 1996. Use of liquefaction-induced features for paleo-seismic analysis. Engineering Geology, v. 44, p. 1-76.

O'Connell, S.C., Dix, G.R. and Barclay, J.E. 1990. The origin, history, and regional structural development of the Peace River Arch, Western Canada. Bulletin of Canadian Petroleum Geology, v. 38A, p. 4-24.

Orchard, M.J. and Tozer, E.T. 1997. Triassic conodont biocronology, its calibration with ammonoid standard, and a biostraigraphic summary for the Western Canada Sedimentary Basin. Bulletin of Canadian Petroleum Geology, v. 45, p. 675-692.

Pelletier, B.R. 1960. Triassic stratigraphy, Rocky Mountain Foothills, northeastern British Columbia 94J and I. Geological Survey of Canada, Paper 60-2.

Pelletier, B.R. 1961. Triassic stratigraphy of the Rocky Mountains and Foothills, northeastern British Columbia. Geological Survey of Canada, Paper 61-8.

Pelletier, B.R. 1963. Triassic stratigraphy of the Rocky Mountains and Foothills, Peace River District, British Columbia, Geological Survey of Canada, Paper 62-26.

Pelletier, B.R. 1964. Triassic stratigraphy of the Rocky Mountain Foothills between Peace and Muskwa rivers, northeastern British Columbia, Geological Survey of Canada, Paper 63-33.

Pelletier, B.R. 1965. Paleocurrents in the Triassic of northeastern British Columbia. In: Primary Sedimentary Structures and their Hydrodynamic Interpretation. G.V. Middleton (ed.). Society of Economic Paleontologists and Mineralogists, Special Publication No. 12, p. 233-245.

Pemberton, S.G. and Frey, R. W. 1984. Ichnology of storm-influenced shallow marine sequences: Cardium Formation (Upper Cretaceous) at Seebe, Alberta. *In*: Scott, D.F. and Glass, D.J., eds, The Mesozoic of middle North America. Canadian Society of Petroleum Geologists Memoir 9, p. 281-304.

Pemberton, S.G. and Frey, R. W. 1985. The *Glossifungites* ichnofacies: modern examples from the Georgia coast, USA *In:* Curran, H.A. (ed.) *Biogenic Structures: Their Use in Interpreting Depositional Environments.* Society of Economic Paleontologists and Mineralogists, Special Publications, Tulsa, Oklahoma, **35**, p. 237-259.

Pemberton, S.G., MacEachern, J.A. and Ranger M.J. 1992. Ichnology and event stratigraphy: The use of trace fossils in recognizing tempestites. In: Pemberton, S.G. eds, Application of ichnology to petroleum exploration, a core workshop. Society of Economic Paleontologists and Mineralogists, Core Workshop 17, p. 85-117.

Pemberton, S.G., MacEachern, J.A. and Saunders, T. 2004. Stratigraphic applications of substrate-specific ichnofacies: delineating discontinuities in the rock record, *in* McIlroy, D., ed., The Application of Ichnology to Paleoenvironmental and Stratigraphic Analysis: Geological Society of London, Special Publication **228**, p. 29-62.

Pemberton, S.G., Spila, M., Pulham, A., Saunders, T., MacEachern, J., Robbins, D. and Sinclair, I. 2001. *Ichnology and Sedimentology of Shallow and Marginal Marine Systems: Ben Nevis and Avalon Reservoirs, Jean D'Arc Basin.* Geological Association of Canada, St John's, Newfoundland, Short Course Notes, **15**.

Pitman, W.C. 1978. Relationship between eustasy and stratigraphic sequences on passive margins. Geological Society of America, Bulletin 89, p. 1389-1403.

Podruski, J.A., Barclay, J.E., Hamblin, A.P., Lee, P.J., Osadetz, K.G., Procter, R.M. and Taylor, G.C. 1988. Conventional Oil Resources of Western Canada. Geological Survey of Canada Paper 87-26, p. 79-92.

Powers, M.C. 1967. Fluid-release mechanisms in the compacting of marine mudrocks and their importance in oil exploration. A.A.P.G. Bulletin, v. 51, p. 79-92.

Prothero, D.R. and Schawb, F. 2003. Sedimentary Geology: *An Introduction to Sedimentary Rocks and Stratigraphy*, second edition, Freeman and Company, New York, p. 557.

Rahman, B. and Henderson, M. 2005. The Nature and Significance of Erosional Surfaces in the Middle Triassic Doig and Halfway Formations, WCSB. CSPG Core Conference, Core Papers and Abstracts, June 23-24, 2005, Calgary, Alberta, p. 298.

Raychaudhuri, I., Howard, G.B., Pemberton, S.G. and MacEachern J.A. 1992. Depositional facies and trace fossils of a low wave energy shoreface succession, Albian Viking Formation, Chigwell Field, Alberta, Canada, *In*: Pemberton, S.G., ed., Application of Ichnology to Petroleum Exploration: A Core Workshop: SEPM Core Workshop 17, Calgary Alberta, p. 319-337.

Raychaudhuri, I. and Pemberton, S.G., 1992. Ichnologic and sedimentologic characteristics of open marine to storm dominated restricted marine settings within the Viking/Bow Island formations, south-central Alberta, in Pemberton, S.G., ed., Application of Ichnology to Petroleum Exploration: A Core Workshop: SEPM Core Workshop 17, Calgary Alberta, p. 119- 139.

Reid, S.A., 2005. Ichnological and Sedimentological Facies Analysis of the Doe Creek Member of the Kaskapau Formation, Northwest Alberta. M.Sc. thesis, University of Alberta, Edmonton, Alberta, 256 p.

Reineck, H.E. and Singh, I.B. 1980. Depositional sedimentary environments with reference to terrigenous clastics (second edition). Springer-Verlag, New York, 549p.

Richards, B.C. 1989. Upper Kaskaskia Sequence: uppermost Devonian and Lower Carboniferous. In: Western Canada Sedimentary Basin - A Case History. B.D. Ricketts (ed.). Canadian Society of Petroleum Geologists, Special Publication no. 30, Calgary, Alberta, p. 164-201.

Richards, B.C, Barclay, J.E., Bryan, D., Hartling, A., Henderson, C.M. and Hinds, R.C., 1994. Carboniferous strata of the Western Canadian Sedimentary Basin, *In*: Geological Atlas of the Western Canadian Sedimentary Basin. G.D. Mossop and I. Shetson (comps.). Canadian Society of Petroleum Geologists and Alberta Research Council, p 221-250.

Riediger, C.L., Foweler, M.G., Brooks, P.W. and Snowdon, L.R. 1990a. Lower and Middle Triassic source rocks, thermal maturation, and oil-source rock correlations in the Peace River Embayment are, Alberta and British Columbia. Bulletin of Canadian Petroleum Geology, v. 38A, p.218-235.

Riediger, C.L., Foweler, M.G., Brooks, P.W. and Snowdon, L.R. 1990b. Triassic oils and potential Mesozoic source rocks, Peace River Arch area, Western Canada Basin. Organic Geochemistry, v. 16, p. 295-305

Riediger, C.L. 1997. Geochemistry of the potential hydrocarbon source rocks of Triassic age in the Rocky Mountain Foothills of northeastern British Columbia and west-central Alberta. Bulletin of Canadian Petroleum Geology, v. 45, p. 719-741.

Robbins, D.J.C. 1999. Sedimentology and sequence biostratigraphic framework of a mixed siliciclastic–carbonate depositional system, Middle Triassic, northeastern British Columbia. Unpublished M.Sc. thesis, University of Alberta, Edmonton, 149 p.

Robertson, G.E. 1984. Origin of varve-type lamination, graded claystones and limestones-shale 'couplets' in the Lower Cretaceous of the western North Atlantic, *In*: Stow D.A.V. and Piper, D.J.W., eds, Fine-grained sediments: deep water proceses

and facies. Geollogical Society of London Special Publication 15, p. 437-452.

Sarnethein and Diester-Haass, L. 1977. M. Sarnthein and L. Diester-Haass, Eolian-sand turbidites, *Journal of Sedimentary Petrology* **47** (1977) (2), pp. 868–890.

Schaeffer, B. and Mangus, M. 1976. An Early Triassic Fish Assemblage from British Columbia. Bulletin of the American Museum of Natural History, 156, p. 515-564.

Seilacher, A. 1964. Sedimentological classification and nomenclature of trace fossils. Sedimentology 3: 253-256.

Seilacher, A. 1984. Sedimentary structures tentatively attributed to seismic events. Marine Geology, v. 55, p. 1-12.

Silberling, N.J. and Tozer, E.T. 1968. Biostratigraphic classification of the marine Triassic in North America. Geological Society of America, Special Paper, 110 p.

Sims, J.D. 1975. Determining earthquake reoccurrence intervals from deformation structures in young lacustrine sediments. Tectono-physics, v. 29, p.144-152.

Stelck, C.R. (1941). Geology of the Pouce Coupe River Area, Alberta and British Columbia. M.Sc. thesis, University of Alberta.

Swift, D.J.P. 1968. Coastal erosion and transgressive stratigraphy. Journal of Geology, v. 76, p. 444-456.

Swift, D.J.P. 1975. Barrier-island genesis: evidence from the central Atlantic Shelf, eastern U.S.A. *Sedimentary Geology*, Vol. 14, p. 1-43.

Thorne, J.A. and Swift, D.J.P. 1991. Sedimentation on continental margins: VI. A regime model for depositional sequences, their component systems tracts, and bounding surfaces. In: Swift, D.J.P., Oertel, G.F., Tillman, R.W., Thorne, J.A. (Eds.), Shelf Sand and Sandstone Bodies-Geometry, Facies and Sequence Stratigraphy. International Association of Sedimentologists Special Publication, v.14, p. 189-255.

Tozer, E.T. 1961. The sequence of marine Triassic faunas in western Canada. Geological Survey of Canada. Paper 61-6. Tozer, E.T. 1963a. Lower Triassic ammonoids from Tuchodi Lakes and Halfway River areas, northeastern British Columbia. Geological Survey of Canada, Bulletin 96, pt. 1, p. 1-28.

Tozer, E.T. 1962. Illustrations of Canadian Fossils, Triassic of Western and Artic Canada. Geological Survey of Canada, Paper 62-19, p. 1-5.

Tozer, E.T. 1963. *Liquidates* and *Maclearnoceras*, new Triassic ammonoids from the

*Nathorstites* Zone of northeastern British Columbia. Geological Survey of Canada, Bulletin 96, part 2, p. 31-38.

Tozer, E.T. 1965. Lower Triassic Stages and Ammonoid Zones of Artic Canada. Geological Survey of Canada, Paper 65-12, p. 1-14.

Tozer, E.T. 1967. A standard for Triassic time. Geological Survey of Canada, Bulletin 156, p. 1-103.

Tozer, E.T. 1982a. Marine Triassic faunas of North America: Their significance for assessing plate and terrain movements. Geologische Rundschau, v. 71, p. 1077-1104.

Tozer, E.T. 1982b. Late Triassic (Upper Norian) and earliest Jurassic (Hettangian) rocks and ammonoid faunas, Halfway River and Pine Pass map areas, British Columbia. In: Current Research, Part A, Geological Survey of Canada, Paper 82-1A, p. 385-391.

Tozer, E.T. 1984. The Trias and its ammonoids: the evolution of a time scale. Geological Survey of Canada, Miscellaneous Report 35.

Twitchett, R.J. and Wignall, B.P. 1996. Trace fossils and the aftermath of the Permo-Triassic mass extinction: eveidence from northern Italy. Paleogeography, Paleoclimatology, Paleoecology, v. 124, p. 137-151.

Vossler, S.M. and Pemberton, S.G. 1989. Ichnology and Paleoecology of offshore siliclastic deposits in the Cardium Formation (Turonian, Alberta, Canada). Paleogeography, Paleoclimatology, Paleoecology, v. 74, p. 217-229.

Walker, R.G. and Davies, S.D. 1991. Control of prograding and incised transgressive shoreface deposits by rapid fluctuations of relative sea level; Viking Formation in the Caroline-Garrington area. *In*: Leckie, D.A., Posamentier, H.W. and Lovell, R.W.W., eds., 1991 NUNA Conference on High Resolution Sequence Stratigraphy. Geological Association of Canada, Program, Proceedings and Guidebook, p. 58-59.

Warren, P.S. 1945. Triassic fauna in the Canadian Rockies. American Journal of Science, v. 243, p. 480-491.

Weatcroft, R.A. 1990. Preservation potential of sedimentary event layers. Geology 18: p.843-845.

Wetzel, A. and Bromley, R. 1994. *Phycosiphon Incertum* Revisited: *Anconichnus Horizontalis* Is Its Junior Subjective Synonym. Journal of Paleontology, v. 68(6), p. 1396-1402.

Willis, A.J. 1992. Reservoir sedimentology of the middle Triassic Halfway Formation,

Wembley Field, Alberta. M.Sc. thesis, University of Alberta, Edmonton, Alberta, 401 p.

Willis, A.J. and Moslow, T.F. 1994. Sedimentology and stratigraphy of tidal inlet reservoirs in the Triassic Halfway Formation, Wembley Field, Alberta. Bulletin of Canadian Petroleum Geology, v. 42, p. 245-262.

Willis, A.J. and Wittenberg, J. 2000. Exploration significance of healing-phase deposits in the Triassic Doig Formation, Hythe, Alberta. Bulletin of Canadian Petroleum Geology, v.48, p.179-192.

Wittenberg, J. and Moslow, T.F. 1991. Origin and variability of overthickened sandstones in the Doig Formation, west-central Alberta (Abstract). In: Opportunities for the Nineties, Program and Abstracts, 1991 Canadian Society of Petroleum Geologists Convention, Calgary, p. 146.

Wittenberg, J. and Moslow, T.F. 1992a. Lateral facies variability and inpact on reservoir heterogeneity, Middle Triassic Doig Formation, Sinclair, Wembley, and Valhalla (East) Fields, Alberta, Canada. Environments of exploration, Program and Abstracts, American Association of Petroleum Geologists and Canadian Society of Petroleum Geologists Convention, Calgary, Alberta, June, 1992, p. 144.

Wittenberg, J. 1992. Origin and stratigraphic significance of several anomalously thick sandstone trends in the Middle Triassic Doig Formation of west-central Alberta. M.Sc. thesis, University of Alberta, Edmonton, Alberta, 600 p.

Wittenberg, J. 1993. The significance and recognition of mass wasting events in cored sequences, impact on the genesis of several anomalously thick sandstone bodies in the Middle Triassic Doig Formation of west-central Alberta. Core workshop guidebook, Carboniferous to Jurassic Pangaea Conference, Canadian Society of Petroleum Geologists, p. 131-161.

Wittenberg, J. and Moslow, T.F. 1992b. Origin and stratigraphic significance of several anomalously thick sandstone trends in the Middle Triassic Doig Formation of west-central Alberta, Canada. Environments of exploration, Program and Abstracts, American Association of Petroleum Geologists and Canadian Society of Petroleum Geologists Convention, Calgary, Alberta, June, 1992, p. 144.

Young, F.G. 1997. Iconoclastic view of mid-Triassic stratigraphy, Umbach-Wargen area, British Columbia. . Bulletin of Canadian Petroleum Geology, v. 45, p. 577-594.

Zhanghua, W., Yoshiki, S., Kazuaki, H., Akihisa, K. and Zhongyuan, C. 2005. Yangtze offshore, China: highly laminated sediments from the transition zone between subaqueous delta and continental shelf. Estuarine, Coastal and Shelf Science, v. 62, p. 161-168.

Zonneveld, J.-P. 1999. Sedimentology and sequence biostratigraphic framework of a mixed siliciclastic–carbonate depositional system, Middle Triassic, northeastern British Columbia. Unpublished PhD Dissertation, University of Alberta, Edmonton, 287 pp

Zonneveld, J-P. 2001, Middle Triassic biostromes from the Liard Formation, British Columbia, Canada: oldest examples from the Mesozoic of NM Pangea: Sedimentary Geology, v. 145, p. 317-341.

Zonneveld, J-P., Beatty, T.W. and Pemberton, S.G. 2005. Lingulide Brachiopods in Western Canadain Triassic Shallow Marine Strata: Implacations for the Post-Extinction Recovery of Triassic Infaunal Communities (Abstract). In: Abstracts Volume. American Association of Petroleum Geologists Convention, Calgary, Alberta, 2005, p. 160.

Zonneveld, J-P., Gingras, M.K. and Pemberton, S.G. 2001. Trace fossil assemblages in a Middle Triassic mixed siliciclastic-carbonate marginal marine depositional system, British Columbia: Palaeogeography, Palaeoclimatology, Palaeoecology, v. 166, p. 249-276.

Zonneveld, J-P., Pemberton, S.G., Saunders, T.D.A. and Pickerill, R.K. 2002. Large robust *Cruziana* from the Middle Triassic of northeastern British Columbia: ethologic, biostratigraphic and paleobiologic significance. Palaios, 17: 435-448.

Zonneveld, J-P. and S.G. Pemberton. 2003. Taxonomy of lingulide derived trace fossils from the lower and middle Triassic of western Canada: Ichnos. 10, p. 25-39.

# APENDIX A: CORE LOGS

# LEGEND

## LITHOLOGY

- SAND/SANDSTO
- silty sand
- shaly sand
- SILT/SILTSTONE
- sandy silt
- clayey silty
- SHALE/MUDSTO
- silty shale
- sandy shale
- organic shale
- Lost Core

## PHYSICAL STRUCTURES

- Current Ripples
- Oscillatory Ripples
- Planar Tabular Bedding
- Low Angle Bedding
- Flaser Bedding
- Wavy Parallel Bedding
- Lenticular Bedding
- Hummocky Cross-strat.
- Scour
- Micro-Fault
- Deformed bedding
- Fracture
- Flame Structures

## LITHOLOGIC ACCESSORIES

- Sand Lamina
- Silt Lamina
- Shale Lamina
- Sid Siderite
- Py Pyrite
- Shell Fragments
- S Sulfur
- Oolitic
- Pisolites
- Fecal Pellets
- Peloids
- P Phosphates
- Anhydrite nodules

## ICHNOFOSSILS

- Skolithos
- Planolites
- Palaeophycus
- Diplocraterion
- Rhizocorallium
- Cylindrichnus
- Asterosoma
- Rosselia
- Thalassinoides
- Chondrites
- Teichichnus
- Scolicia
- Phycosiphon
- Fugichnia
- Lockeia
- Anconichnus

## FOSSILS

- Fish Remains
- Plant Remains
- Vertebrates

## BIOTURBATION

- Abunda
- Comno
- Modera
- Rare
- Barren

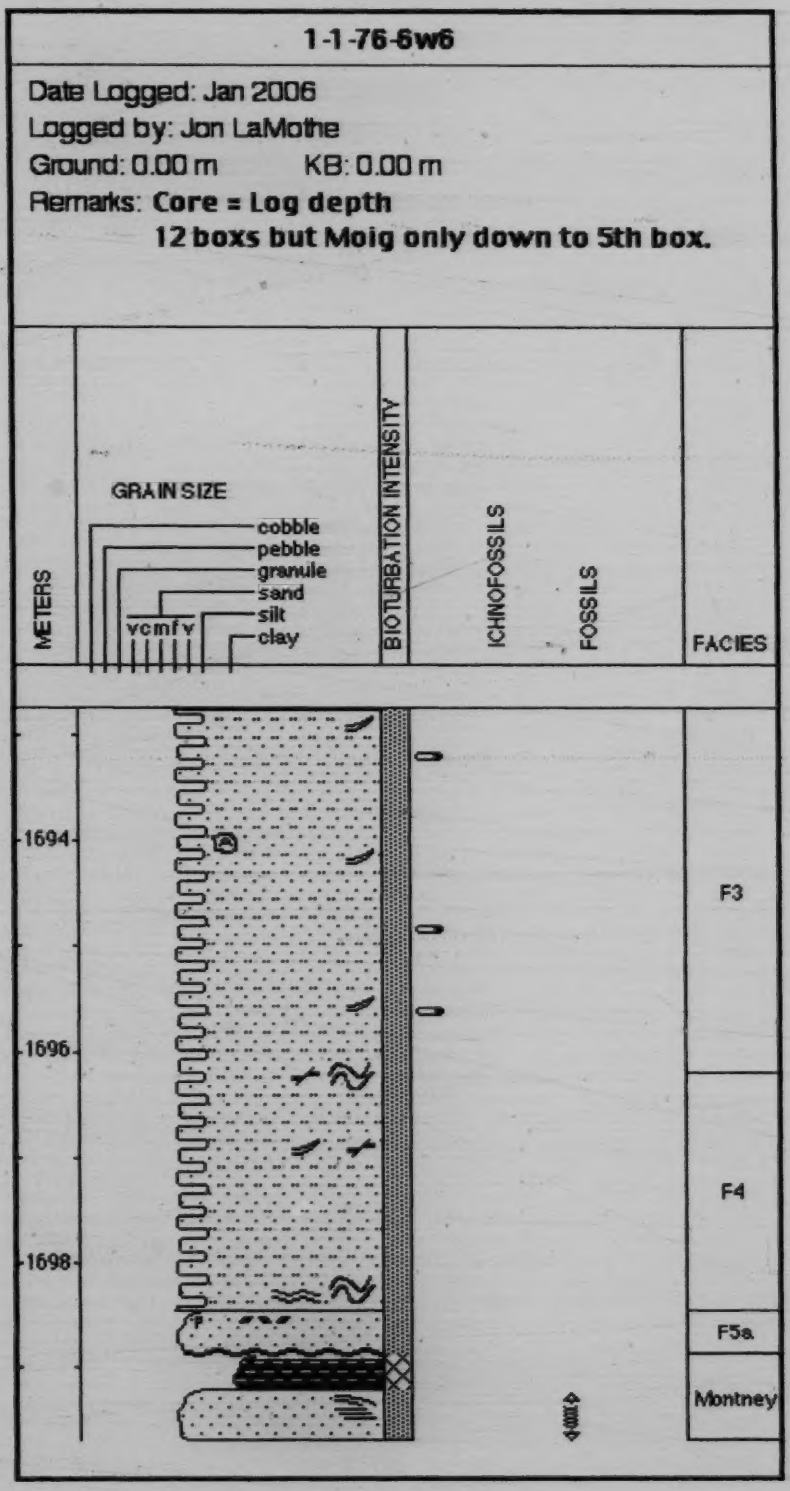
1-1-76-6w6
Date Logged: Jan 2006
Logged by: Jon LaMothe
Ground: 0.00 m KB: 0.00 m
Remarks: Core = Log depth
12 boxs but Moig only down to 5th box.
METERS
GRAIN SIZE
cobble
pebble
granule
sand
silt
clay
vc m f v
BIOTURBATION INTENSITY
ICHNOFOSSILS
FOSSILS
FACIES
1694
1696
1698
F3
F4
F5a
Montney

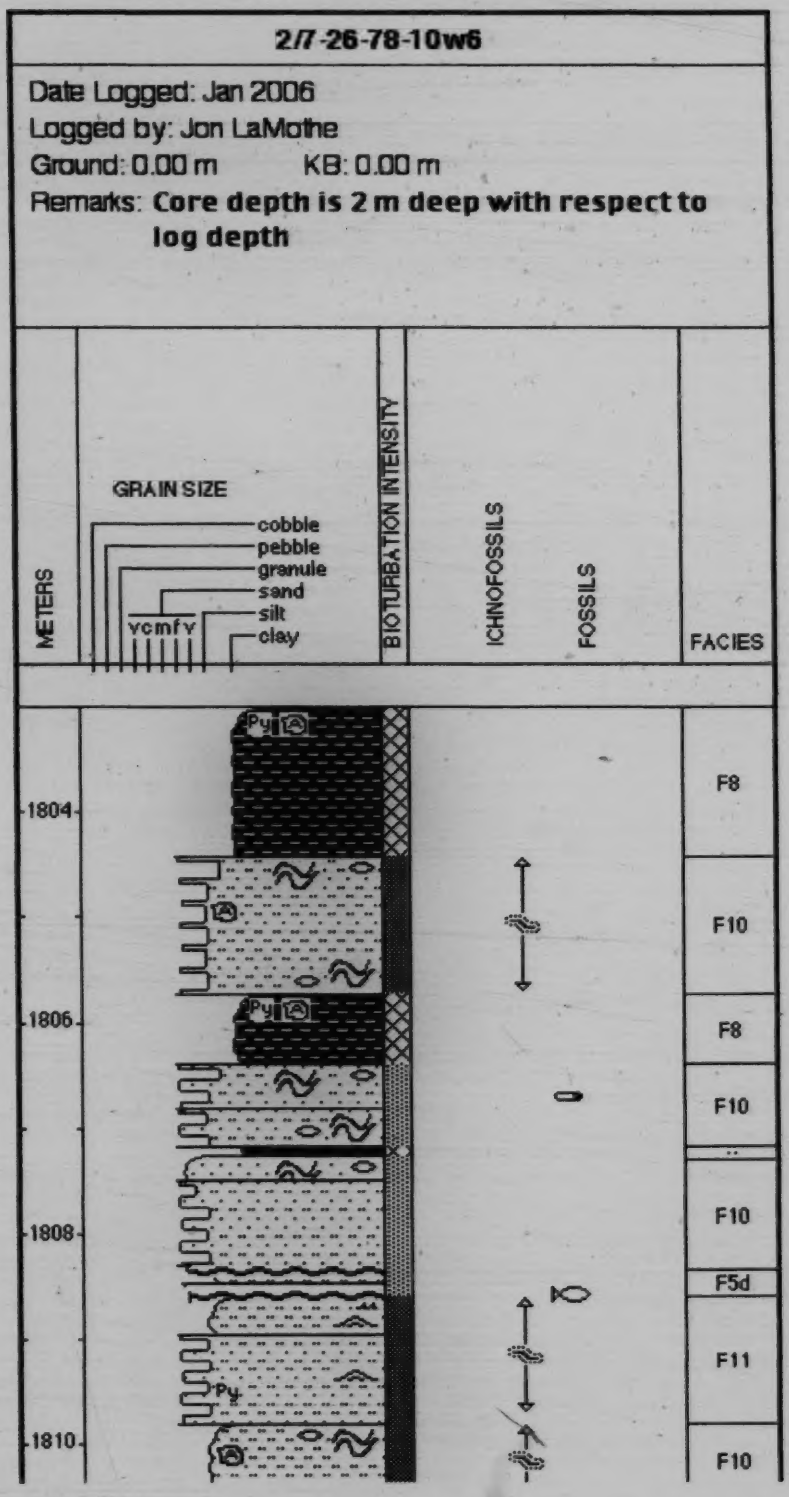
2/7-26-78-10w6
Date Logged: Jan 2006
Logged by: Jon LaMothe
Ground: 0.00 m KB: 0.00 m
Remarks: Core depth is 2 m deep with respect to log depth
METERS
GRAIN SIZE
cobble
pebble
granule
sand
silt
clay
vcmfv
BIOTURBATION INTENSITY
ICHNOFOSSILS
FOSSILS
FACIES
1804
1806
1808
1810
Py
F8
F10
F8
F10
F10
F5d
F11
F10

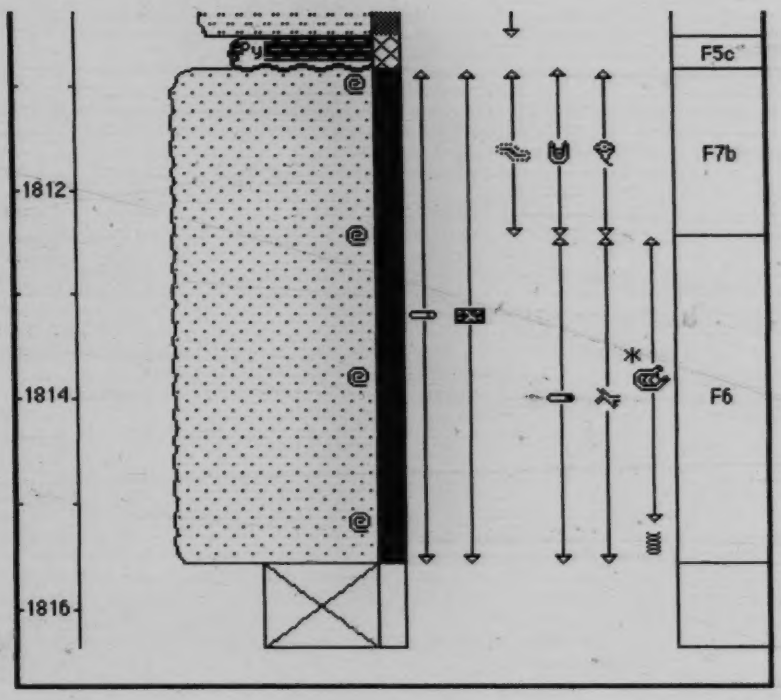
Py
F5c
F7b
F6
1812
1814
1816

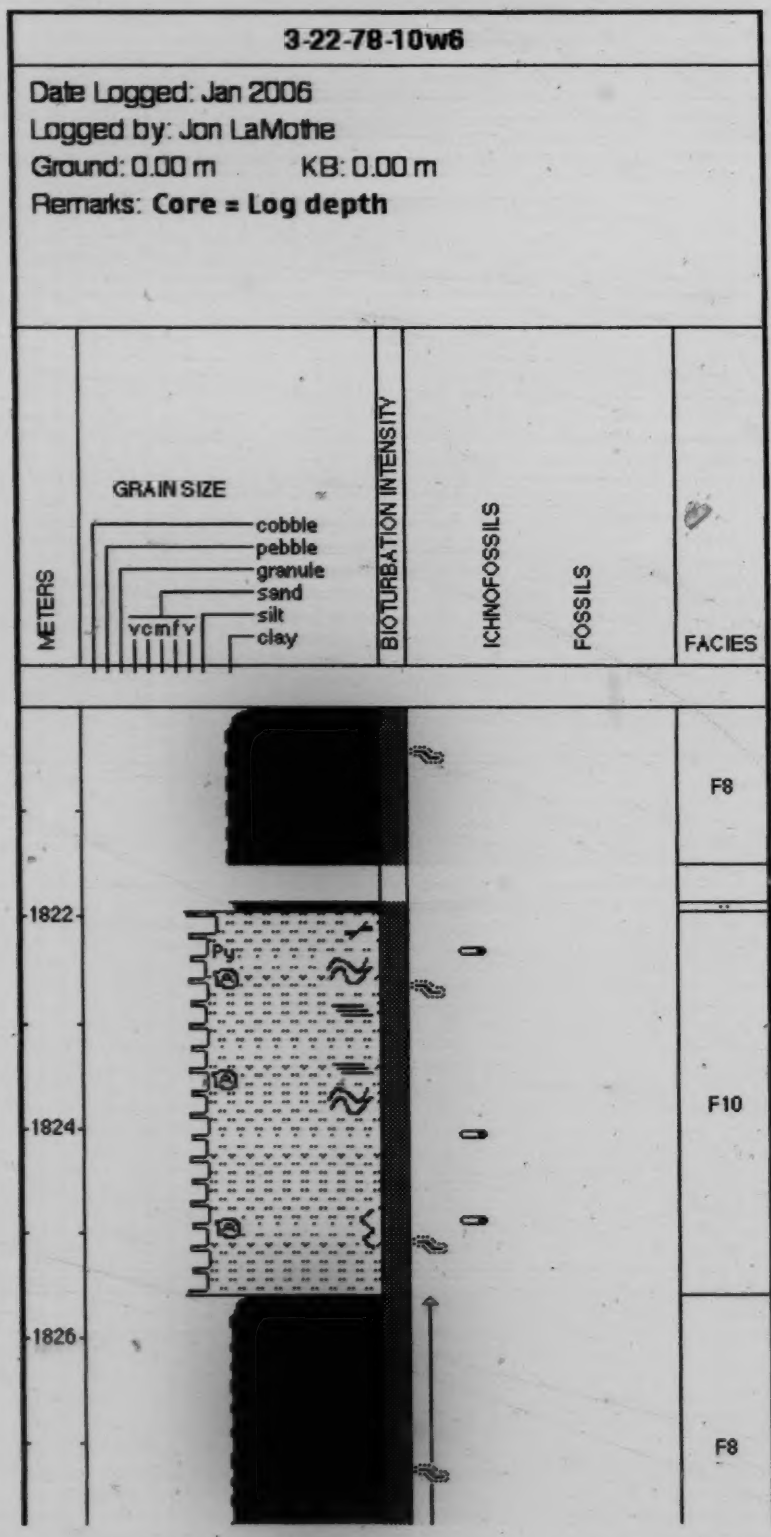
3-22-78-10w6
Date Logged: Jan 2006
Logged by: Jon LaMothe
Ground: 0.00 m KB: 0.00 m
Remarks: Core = Log depth
METERS
GRAIN SIZE
cobble
pebble
granule
sand
silt
clay
vcmfv
BIOTURBATION INTENSITY
ICHNOFOSSILS
FOSSILS
FACIES
1822
1824
1826
Py
F8
F10
F8

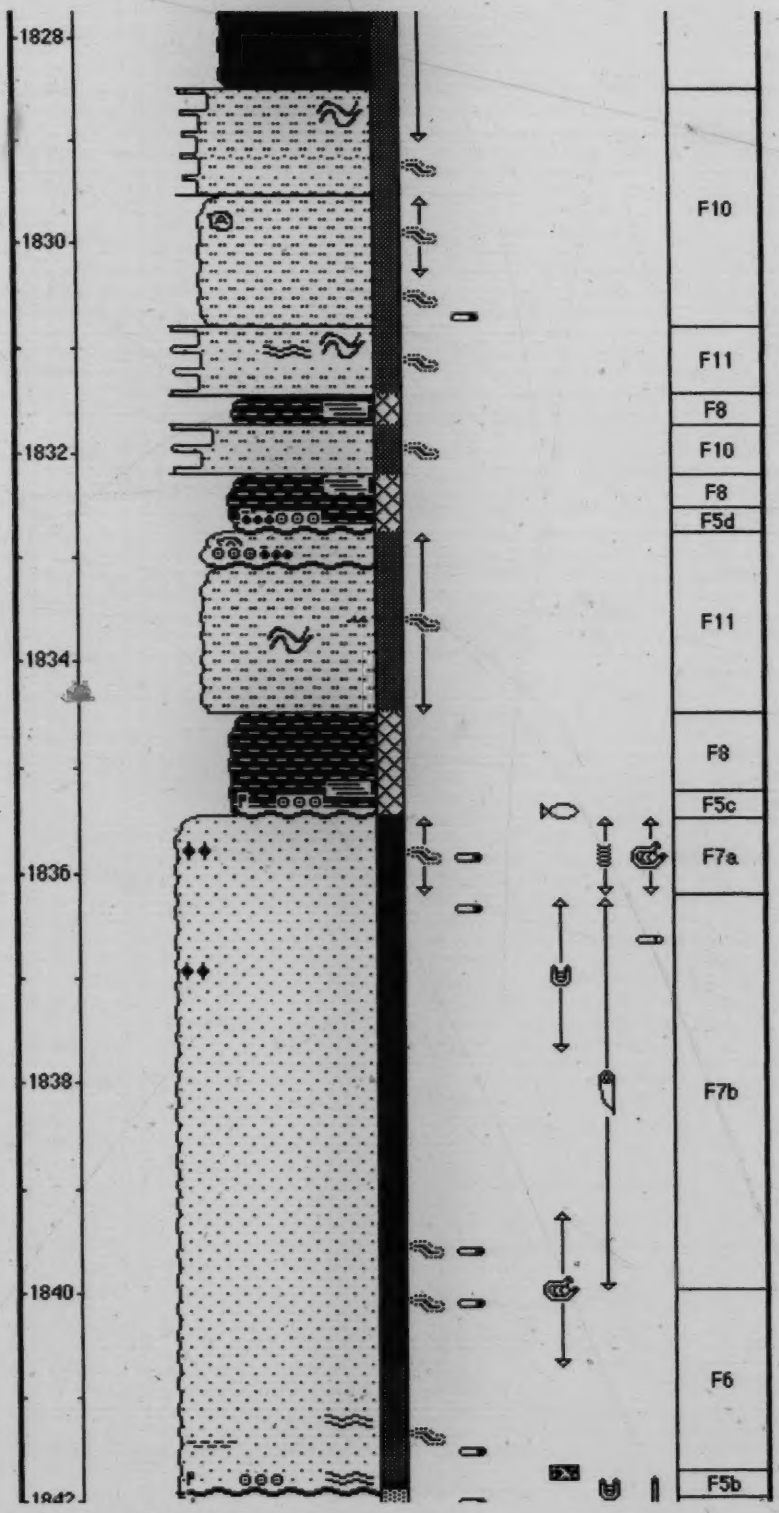
1828
1830
1832
1834
1836
1838
1840
1842
F10
F11
F8
F10
F8
F5d
F11
F8
F5c
F7a
F7b
F6
F5b

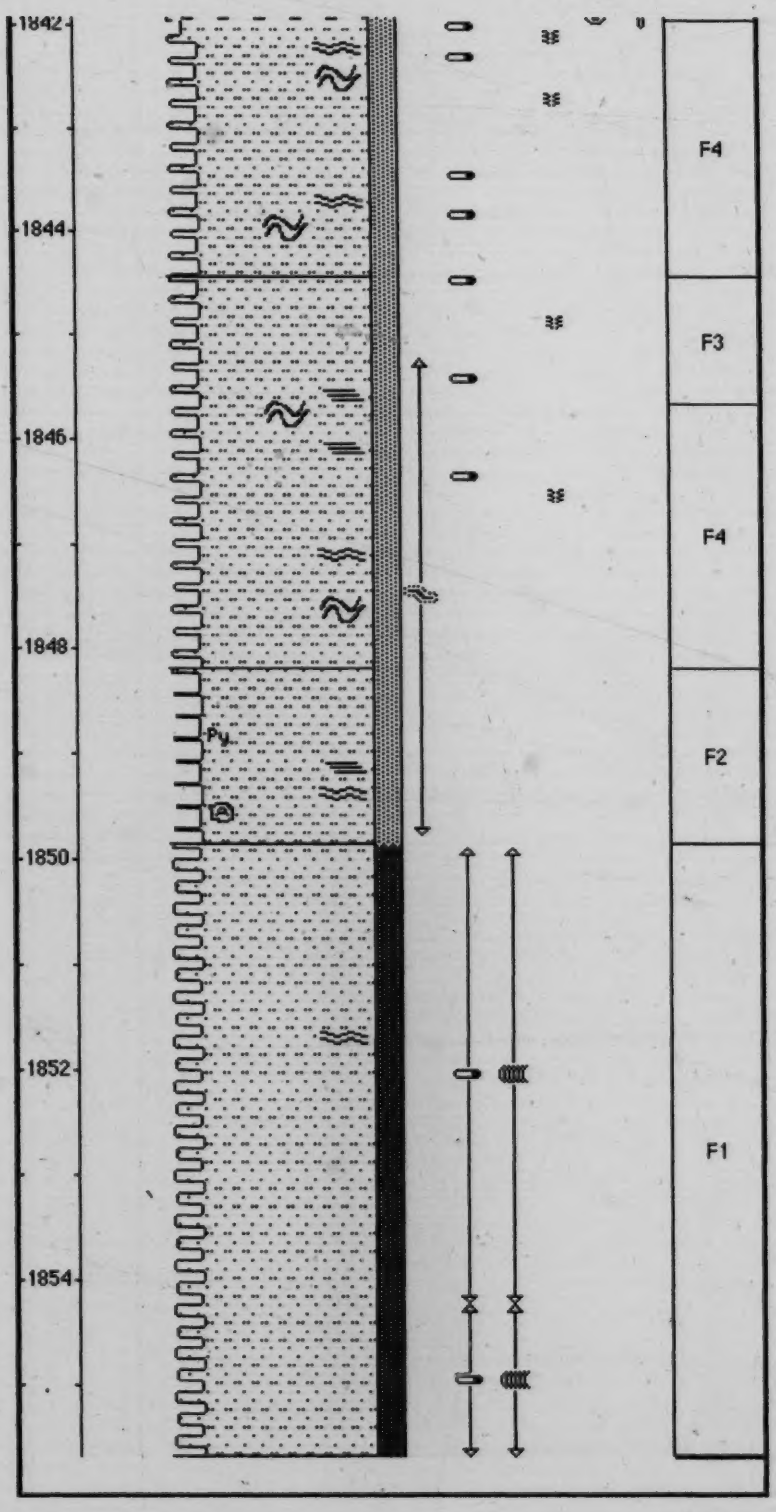
1842
1844
1846
1848
1850
1852
1854
F4
F3
F4
F2
F1

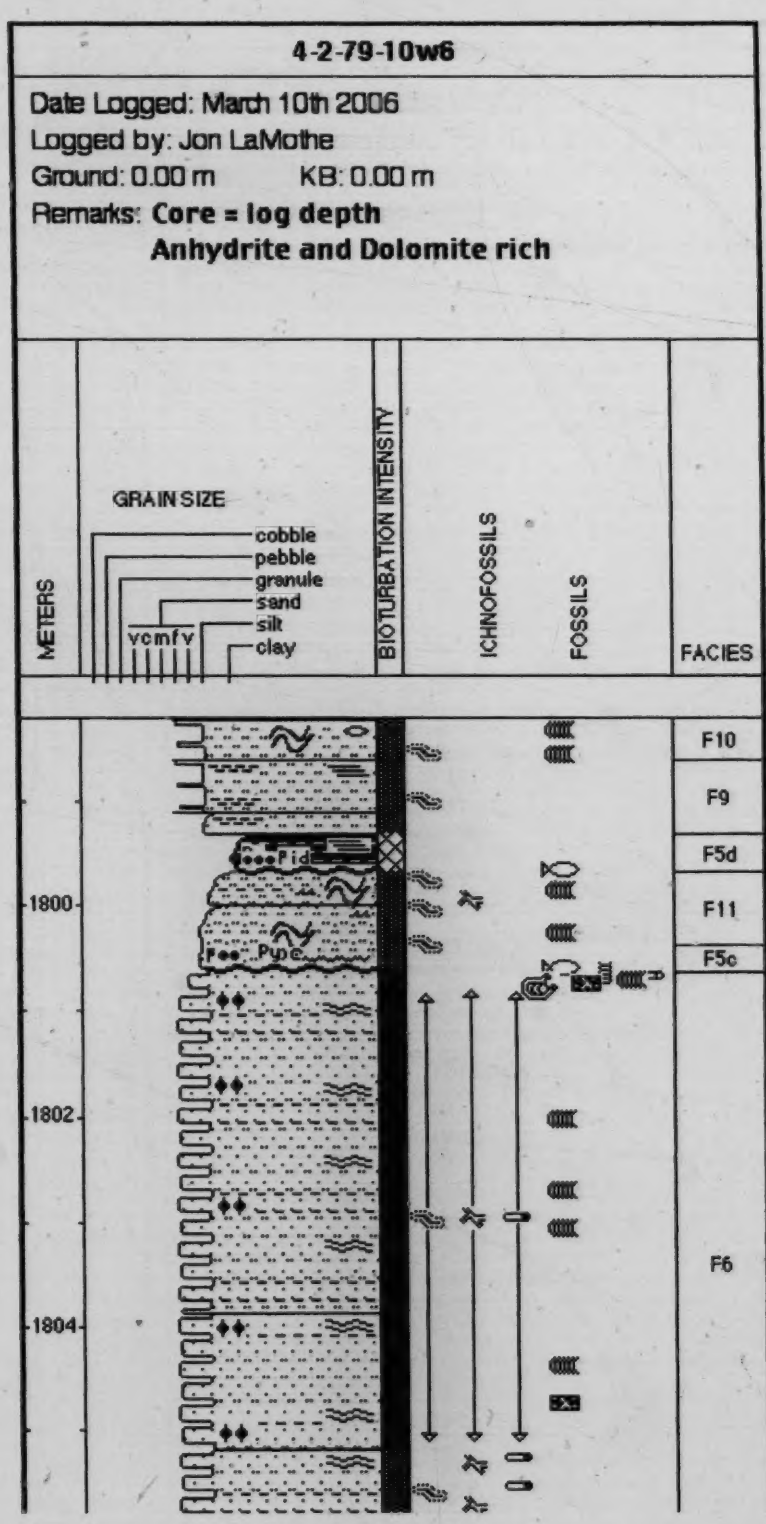
4-2-79-10w6
Date Logged: March 10th 2006
Logged by: Jon LaMothe
Ground: 0.00 m KB: 0.00 m
Remarks: Core = log depth
Anhydrite and Dolomite rich
METERS
GRAIN SIZE
cobble
pebble
granule
sand
silt
clay
vcmfv
BIOTURBATION INTENSITY
ICHNOFOSSILS
FOSSILS
FACIES
1800
1802
1804
F10
F9
F5d
F11
F5c
F6

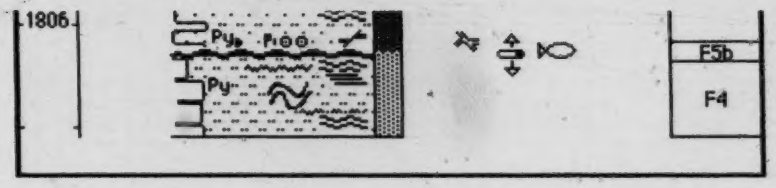
1806
Py
Py
F5b
F4

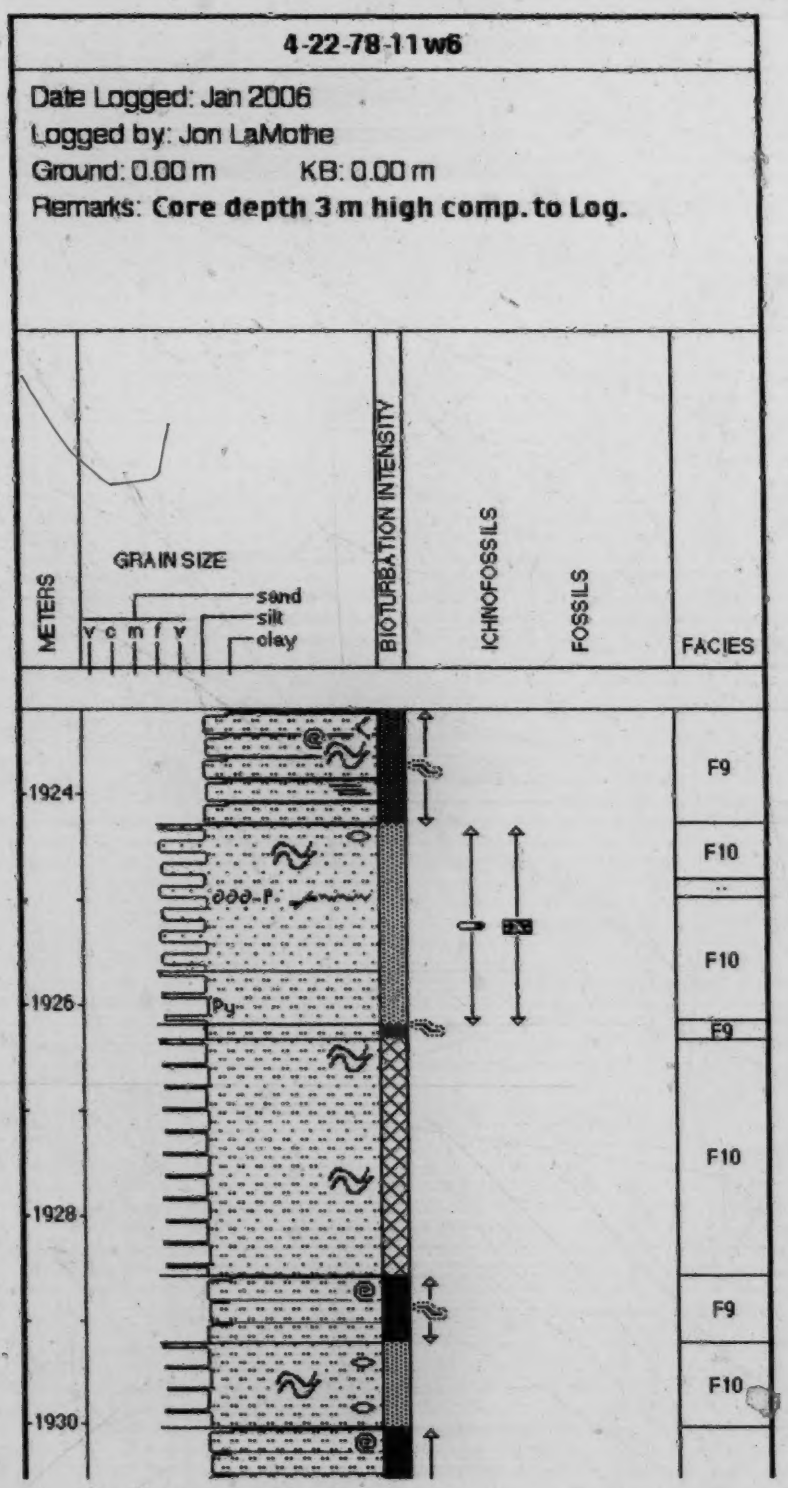
4-22-78-11w6
Date Logged: Jan 2006
Logged by: Jon LaMothe
Ground: 0.00 m KB: 0.00 m
Remarks: Core depth 3 m high comp. to Log.
METERS
GRAIN SIZE
sand
silt
clay
v c m f v
BIOTURBATION INTENSITY
ICHNOFOSSILS
FOSSILS
FACIES
1924
1926
1928
1930
Py
F9
F10
F10
F9
F10
F9
F10

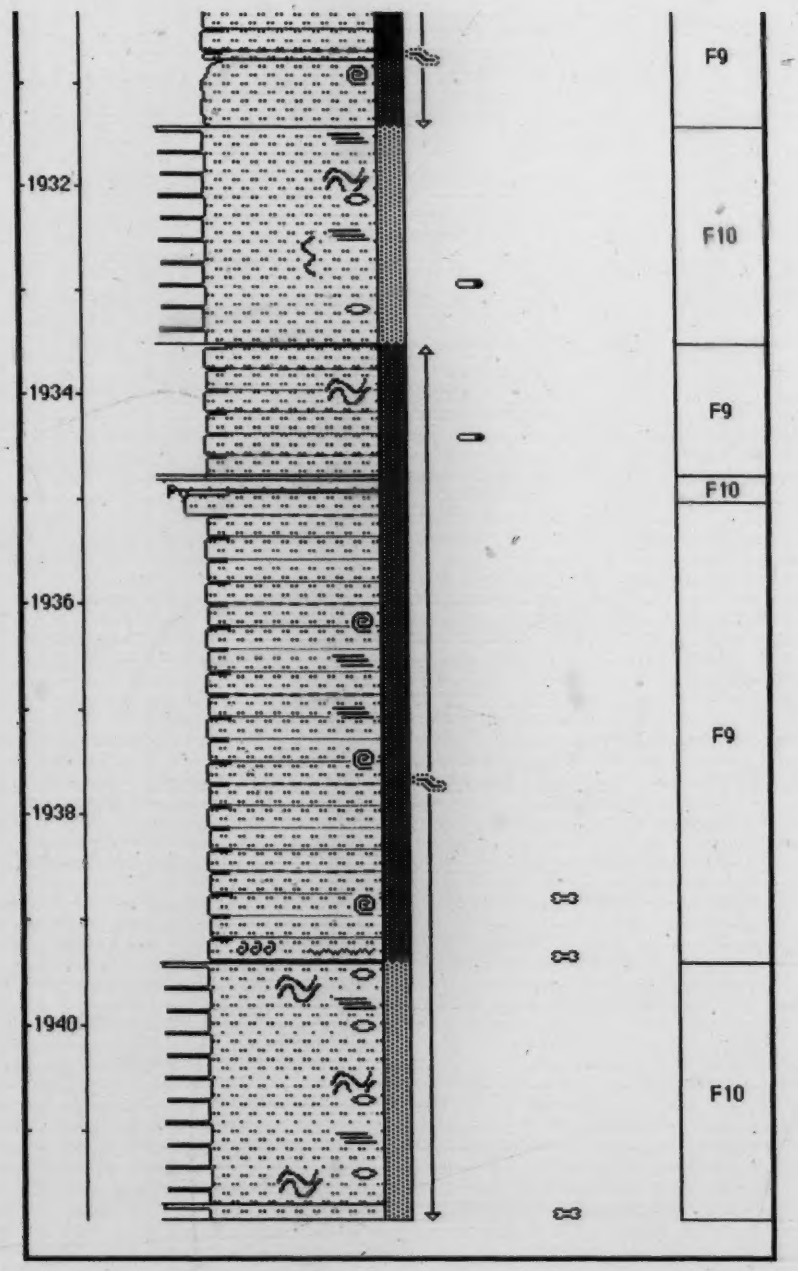
1932
1934
1936
1938
1940
F9
F10
F9
F10
F9
F10

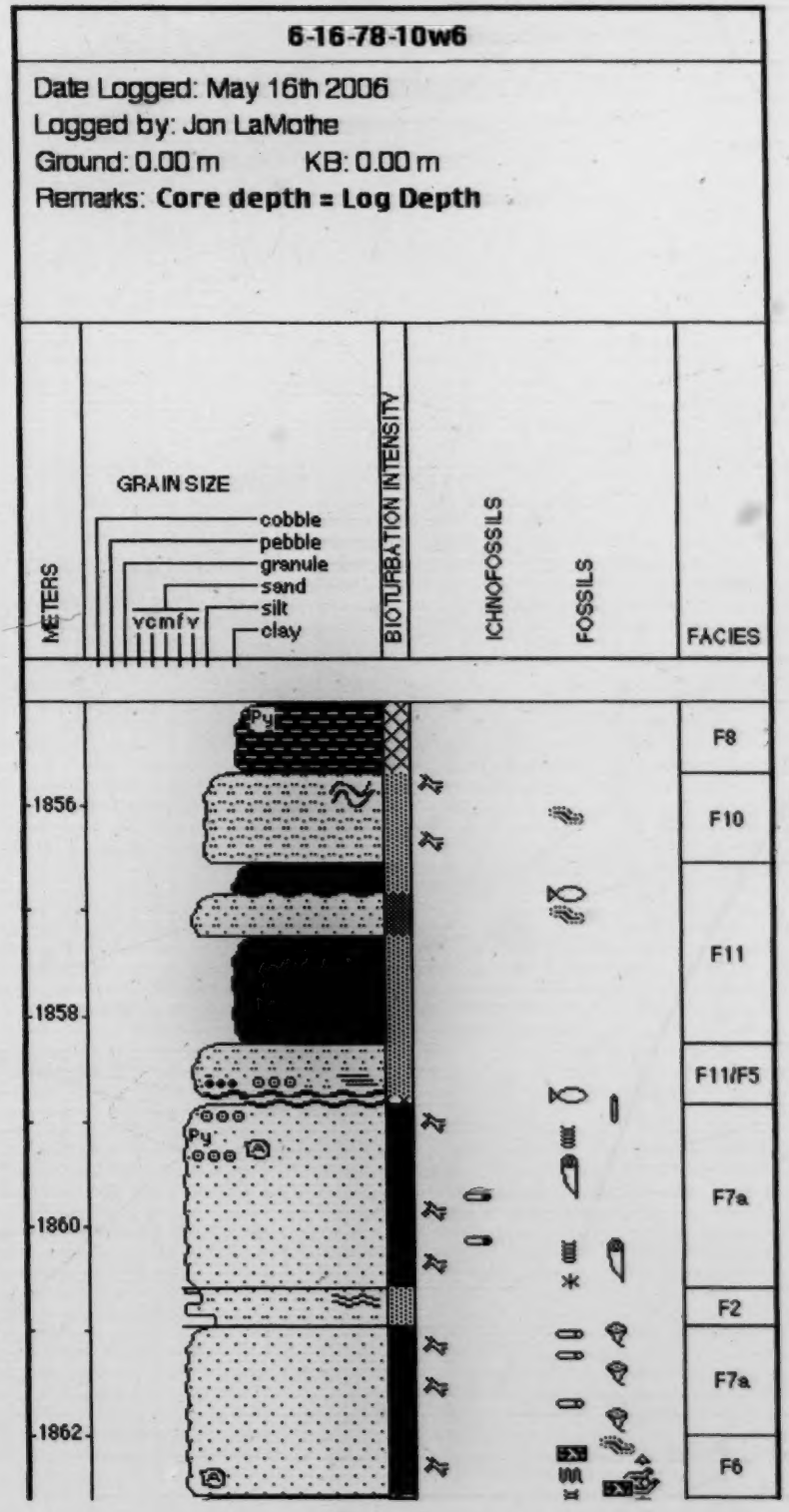
6-16-78-10w6
Date Logged: May 16th 2006
Logged by: Jon LaMothe
Ground: 0.00 m KB: 0.00 m
Remarks: Core depth = Log Depth
METERS
GRAIN SIZE
cobble
pebble
granule
sand
silt
clay
vcmfv
BIOTURBATION INTENSITY
ICHNOFOSSILS
FOSSILS
FACIES
1856
1858
1860
1862
Py
F8
F10
F11
F11/F5
F7a
F2
F7a
F6

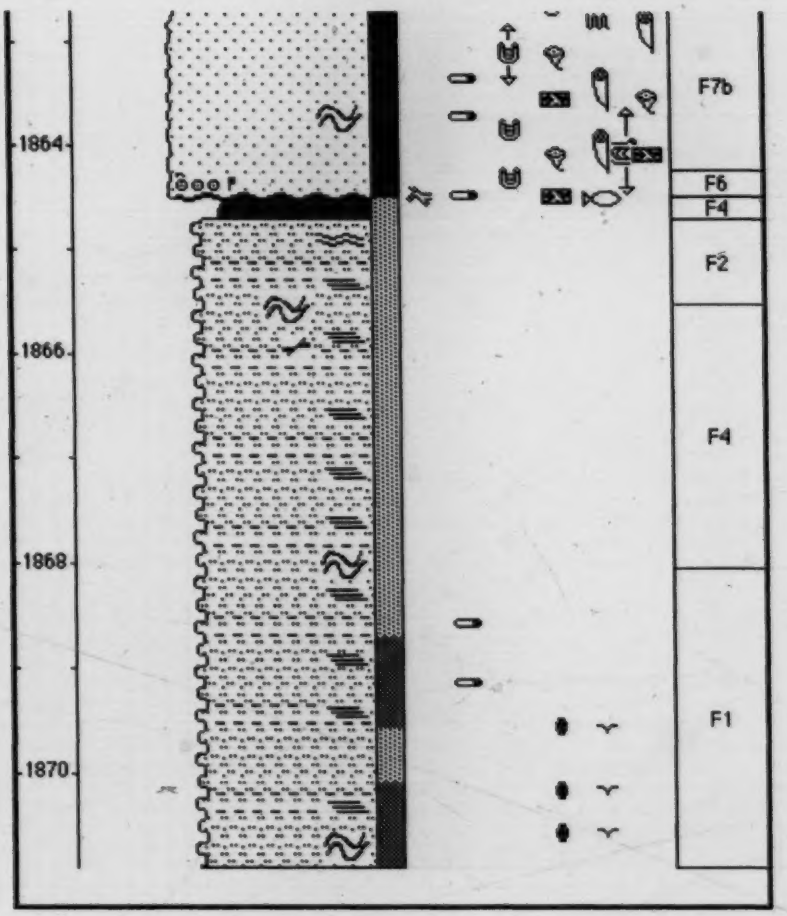
1864
1866
1868
1870
F7b
F6
F4
F2
F4
F1

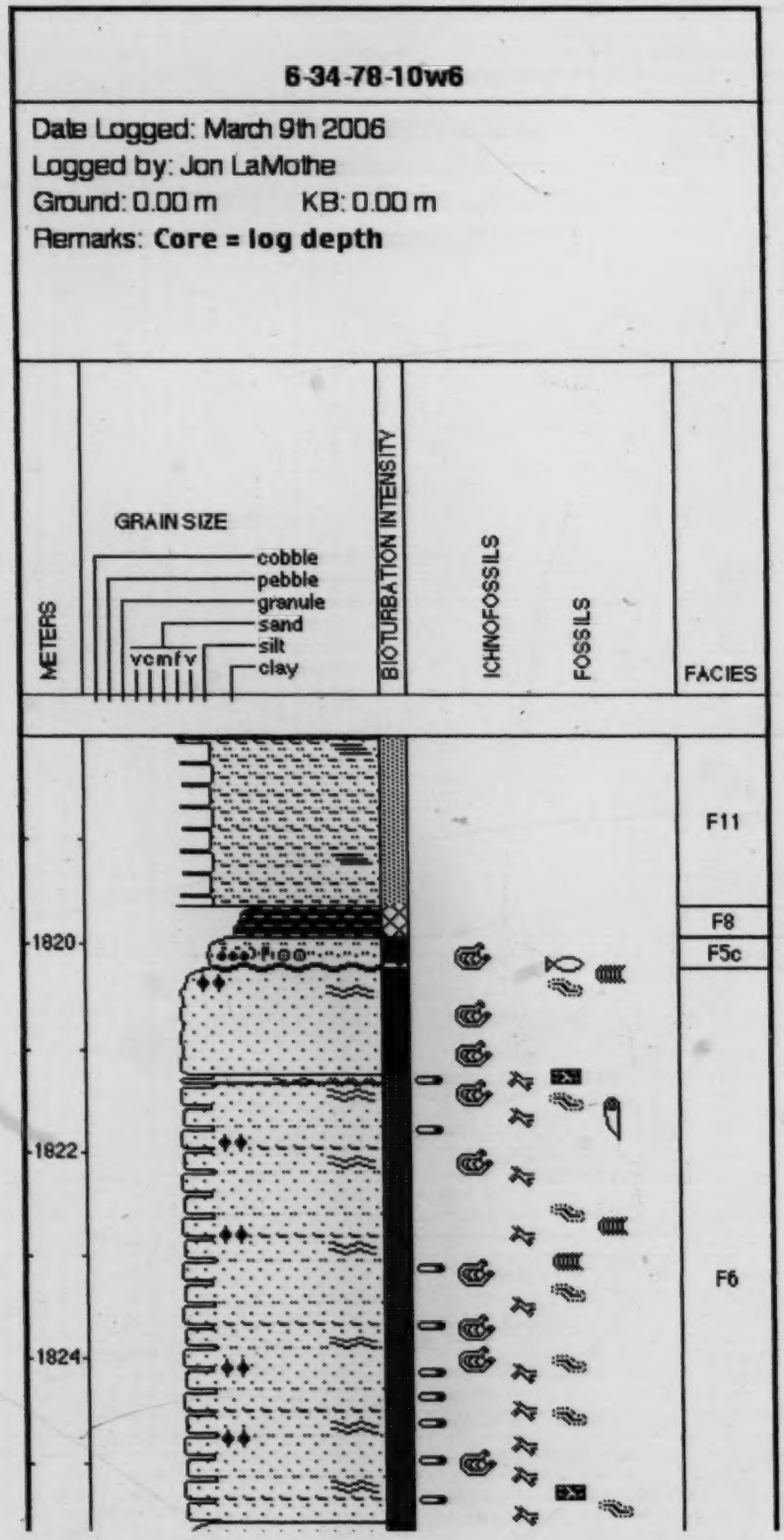
6-34-78-10w6
Date Logged: March 9th 2006
Logged by: Jon LaMothe
Ground: 0.00 m KB: 0.00 m
Remarks: Core = log depth
METERS
GRAIN SIZE
cobble
pebble
granule
sand
silt
clay
vc m f v
BIOTURBATION INTENSITY
ICHNOFOSSILS
FOSSILS
FACIES
1820
1822
1824
F11
F8
F5c
F6

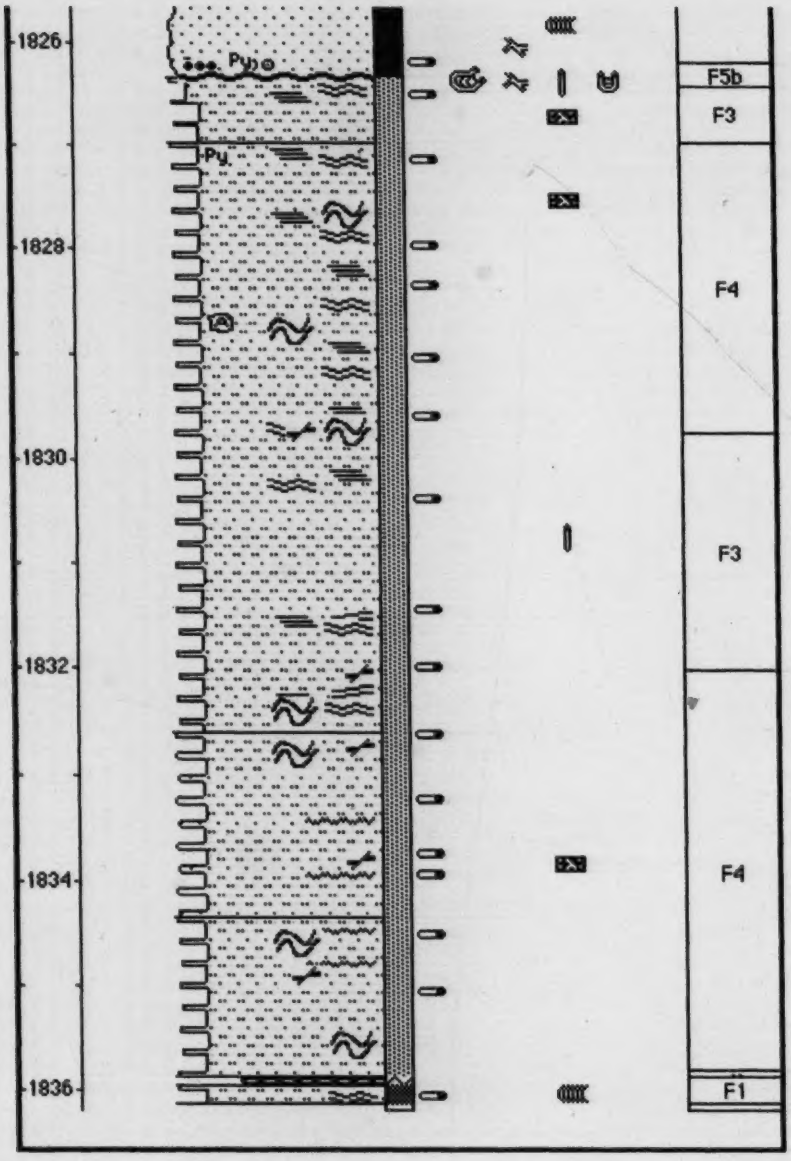
1826
1828
1830
1832
1834
1836
Py
Py
F5b
F3
F4
F3
F4
F1

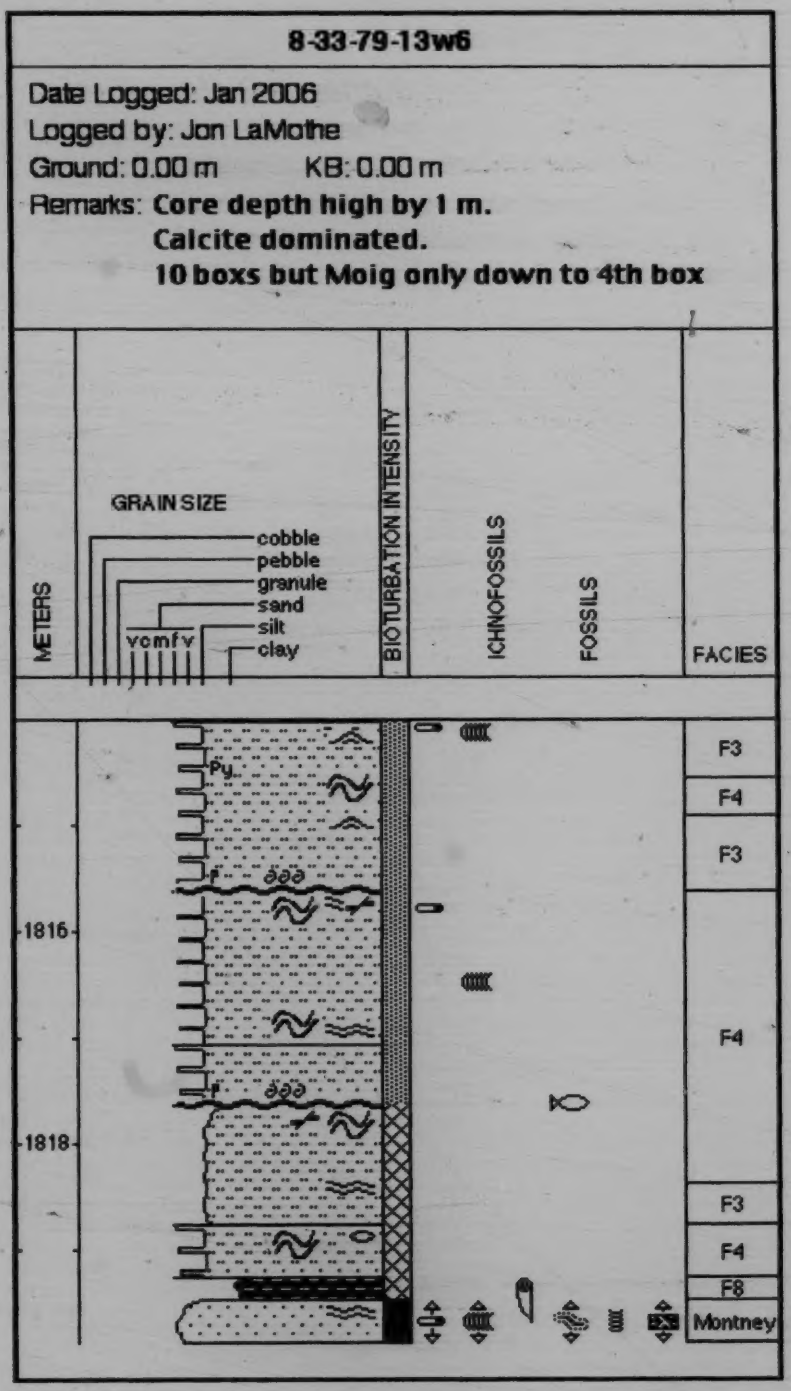
8-33-79-13w6
Date Logged: Jan 2006
Logged by: Jon LaMothe
Ground: 0.00 m KB: 0.00 m
Remarks: Core depth high by 1 m.
Calcite dominated.
10 boxs but Moig only down to 4th box
METERS
GRAIN SIZE
cobble
pebble
granule
sand
silt
clay
vcmfv
BIOTURBATION INTENSITY
ICHNOFOSSILS
FOSSILS
FACIES
Py
1816
1818
F3
F4
F3
F4
F3
F4
F8
Montney

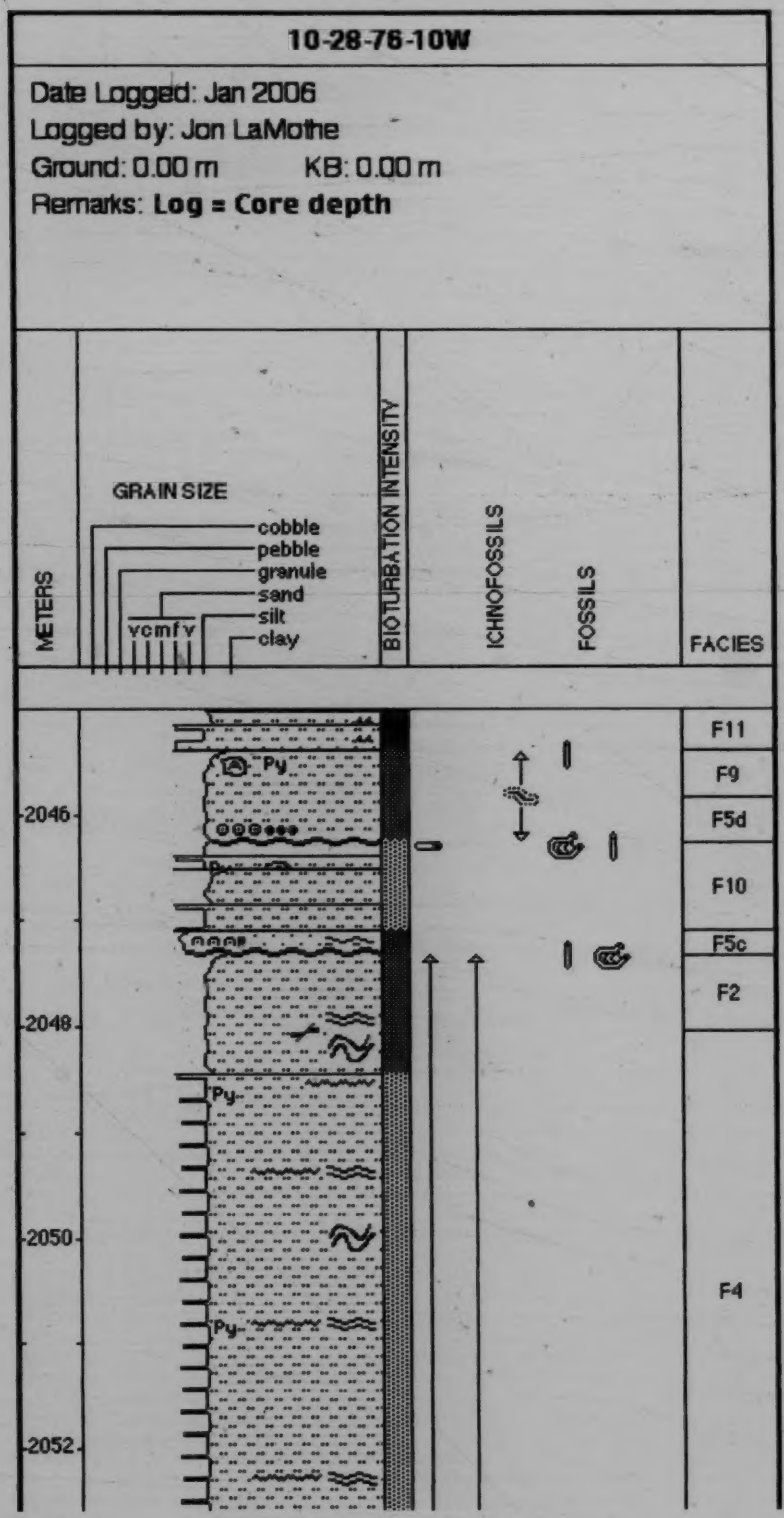
10-28-76-10W
Date Logged: Jan 2006
Logged by: Jon LaMothe
Ground: 0.00 m KB: 0.00 m
Remarks: Log = Core depth
METERS
GRAIN SIZE
cobble
pebble
granule
sand
silt
clay
vcmfv
BIOTURBATION INTENSITY
ICHNOFOSSILS
FOSSILS
FACIES
2046
2048
2050
2052
Py
F11
F9
F5d
F10
F5c
F2
F4

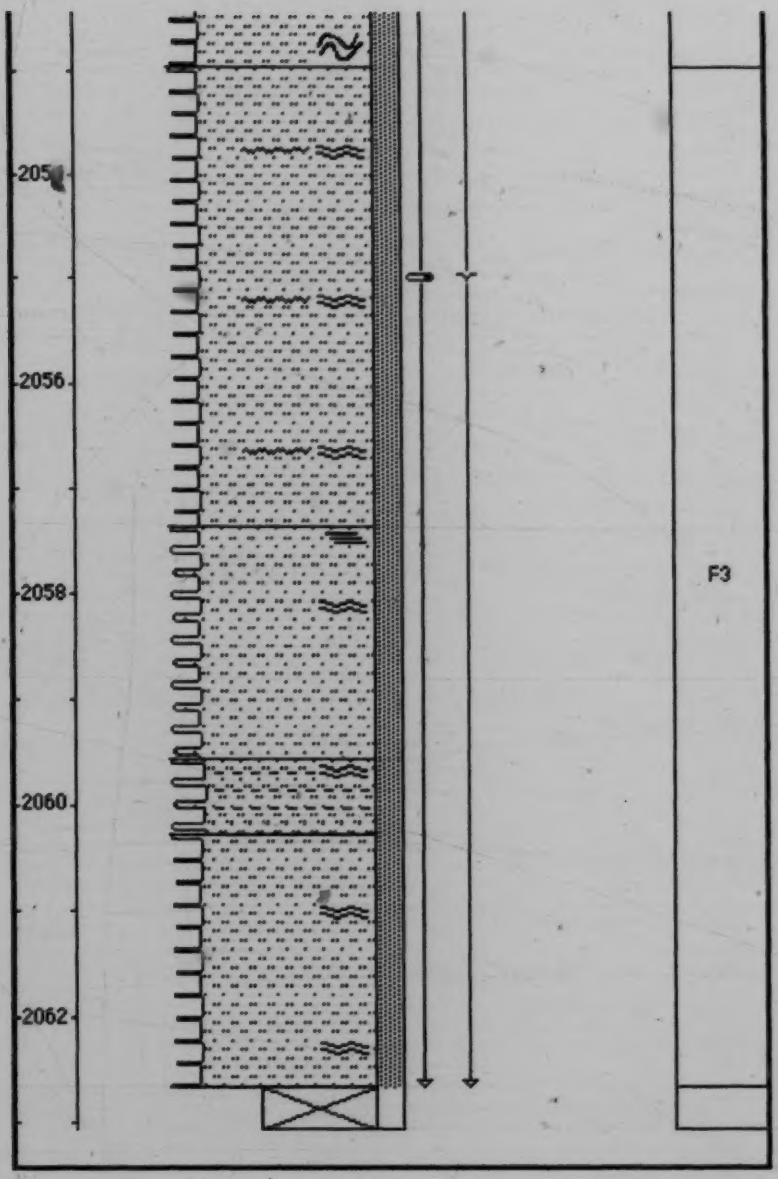
2054
2056
2058
2060
2062
F3

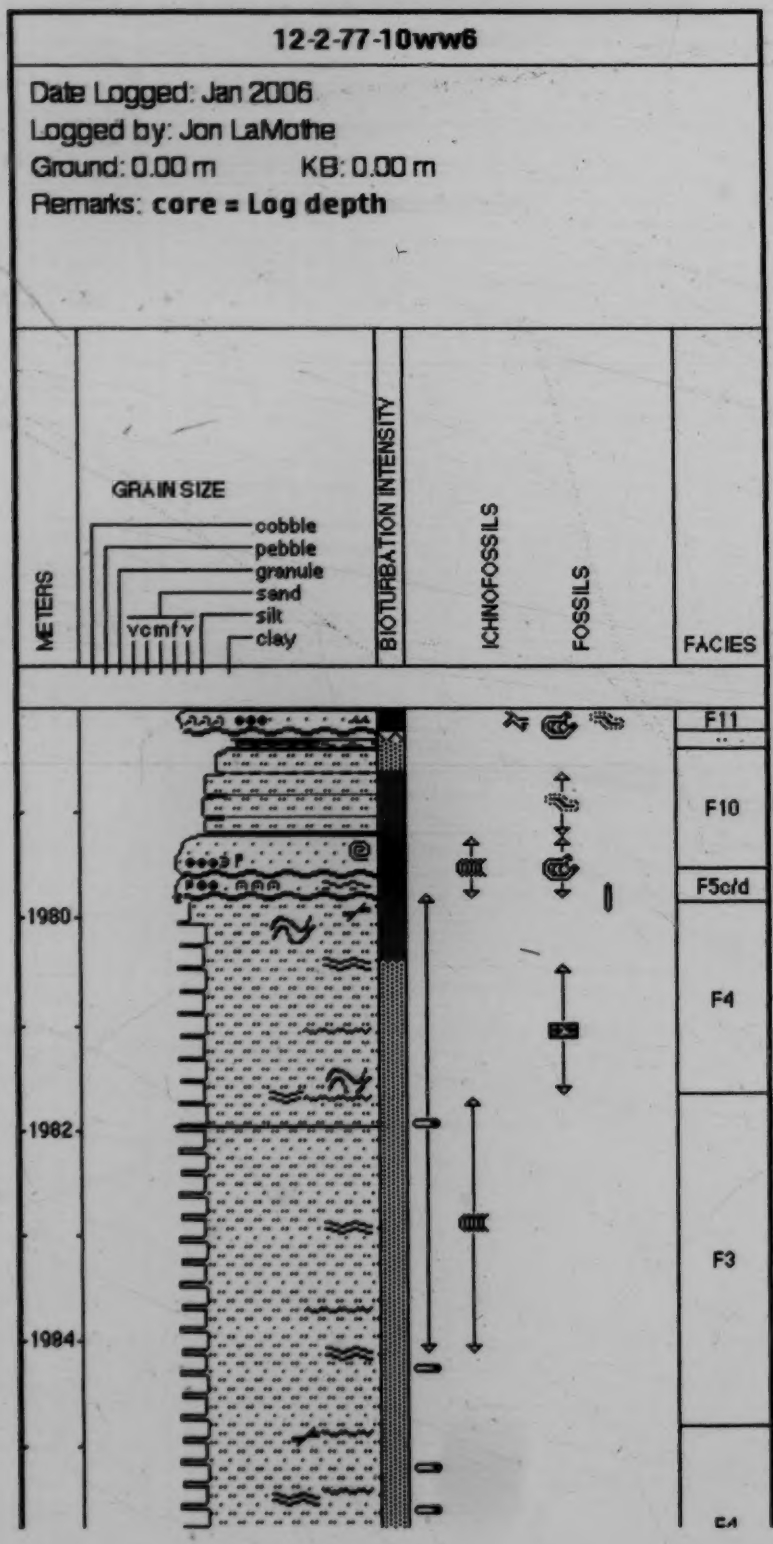
12-2-77-10ww6
Date Logged: Jan 2006
Logged by: Jon LaMothe
Ground: 0.00 m KB: 0.00 m
Remarks: core = Log depth
METERS
GRAIN SIZE
cobble
pebble
granule
sand
silt
clay
vc m f v
BIOTURBATION INTENSITY
ICHNOFOSSILS
FOSSILS
FACIES
1980
1982
1984
F11
F10
F5c/d
F4
F3

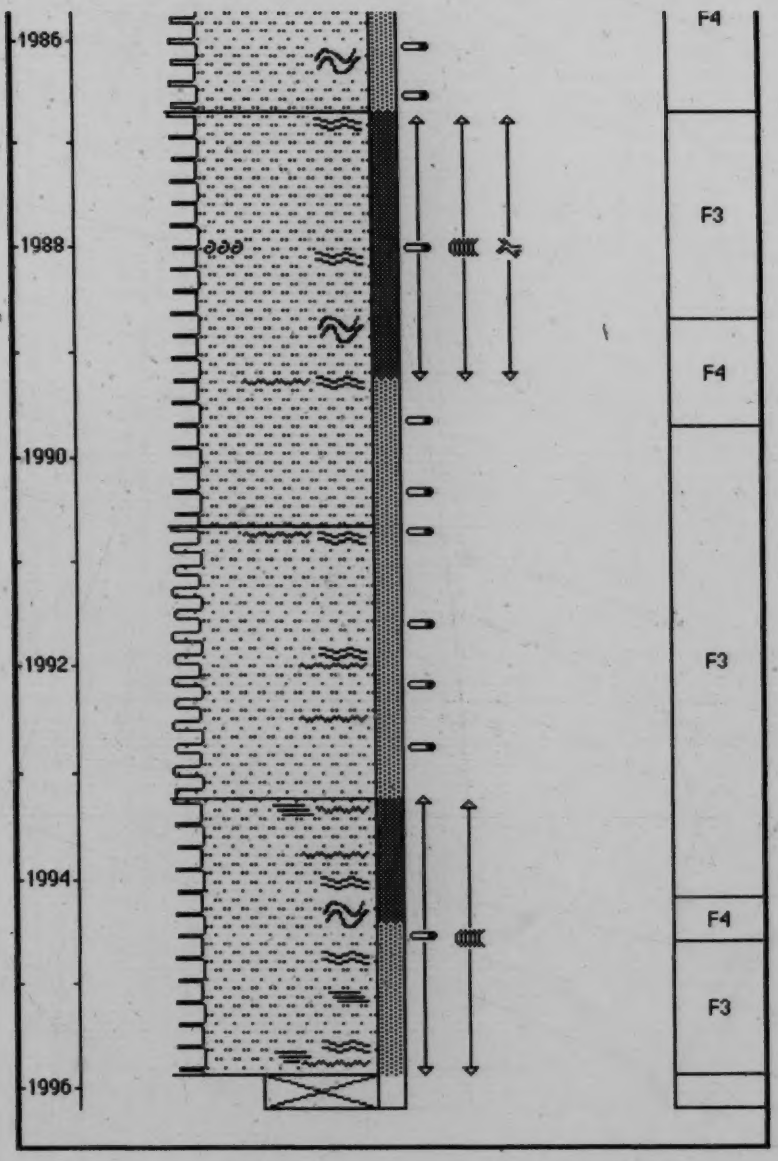
1986
1988
1990
1992
1994
1996
F4
F3
F4
F3
F4
F3

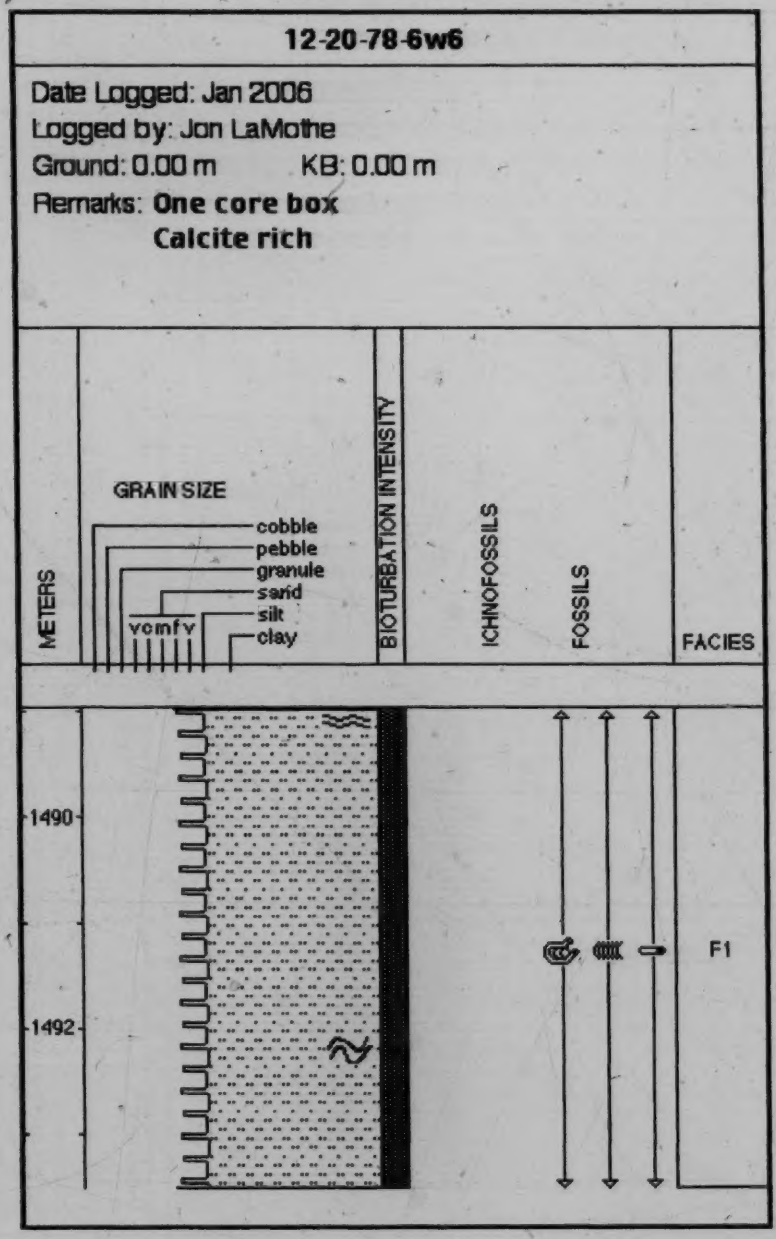
12-20-78-6w6
Date Logged: Jan 2006
Logged by: Jon LaMothe
Ground: 0.00 m KB: 0.00 m
Remarks: One core box
Calcite rich
METERS
GRAIN SIZE
cobble
pebble
granule
sand
silt
clay
vcmfv
BIOTURBATION INTENSITY
ICHNOFOSSILS
FOSSILS
FACIES
1490
1492
F1

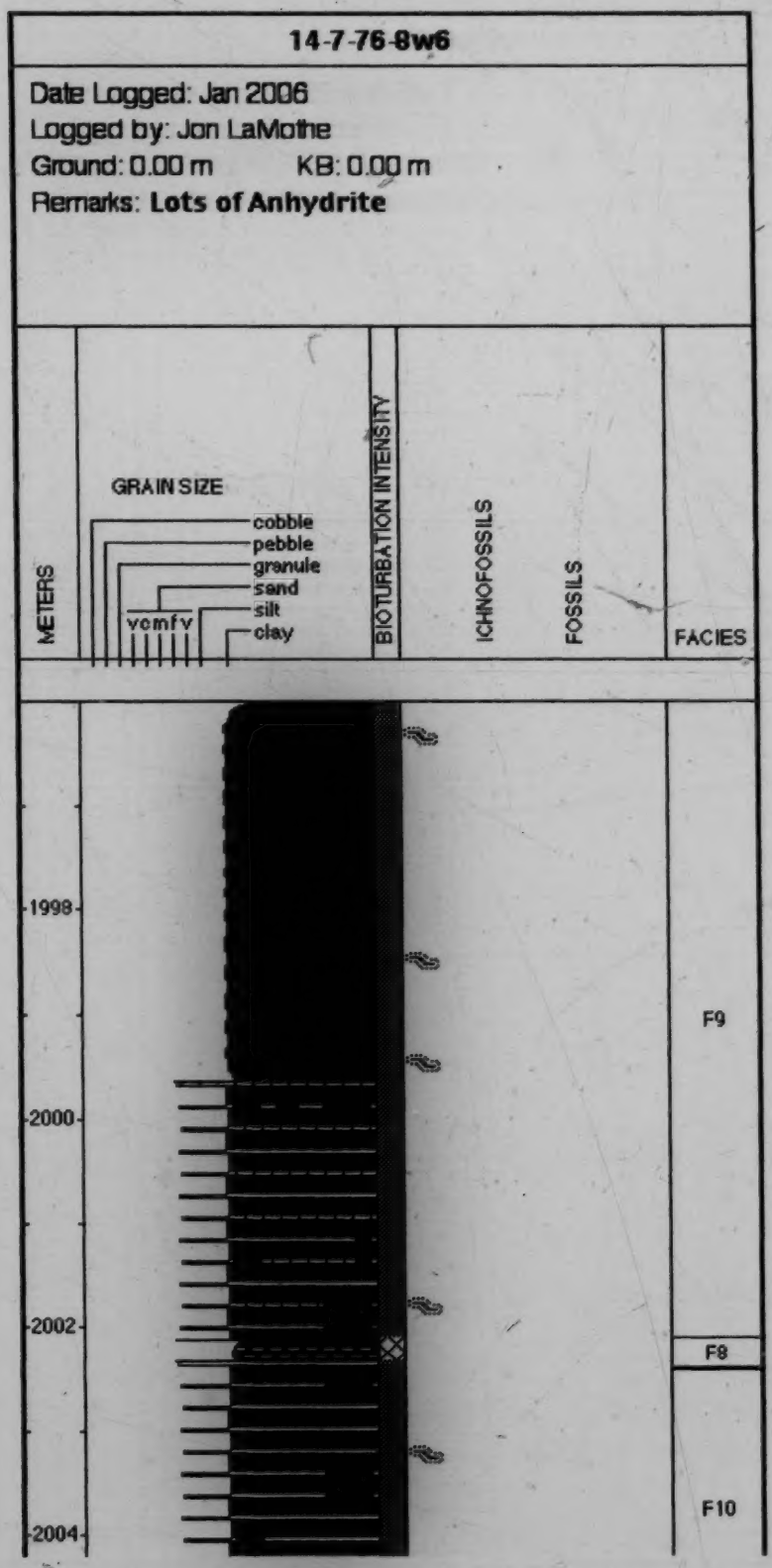
14-7-76-8w6
Date Logged: Jan 2006
Logged by: Jon LaMothe
Ground: 0.00 m KB: 0.00 m
Remarks: Lots of Anhydrite
METERS
GRAIN SIZE
cobble
pebble
granule
sand
silt
clay
vcmfv
BIOTURBATION INTENSITY
ICHNOFOSSILS
FOSSILS
FACIES
1998
2000
2002
2004
F9
F8
F10

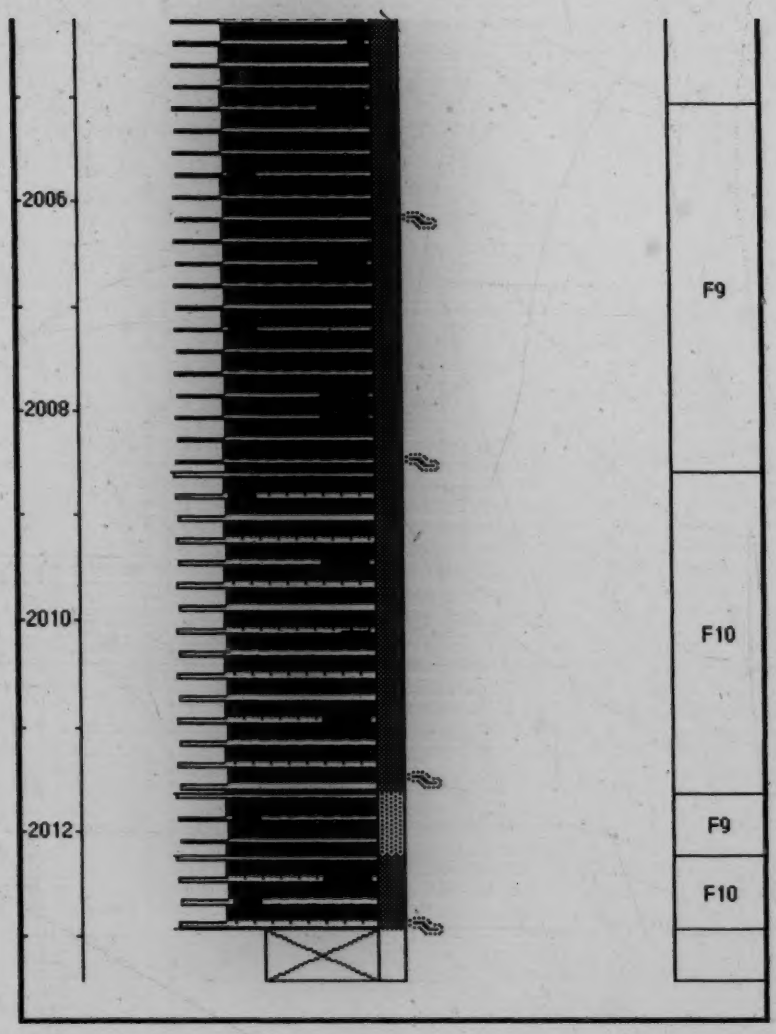
2006
2008
2010
2012
F9
F10
F9
F10

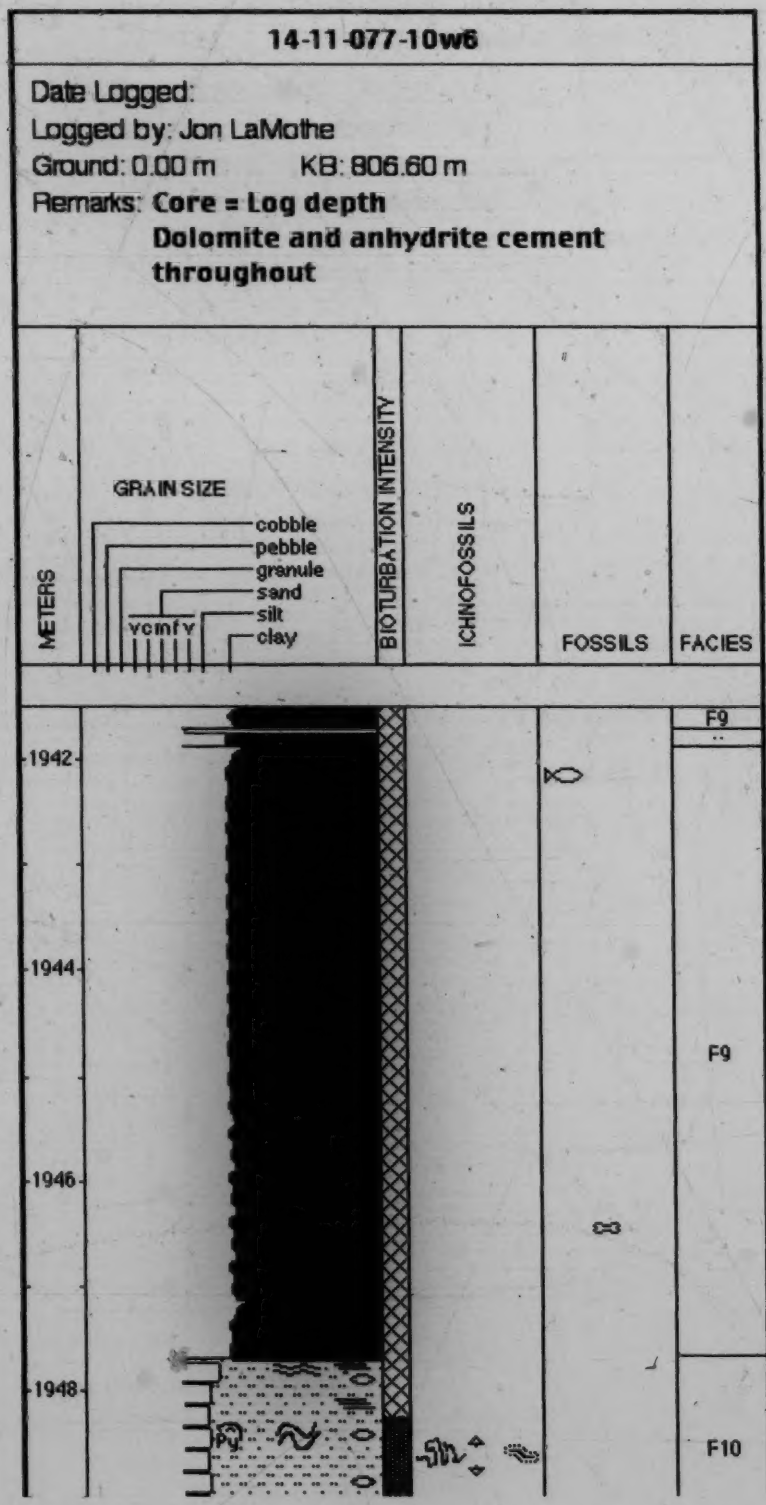
14-11-077-10w6
Date Logged:
Logged by: Jon LaMothe
Ground: 0.00 m KB: 806.60 m
Remarks: Core = Log depth
Dolomite and anhydrite cement throughout
METERS
GRAIN SIZE
cobble
pebble
granule
sand
silt
clay
vcmfv
BIOTURBATION INTENSITY
ICHNOFOSSILS
FOSSILS
FACIES
1942
1944
1946
1948
F9
F9
F10

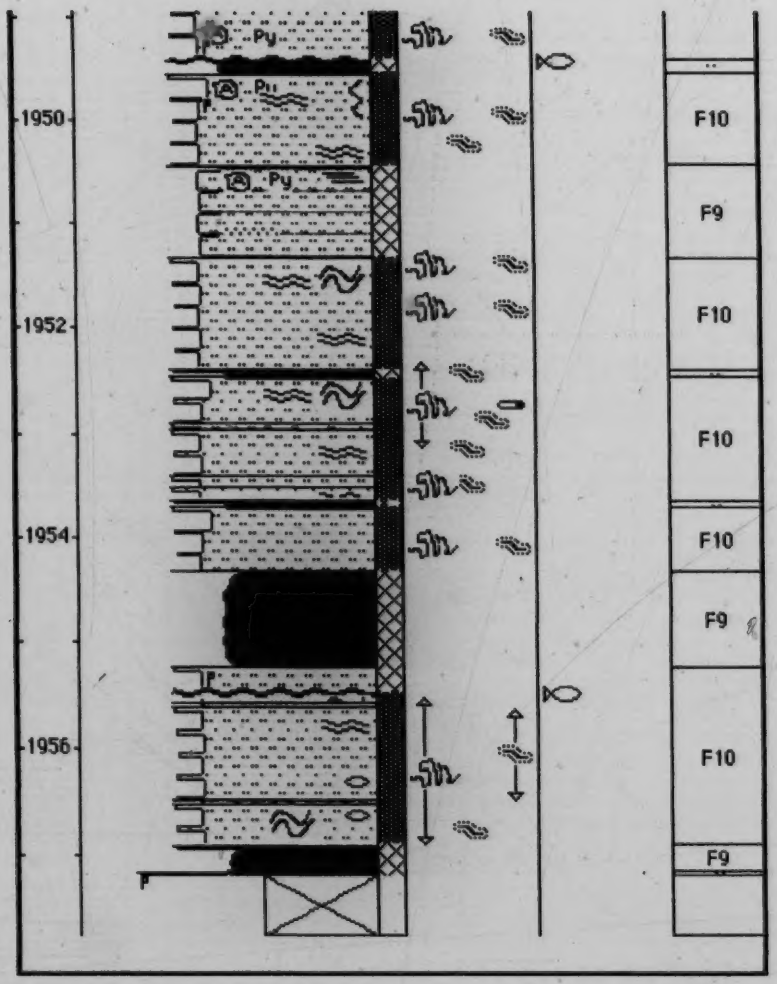
1950
1952
1954
1956
Py
Pu
Py
Sh
F10
F9
F10
F10
F10
F9
F10
F9

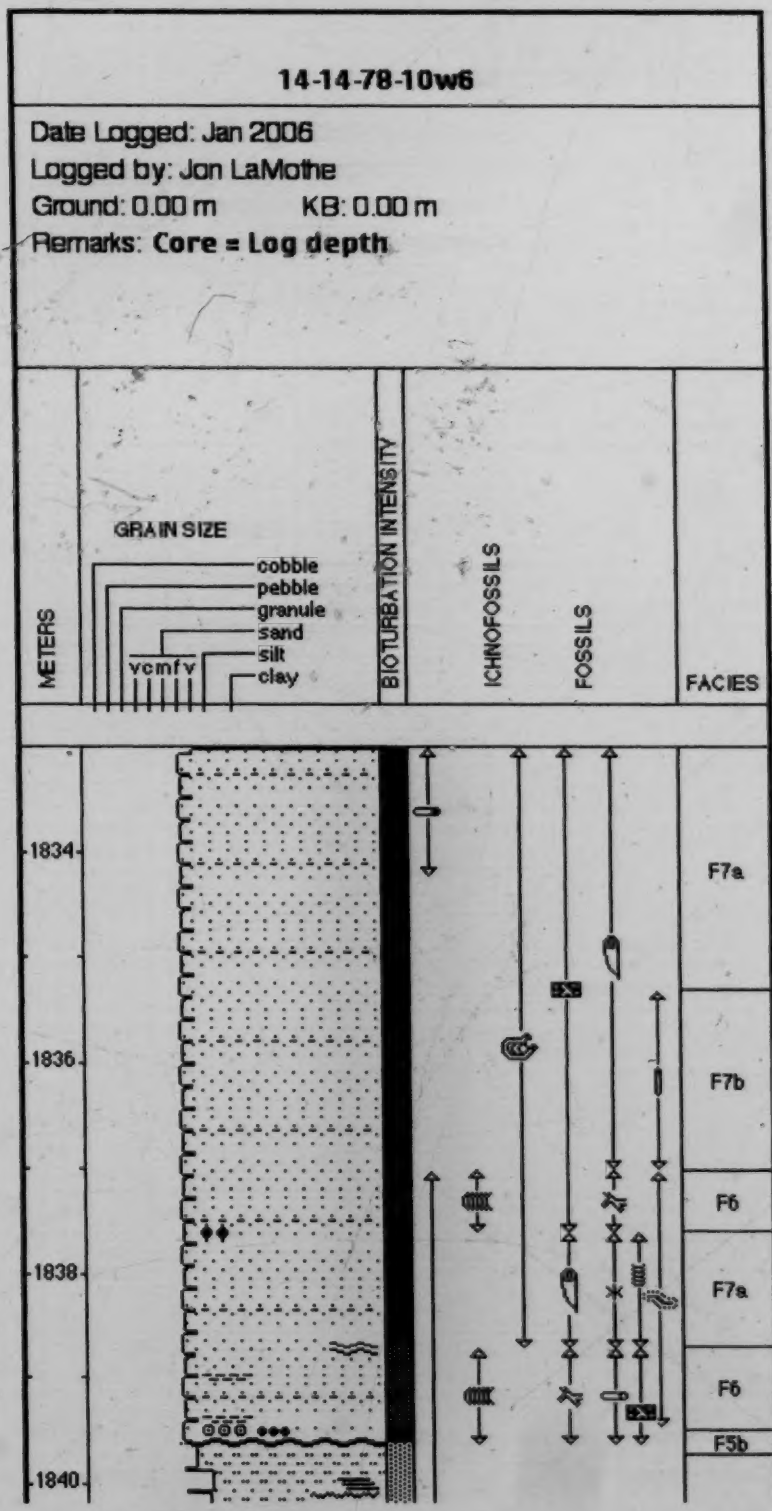
14-14-78-10w6
Date Logged: Jan 2006
Logged by: Jon LaMothe
Ground: 0.00 m KB: 0.00 m
Remarks: Core = Log depth
METERS
GRAIN SIZE
cobble
pebble
granule
sand
silt
clay
vcmfv
BIOTURBATION INTENSITY
ICHNOFOSSILS
FOSSILS
FACIES
1834
1836
1838
1840
F7a
F7b
F6
F7a
F6
F5b

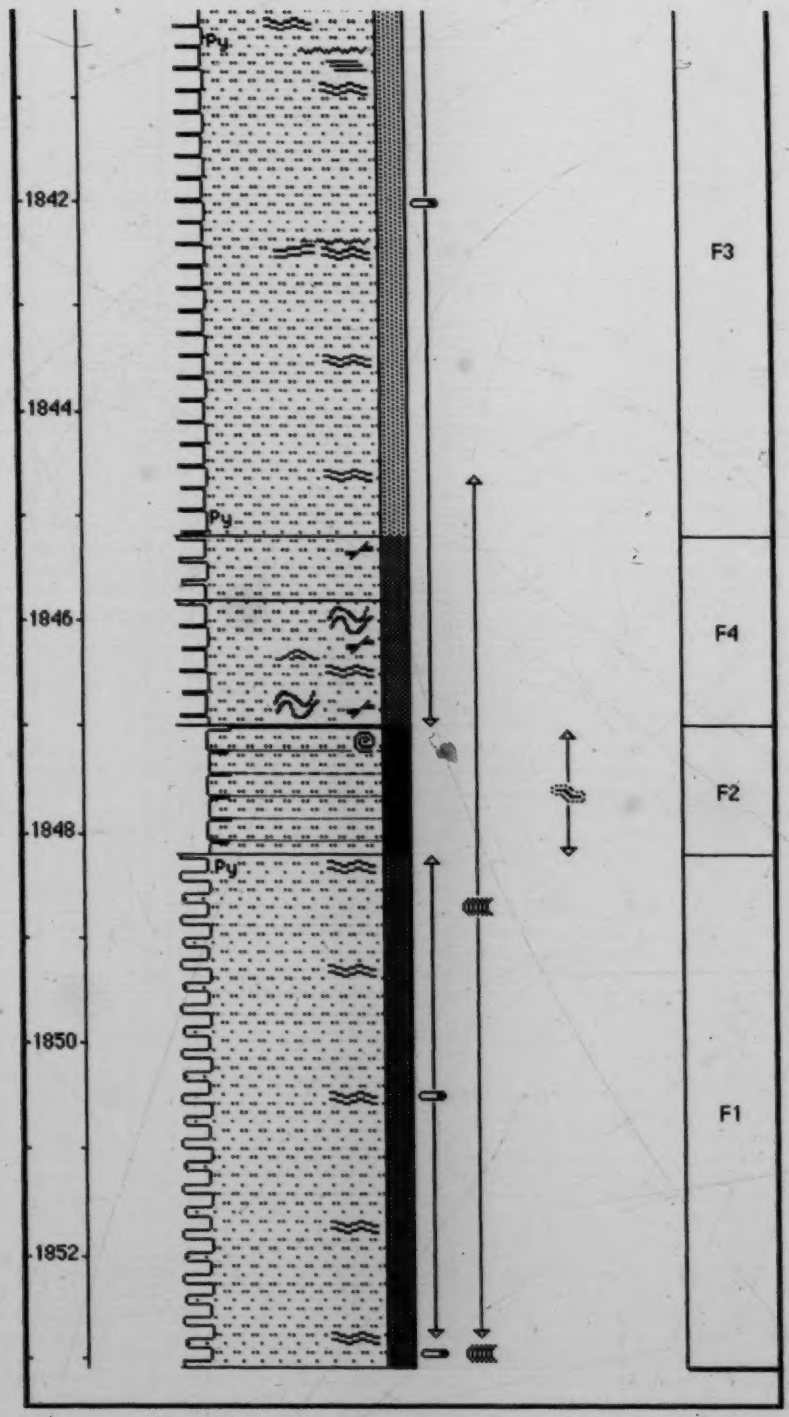
1842
1844
1846
1848
1850
1852
Py
Py
Py
F3
F4
F2
F1

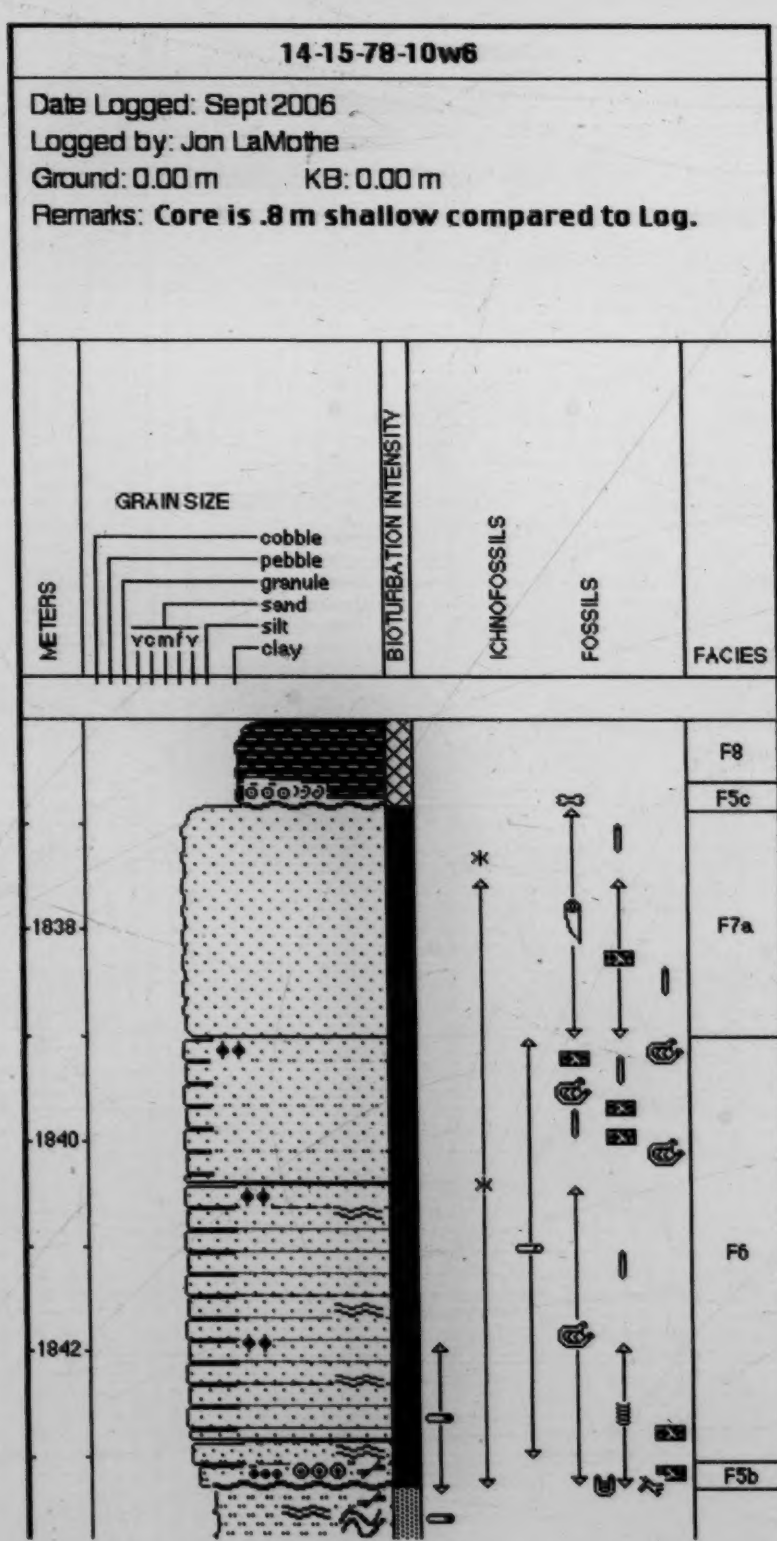
14-15-78-10w6
Date Logged: Sept 2006
Logged by: Jon LaMothe
Ground: 0.00 m KB: 0.00 m
Remarks: Core is .8 m shallow compared to Log.
METERS
GRAIN SIZE
cobble
pebble
granule
sand
silt
clay
vcmfv
BIOTURBATION INTENSITY
ICHNOFOSSILS
FOSSILS
FACIES
1838
1840
1842
F8
F5c
F7a
F6
F5b

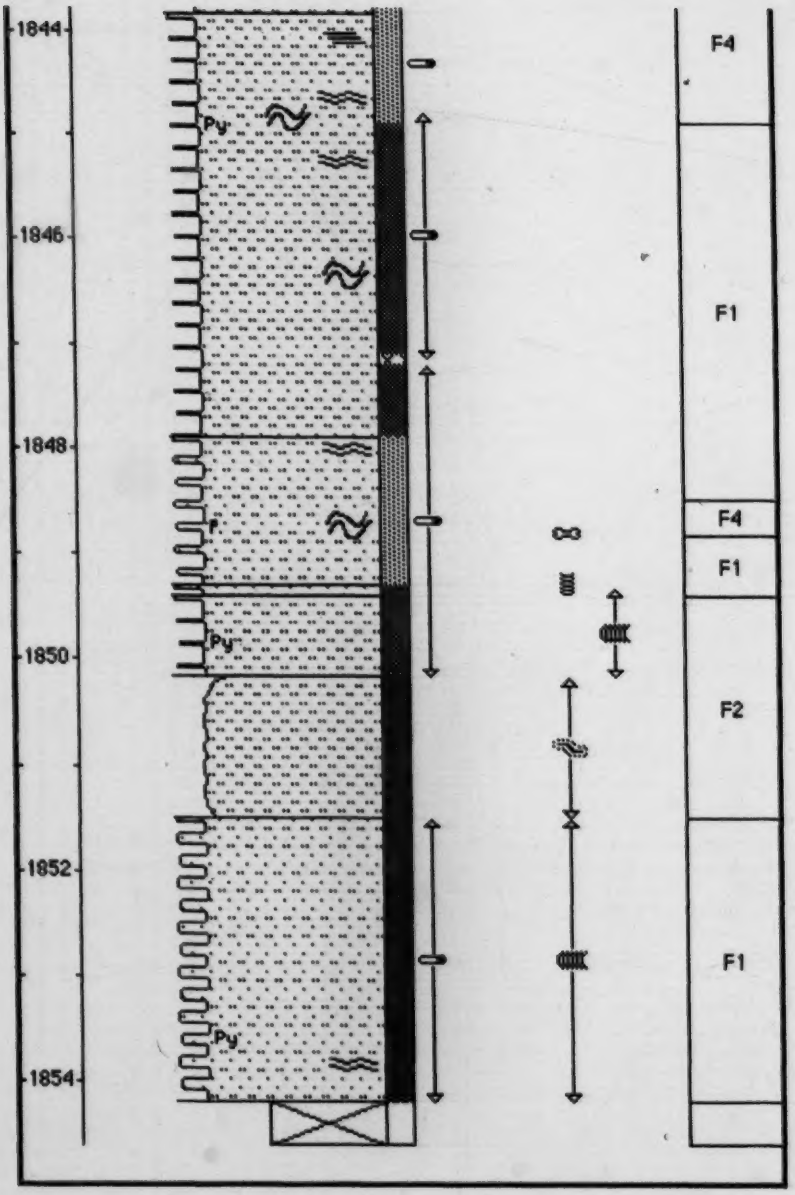
1844
1846
1848
1850
1852
1854
Py
Py
Py
F4
F1
F4
F1
F2
F1

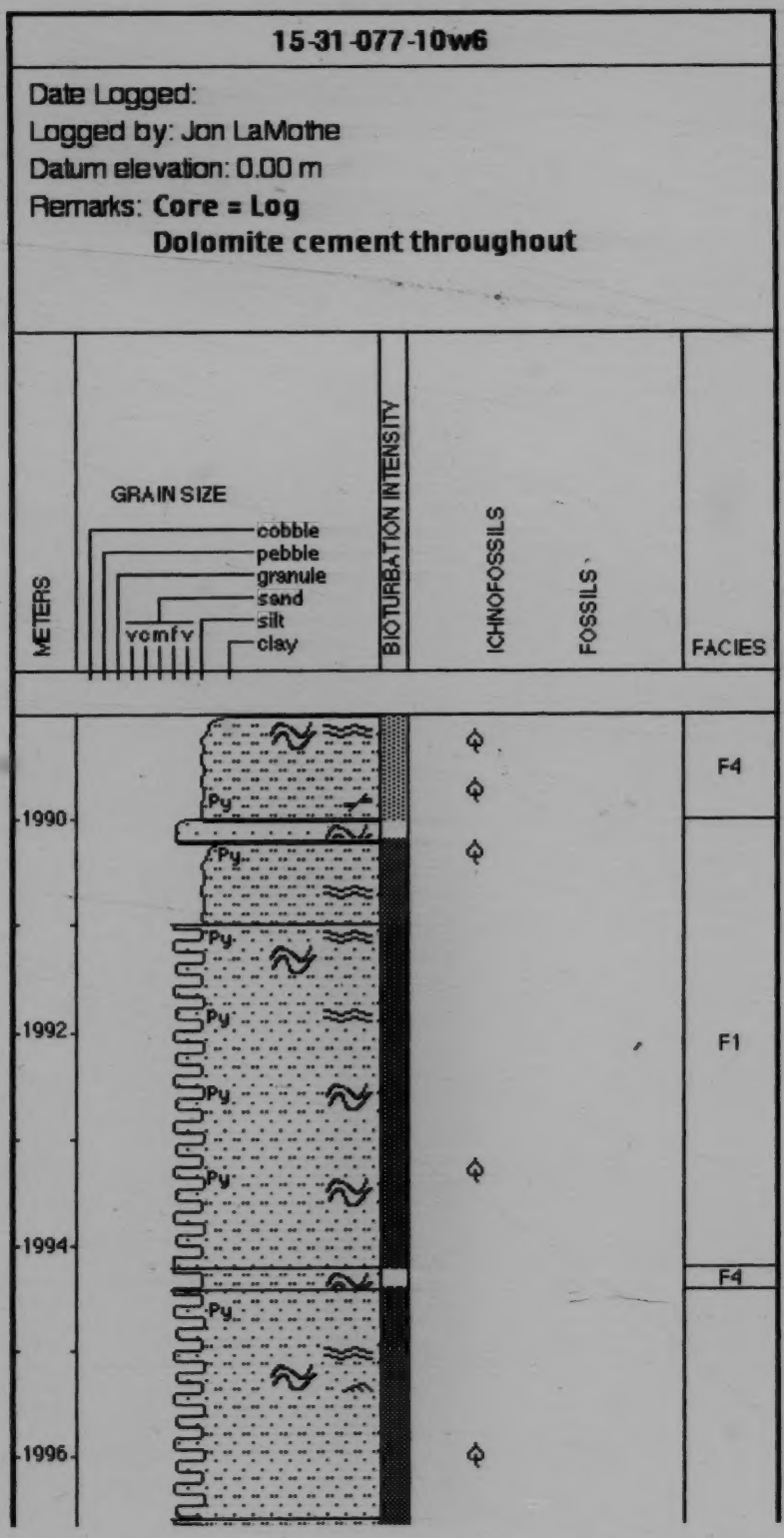
15-31-077-10w6
Date Logged:
Logged by: Jon LaMothe
Datum elevation: 0.00 m
Remarks: Core = Log
Dolomite cement throughout
METERS
GRAIN SIZE
cobble
pebble
granule
sand
silt
clay
vcmfv
BIOTURBATION INTENSITY
ICHNOFOSSILS
FOSSILS
FACIES
1990
1992
1994
1996
Py
F4
F1
F4

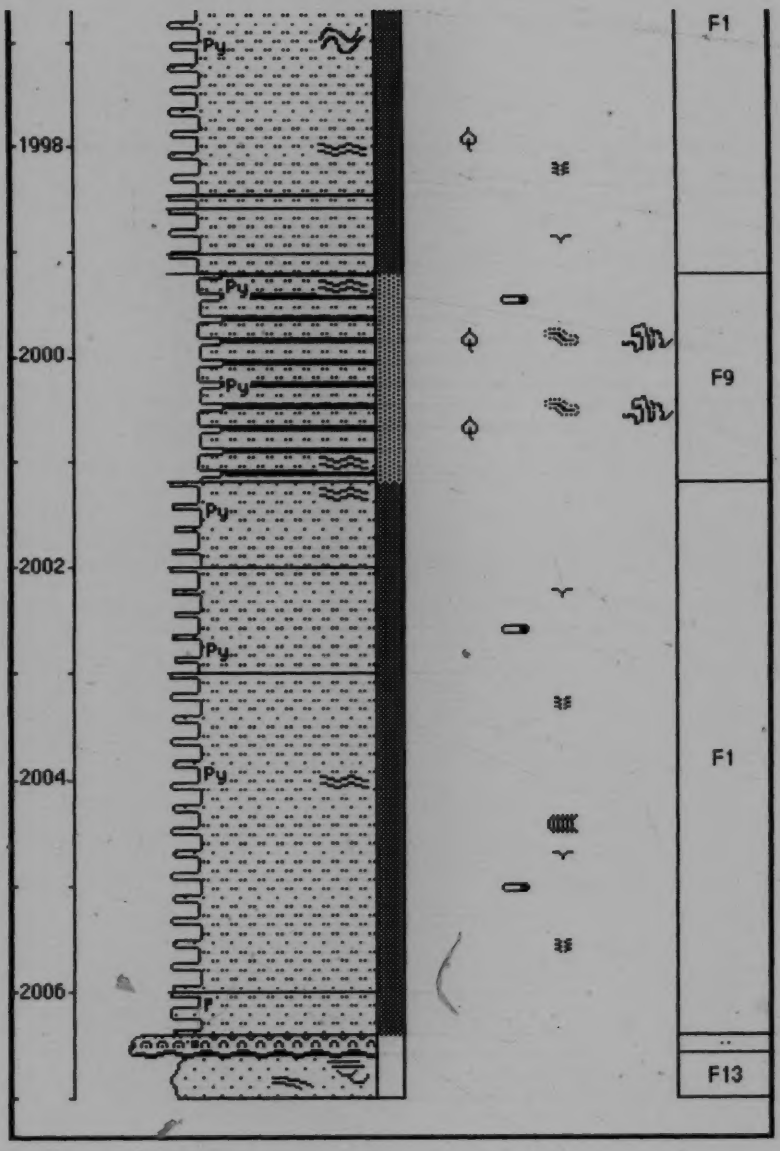
1998
2000
2002
2004
2006
Py
Py
Py
Py
Py
P
F1
F9
F1
F13